FRACTAL ANALYSIS OF CREEPING DISCHARGES PROPAGATING OVER SOLID INSULATORS IMMERSED IN INSULATING OIL

Warnakula Ediriweera Patabandige Sampath Ediriweera

178070P

Degree of Master of Science

Department of Electrical Engineering

University of Moratuwa

Sri Lanka

October 2018

FRACTAL ANALYSIS OF CREEPING DISCHARGES PROPAGATING OVER SOLID INSULATORS IMMERSED IN INSULATING OIL

Warnakula Ediriweera Patabandige Sampath Ediriweera

178070P

Thesis submitted in partial fulfilment of the requirements
for the degree of Master of Science

Department of Electrical Engineering

University of Moratuwa
Sri Lanka

October 2018

DECLARATION

I declare that this is my own work and this dissertation does not incorporate without acknowledgement any material previously submitted for a Degree or Diploma in any other University or institute of higher learning and to the best of my knowledge and belief it does not contain any material previously published or written by another person except where the acknowledgement is made in the text.

Also, I hereby grant to University of Moratuwa the non-exclusive right to reproduce and distribute my dissertation, in whole or in part in print, electronic or other medium. I retain the right to use this content in whole or part in future works (such as articles or books).

Signature: Date:

The above candidate has carried out research for the Master's thesis under my supervision.

Signature of the Supervisor(s):

Dr. Rasara Samarasinghe Date:

Prof. Rohan Lucas Date:

Abstract

A solid/liquid insulation interface is considered to be one of the weakest points in a composite insulation system as it facilitates creeping discharges on the interface when the electric field strength exceeds a threshold value. This thesis presents an original study on the use of alternative liquid and solid insulation materials to minimize the effect of damages which occur due to creeping discharge activity. A point-plane electrode arrangement based test apparatus energized by a high voltage supply is used for analysing propagation of creeping discharges over solid/liquid interfaces using visual observation. Firstly, an algorithm is developed to determine the fractal dimension of creeping discharges propagating over various solid/liquid insulating interfaces. In particular, it focuses on the variation in creeping discharge patterns with the use of pure epoxy and Nano-composite epoxy samples. The results show that the pattern propagation depends on the surface profile and the dielectric constant of the solid material. Next, the effect of the thickness of solid materials on the propagation characteristics of creeping discharges is studied and the results show that capacitive mechanism plays a major role on pattern propagation irrespective of the kind of solid material. Next, the effect of oil level on creeping discharge propagation over solid/liquid interfaces is studied and the results show that when the oil level increase, amount of ramification and propagation of streamers decreases. Finally, this thesis studies the effect of using alternative oils such as copra type coconut oil, virgin type coconut oil, soya bean oil and sunflower oil on creeping discharge propagation. The results show that there is an inverse relationship between the amount of tree formation and the dielectric constant of the liquid. The investigations show that use of nano-composite materials and alternative oils have a significant effect on creeping discharge propagation over solid/liquid insulating interfaces.

***Keywords*-Gaseous Mechanism, Creeping Discharges, Fractal Dimension, Promotional Effect, Fractal Characteristics**

ACKNOWLEDGEMENTS

First and foremost, I would like to express my sincere gratitude to my supervisors, Prof. Rohan Lucas and Dr. Rasara Samarasinghe for the guidance and support during my M.Sc. studies. I thank them for sharing their experiences on the subject and specially for making time in their busy schedule to help me with my research.

I also wish to express my sincere gratitude to the member of the progress review panels, Dr. Asanka Rodrigo and Dr. Lidula Widanagamaarachige for their valuable suggestions, guidance, encouragement and judgements that helped me to successfully complete my research, and to all the lectures for their valuable ideas.

I would like to thank the Senate Research Committee at University of Moratuwa for providing me the financial support and to the University of Moratuwa for providing the Department of Electrical Engineering a new high voltage lab which made a good working environment to conduct my research. Special thanks should go to the technical officer of the power systems and high voltage laboratory, Mr. Ashoka Chandana and the lab assistant, Mr. Jagath Mahanthe for their valuable ideas and support during my experiments. I express my thanks to all the staff of material science and engineering of the University of Moratuwa for proving me their facilities to prepare material samples, and for sharing their knowledge with me.

I would also like to thank all my colleagues and friends specially Mr. Promod Jayarathne, for giving their assistance throughout the time of research and for making my time at the university enjoyable.

Last but not least, I wish to give my heartful thanks to my parents and sister for their understanding, motivation and patience even though the research took more than a year.

TABLE OF CONTENTS

LIST OF FIGURES

LIST OF TABLES

LIST OF APPENDICES

CHAPTER 1

INTRODUCTION

1.1 Background

A quality electricity supply has become one of the basic necessities in the modern society, demanding an efficient and uninterrupted power supply. A power system consists of many essential and critical oil filled high voltage (HV) assets such as cables, transformers, capacitors and circuit breakers with many solid/liquid interfaces present. The failure of these assets may lead to catastrophic events, resulting in economic losses and injury to humans. Therefore, it is important for the power utilities to maximize their effect in maintaining reliable operation of their high voltage assets [1].

The potential gradient inside the HV assets can be high depending on the energizing levels of the asset, and some parts of the equipment inside the oil-filled apparatus can be at very high potentials compared to the earthed outer cases. As an example, winding and leads in a transformer are at a higher potential compared to the core and the tank. Normally different insulation materials are used to separate these components with different voltage levels in order to prevent direct discharges and complete failure [2].

Petroleum-based mineral oils are widely used as an insulation and cooling medium in HV assets. In the case of transformers, the insulation system consists of insulating dielectric liquid and cellulose insulation such as paper and pressboard. The dielectric liquid can act as electrical insulation and a medium to carry the dissipated heat [2].

Composite insulating structures must withstand the electric stress generated by nomi-

nal operating voltages and sometimes transients such as lightning surges and switching impulse voltages. There can be partial discharges in the structure due to high electric stresses, which may deteriorate the insulation structure with time, even at normal operating voltages. On the other hand, solid/liquid interface of oil-filled apparatus is considered to be a weak point as it facilitates the creeping discharge propagation over the interface, which may lead to flashovers in the long run. Ultimately, the complete failure of the assets will occur instantly. Most of the investigations have shown that the main reason of the HV equipment failure under normal operating conditions is insulation failure due to events such as partial discharges, surface discharges and creeping discharges that occur over time [3, 4].

Therefore, at the design stage of a power system, it is important to take necessary actions in order to ensure that the electric stress is lower than the withstand capability of the composite insulation system. Thus, manufacturing companies make necessary efforts to ensure that a certain level of tolerance is maintained based on their experience during the design stage of HV assets.

1.2 Solid/liquid Insulating Interfaces

Dielectric liquids are being used in the industry in association with solid insulating material to serve as an insulation, impregnation and cooling medium. In some cases, the solid barrier materials are used to improve the dielectric strength of gas and oil gaps [5]. Figure 1.1 gives an example of the oil/pressboard insulation structure where pressboard cylinders have been used for partitioning the oil gaps into smaller gaps with higher breakdown strength. There are two concepts which explain the increase of the breakdown strength of the liquid gaps with insulating barriers: barrier effect [6, 7] and volume effect [8, 9].

According to the volume effect, gaps with large electrode areas and long distances can reduce the dielectric strength of insulating liquids due to the presence of defects on

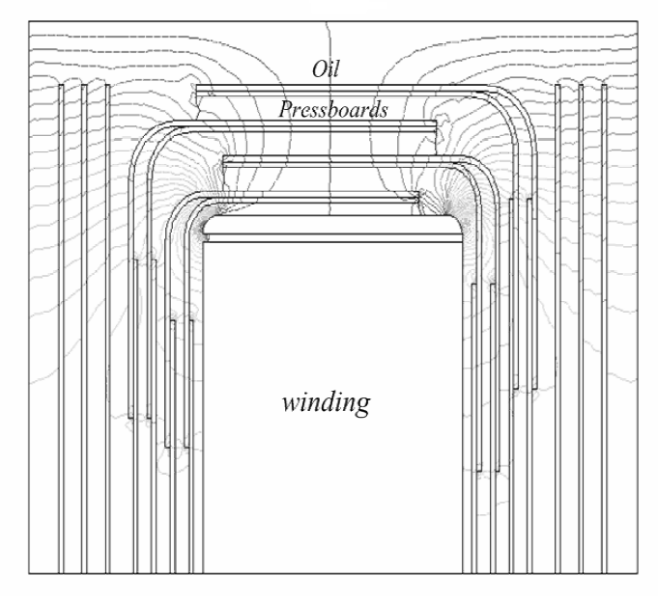

Figure 1.1: Structure of an oil press-board composite insulation system in a transformer [2]

electrode surface and weak links in the insulating liquid. The local electric field is influenced by craters and asperities on the electrode surface and it affects the initiation of the breakdown. On the other hand, the presence of weaker links such as ionized molecules and water will promote the initiation of discharge and their development. The number of weak links is considered to be increased with the gap distance [2].

Barriers can change the space charge distribution and distort the electric field inside the oil gaps. The barrier makes the charges injected by an electrode or induced by the ionization process to be blocked and spread over its surface. Then the electric field between the surface charge layer and one of the electrode become uniform. As a result of the field distribution, breakdown voltage increases.

1.3 Creeping Discharges

Dielectric liquid and solid barriers can increase the dielectric strength of HV oil filled assets. However, the arrangement of the composite insulation system is also one of the

key points that has to be considered. As an example, angled pressboard rings are used inside transformers to limit the tangential electric field along the pressboard below 1-2 kV/mm, which is considered as the driving force of creeping discharges [2].

Once a discharge initiates inside oil, it tries to propagate along the direction of the highest electric field. However, once it reaches a solid dielectric, it can hardly penetrate the solid material. Instead, the discharge would propagate on the surface of the solid dielectric given that the tangential electric field component is sufficient for discharge propagation. These discharges are commonly called creeping discharges. The tangential component of the electric field will drive the creeping discharge over the solid/liquid interface. This discharge can make irrecoverable damage to the insulation system and cause flashover which undermines the use of a composite insulation system.

The development of creeping discharges on a solid surface is a dynamic process. The concentration of charge carrier and the external electric field determine the electric field in streamer channels. In addition to that, there are a few influencing parameters such as surface smoothness, hydrostatic pressure and electron emission from the solid surface [2].

1.4 Alternative Insulating Liquids

A conventional transformer oil is of petroleum origin and consists of hydrogen and carbon atoms in basic three different structures: aromatic, naphthenic and paraffinic. Figure 1.2 shows the basic structure in mineral oil. The paraffinic structure has either straight or branched molecule groups. If the oil contains more straight groups, normally it is called as normal-alkanes and their free flow become limited as the temperature decreases. Therefore, the content of normal-alkanes is required to be removed prior to the usage at cold climates. This structure decreases the solubility in water and the by-products generated by oxidation can lead to the development of sludge. Thermal

stability of these molecules can be considered to have a lower value compared to the other two type of structures. Therefore, naphthenic oil has become more popular in the industry as it can overcome these problems. With the naphthenic structure, oil has low temperature properties. Normally, all type of mineral oil contains aromatic structures to some extent. Alternating double and single bonds of the structure have made the chemical and physical properties completely different from the other two structures. Gas generated by a fault can be absorbed by this structure. However, the structure can reduce the dielectric characteristics of mineral oil due to their low ionization potential and electron affinity [10, 11].

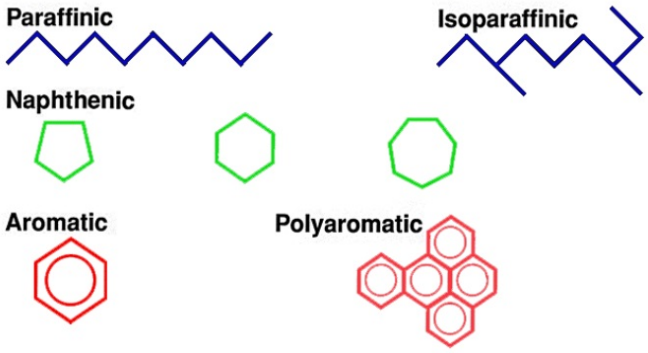

Figure 1.2: Basic hydrocarbon structure in mineral oil molecules [11]

Mineral oils have been used in oil filled high voltage apparatus such as transformers, switchgear and circuit breakers for decades. However, their applications have been more restricted due to a few facts such as the requirement of fire safety and environmental protection and limited petroleum sources. Under this background, researchers have progressed into studies about the capability of esters as a liquid insulation. Even though there are high dielectric losses with esters, it can reduce the concentration of local electric fields inside high voltage assets. Usually, esters have higher conductivity, viscosity and the ability to dissolve water. Non-toxic, environmentally friendly and less flammable nature has made the esters popular in the industry [2, 10, 12]. Generally, esters can be divided into two categories as natural esters and synthetic esters.

Over the past decades, natural seed oils have been studied for use inside power transformers. The chemical structure of natural ester oil is shown in figure 1.3. Unsaturated

Table 1.1: Characteristics comparison between mineral oil and ester oil

Criteria	Mineral Oil	Ester Oil
Key Properties	Non-renewable material	Renewable sources
Environmental Properties	Poorly biodegradable and slightly toxic	Highly biodegradable and non-toxic
Leak and Spill	Spills clean-up are required by regulation	Spills clean-up can be eliminated because relatively rapid biodegradable

bonds in the structure have made the ester more susceptible to oxidation. Esters nourish the generation of some bacteria, and acids generated by them can cause degradation of the insulation system. Therefore, additives are usually used before their application. On the other hand, synthetic esters are more biodegradable than mineral oil. However, it requires a higher cost to synthesis the esters compared to other dielectric liquids. Figure 1.4 shows the chemical structure of synthetic ester oil. The longer chain structure of the esters has given them a higher flash point and a density making them more flame-retardant [12, 13]. Table 1.1 shows a comparison of few characteristics between mineral oil and ester oil.

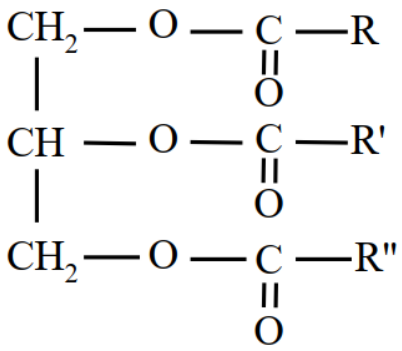

Figure 1.3: Chemical structure of natural ester oil [12]

Vegetable oils (natural esters) have become more popular due to their full biodegradability and the availability of natural resources. However, researchers have identified the need of powerful oxidation inhibitors to reduce its biodegradability within a short time before the usage because once the high voltage asset is installed, sealed unit is going to remain as it is for many years unless the oil is changed [14].

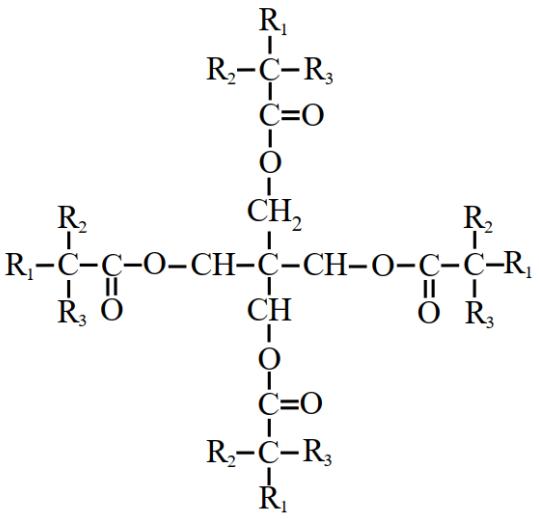

Figure 1.4: Chemical structure of synthetic ester oil [12]

1.5 Epoxy Based Nano-Composites

Generally, the word epoxy is being used to address both pre-polymers and cured resin in which reactive groups have reacted with each other. The discovery of epoxy occurred as early as 1891. However, it did not become a commercially available product until Pierre Castan in Switzerland and Sylvan Greenlee in the United States synthesized the first bisphenol-A epichlorohydrin-based resin material [15].

Epoxy resin based materials are being used in several applications such as coating, electrical insulation, adhesives. Epoxy resin insulating systems are widely used in HV applications such as in bushings, transformers, generators due to their mechanical and dielectric properties [16–18]. Unless a drop of the curing agent is not mixed with the resin, it has an indefinite lifetime. The main advantage of the epoxy resin is the ability to transform from thermoplastic state to thermo-set state by a chemical called as a hardener. Some agents promote the hardening process of epoxy by catalytic action, while others are absorbed by epoxy to make the cross-linked structure. Sometimes these reactions can be carried out in room temperature with the heat produced by an exothermic reaction. However, epoxy cured in higher temperature improves the properties

such as mechanical strength, dielectric strength and glass transition temperature [15].

In recent years, researchers have paid more attention towards insulating materials which offer higher thermal conductivity. Polymers, such as epoxies, can be used in insulation systems of high voltage assets. However, their application had been limited due to low thermal conductivity and high thermal expansion coefficient. In order to increase the thermal conductivity while preserving the dielectric properties of polymers, filler materials such as glass, silicon dioxide and mica are used to prepare polymer-based composites. Reinforcement of polymers with organic and inorganic fillers make low weight materials while improving the mechanical, thermal and electrical properties which are affected by characteristics of the filler such as the shape, dimension and nature [19–21].

Polymer nano-composites consist of fillers with smaller particle size so that it has a mixture of two phases: a polymer matrix and the solid phase. In early days, polymer composites were manufactured with micrometre sized particles in higher concentrations. However, nowadays, nano-composite materials are developed with nano-sized particles in low concentrations and new fillers have been introduced providing the researchers a path for the development of high-performance nano-composites [22, 23]. Few advantages of nano-fillers are as follows.

1. Modification of mechanical properties.
2. Improvement the fire retardants.
3. Modification of electrical and magnetic properties.
4. Modification of surface properties.
5. Improvement of processability.

1.6 Problem and Research Motivation

Solid dielectrics such as cellulose paper, pressboard, porcelain, glass and ceramic are the main insulating materials used in HV industry to increase the dielectric strength of the insulation of an equipment. Miniaturization and alternative for conventional insulation with simplified structures are required to increase the reliability, competitiveness and to reduce the production cost of oil-filled assets. It would make the distances between the insulations narrow [24, 25].

Figures 1.5a, 1.5b and 1.5c show failure of transformers due to flash over associated with creeping discharges on the mineral oil/press-board interface. The difference in permittivity between the solid and the liquid seems to be the main reason for initiation of creeping discharges propagating along the interface. Even with the use of advanced manufacturing and monitoring technologies, most of the faults occur unexpectedly without any obvious cause [26]. Figure 1.6 shows the traces of creeping discharges occurring inside a distribution switchgear. Creeping discharges can propagate up to the flashover point according to the electric field distribution. The flashover along solid/liquid interfaces leaving behind conducting traces are generally called as surface tracking, which can be divided into two categories. Sustaining AC stress drives one type, and transients and surges trigger the other type and will cause instant flash over [2,27]. Discharges can propagate easily with the traces of previous discharges, causing partial or total irrecoverable damages to the asset, requiring the repair of the apparatus or even its replacement [28].

Normally dielectric constants of insulation liquids are lower than that of solid insulation. Therefore, electrical stress is divided among them unequally. As an example, dielectric constant of mineral oil is about half of that of pressboard, making the stress inside oil twice than that in pressboard inside the transformer. To worsen the case, breakdown voltage of a solid insulating material is higher than that of liquid insulation. Therefore, partial discharges and breakdown can occur easily inside oil compared to solid insulator [2].

(a) (b)

(c)

Figure 1.5: Creeping discharge failure of insulation (a) to (c) [25]

Figure 1.6: Discharge formation in a distribution switchgear [29]

Alternative natural ester oils are used inside oil-filled high voltage apparatus in conjunction with solid materials specially in power transformers. In 2001, a coconut oil

filled seal type distribution transformer was installed in Wathara area in kesbewa, Sri Lanka, which is shown in figure 1.7, in its installed location. 160 kV transformer is supplying power to a rubber factory and to domestic consumers through 400 V feeders [30]. The transformer had been loaded about 40 % of its rated power during its operation throughout these years and this transformer is still operating without any faults or failures [31]. However, the transformer manufacturers are not willing to risk the consequences of designing a HV apparatus filled with ester oil without a proper understanding of discharge behaviour under divergent oil gaps, especially in conjunction with solid materials. Therefore, it is of vital importance to study the propagation of creeping discharges along the surface of solids materials immersed in ester oils and to compare their behaviour with those with the use of mineral oil. It is necessary to ensure that the dielectric liquid can withstand the generated stress to minimize the partial discharges and flashover conditions at the design stage of an HV asset. Other than that, comprehensive studies should be carried out in order to predict the initiation, development and propagation of creeping discharge in solid/liquid insulating systems, for upgrading the insulating system during its design. The conditions under which the discharge initiates and the parameters influencing the discharge development up to the flashover are of utmost importance for design optimization of high voltage apparatus and their insulating parts such as bushings and spaces.

Some work has already been carried out to study the discharge propagation in solid/liquid insulator interfaces, especially using mineral oils [2]. However, creeping discharge characteristics along the insulating material immersed in natural esters subjected to alternating voltage have to be studied thoroughly in order to understand the usability of natural esters in a highly stressed environment.

A lot of research work has recently been devoted to improving the dielectric properties of insulating materials by adding specific nano-fillers to polymer-based materials, changing the dielectric and mechanical properties. Nano-composite polymer materials show better performance as insulating properties [32, 33]. Other than the electrical characteristics, they show higher tensile strength and chemical, thermal stabilities over

conventional insulators [34].

Some work has already been carried out to study the improvements to the dielectric properties of a material such as breakdown strength, dielectric dissipation factor and partial discharge formation [33]. However, there are other important mechanisms such as the development of creeping discharges over nano-composite insulating materials and the behaviour of such insulating material in a solid/liquid insulating interface, which can affect the performance of the dielectric material.

Therefore, studying the creeping discharge characteristics of epoxy nano-composites immersed in insulating oil based is among the main objectives of this thesis.

Figure 1.7: Coconut oil filled 160 kVA, 33/0.4 kV distribution transformer installed at Wathara, Kesbewa, Sri Lanka [31].

1.7 Objectives of the Thesis

Thesis research is focused on investigating the creeping discharge characteristics of epoxy nano-composites immersed in insulating oil based on the experimental analysis.

1. To design and implement a test apparatus to investigate creeping discharge development in a laboratory environment, and to analyse the creeping discharge formation in various solid/liquid interfaces using samples of pure epoxy and nano-composite epoxy.

2. To determine the final discharge length, radial discharge length and fractal dimension of the creeping discharges based on the optical characteristics of creeping discharges, and, to select the materials with the lowest electrical tree formation.

3. To perform a detail investigation in order to determine the effect of parameters such as oil level, thickness of solid material and type of natural esters on characteristics of creeping discharge propagation.

1.8 Thesis Outline

Chapter 2

Chapter 2 presents a detailed discussion on creeping discharge development on solid/liquid and solid/gas insulating interfaces and fractal analysis methods used to quantify the creeping discharges. This chapter includes background study of the work carried out by past researchers on experimental and simulation studies on creeping discharges. This thesis is mainly focused on analysing creeping discharge patterns propagating over various solid/liquid interfaces using their fractal characteristics. Therefore, properties of fractals, fractal analysis methods and past studies carried out on fractal analysis of experimental and simulated discharges are also discussed in this chapter.

Chapter 3

Chapter 3 discusses the methods used in the current study to analyse creeping discharge patterns and their adaption. The chapter also discusses the processing program used to

calculate the fractal dimension of the creeping discharges.

Chapter 4

This chapter discusses the experimental studies of creeping discharge propagation on glass, acrylic, pure epoxy and nano-composite surface in a divergent electric field generated by the experimental test setup under AC stress by means of the High-speed CCD camera. The first part of the chapter discusses the synthesizing procedure of pure epoxy and nano-composite samples. The second part of the chapter discusses the experimental setup used to capture the various creeping discharge figures, including the reason to select a point-plane electrode system for testing purposes. Finally, the creeping discharge characteristics are compared in term of discharge lengths, fractal dimension and surface profile.

Chapter 5

This chapter analyses two different factors that can affect creeping discharge propagation over solid / liquid interface, namely material thickness and oil pressure. The first part of the chapter discusses the experimental studies carried out on creeping discharge propagation on glass, acrylic and pure epoxy surfaces with samples of different thicknesses in a divergent electric field under ac stress, where the main focus is to analyse the effect of material thickness on creeping discharge development in terms of discharge lengths and fractal dimension. The second part of the chapter discusses the creeping discharge propagation on glass surfaces immersed in insulating oil with different oil heights, where the main focus is to see the effect of oil pressure on the soil/liquid interface generated by the mass of the oil. Creeping discharge propagation with different oil levels is compared using corresponding discharge lengths and fractal dimension values.

Chapter 6

Chapter 6 discusses the experimental studies carried out on creeping discharge propagation on glass samples immersed in different type of natural ester oils. Four different types of insulating oils; copra type coconut oil, virgin coconut oil, soybean oil and sunflower oil are used for the experiments. Suitability of each oil as a dielectric insulation is analysed according to the severity of creeping discharge propagation.

Chapter 7

Chapter 7 presents the conclusions of this research, summarizing discoveries made from the research and suggestions for future work.

1.9 Publications List

1. W. E. P. Sampath Ediriweera, K. L. I. M. P. B. Jayarathna, J. R. Lucas and R. Samarasinghe, ”Effect of the Shape of the Insulator on Fractal Characteristics of Creeping Discharges,” *2018 Moratuwa Engineering Research Conference (MERCon)*, Moratuwa, 2018, pp. 506-510.

2. W. E. P. S. Ediriweera, K. L. I. M. P. B. Jayarathna, R. Samarasinghe and J. R. Lucas, ”Effect of Barrier and Its Shape Over the Breakdown Voltage of Oil Gaps,” *2018 2nd International Conference On Electrical Engineering (EECon)*, Colombo, Sri Lanka, 2018, pp. 76-80.

CHAPTER 2

BACKGROUND STUDY AND LITERATURE REVIEW

2.1 Introduction

Insulation failure is a major problem faced by power utilities. These failures affect the electricity consumers and it can cost the utility companies for the repair or replacement of the assets. Creeping discharge, which propagates over solid/liquid interface is one of the reasons of insulation failure. This thesis provides a comprehensive study of creeping discharge propagation and fractal analysis of creeping discharges over various solid/liquid insulating interfaces under different conditions.

This chapter provides a detailed description of past studies on creeping discharges from the point of discovery of the surface discharge to the present, numerical methods that can be used to model the creeping discharge propagation over solid/liquid interfaces, and a comprehensive study of fractal geometry including fractal analysis methods, past studies about fractal analysis of creeping discharges on both experimental and simulated patterns.

Creeping discharges over solid/liquid interfaces is another aspect of partial discharges. These are characterized by the propagation of streamers, formation of branches and intensive light spots. The branches will extend in length and in width with the time. The more frequent occurrence of these discharges makes the dielectric medium more conductive. Figure 2.1 shows a discharge pattern which is propagating over a glass/SF6 interface.

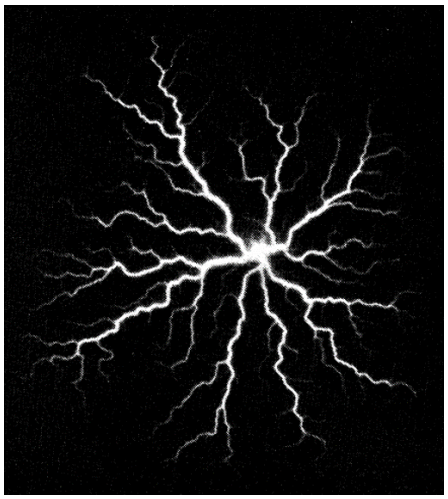

Figure 2.1: surface leader discharge on' a 2-mm glass plate in 0.3-MPa SF_6 [35]

2.2 Creeping Discharges

Investigations of creeping discharge development have been carried out under several experimental conditions such as electrode arrangement and polarity of the voltage. The earliest studies have been started with the breaking discovery of the Lichtenberg figures in eighteenth-century [36–40].

2.2.1 Lichtenberg Figures

When a powder is dusted on a charged surface of a dielectric material, the powder becomes glued to the surface to make a characteristic pattern. A photographic film also can be used to obtain such patterns. These types of patterns are called as Lichtenberg figures. This phenomenon was discovered unexpectedly by German physicist Georg Christoph Lichtenberg in 1777 [40]. A report stating his discovery was read by his teacher at the royal society of science of Gottingen on May 3, 1777. Later Lichtenberg wrote a report about his discovery and read it in a public meeting on February 21st, 1978. The report had the title as "*De nova methodo naturam ac motum fluidi electrici investigandi*" (On a new method to investigate the motion of electric fluid). A part of

the report given below states the situation that led to his own finding [41].

"*At that time Lichtenberg made a huge electrophorus of about 2 m in diameter. It was so powerful that a spark of about 40 cm in length could be produced. The occasion of observing this phenomenon (dust figure) was as follows:*"

"*About the beginning of spring 1777 my electrophorus was just finished. In my room all was still covered with very fine rosin powder that had risen during planning and polishing of the cake and the metal disk, and later it lay on walls and books. When air motion occurred, it deposited on the metal disk of the electrophorus, to my great annoyance. However, it was not until I had hung the disk on the ceiling of the room many times, that the powder deposited on the cake; then I could not cover it uniformly as had occurred on the metal disk, but to my great joy it was arranged like small stars at certain points. These were dull in the beginning and difficult to see; when I sprinkled more dust intentionally, however, they became very clear and often resembled embossed work. Sometimes innumerable stars, the Milky Way and bigger suns appeared.*"

"*The bows were dull on their concave side, and decorated manifoldly with rays on their convex side. Marvelous small twigs emerged; the twigs produced by frost on window glass resemble them. Small clouds of many various forms and grades of shading and finally different figures of particular shape were seen .... However, a very pleasant play occurred to me, when I saw that these figures could scarcely be destroyed. Even if I wiped off the dust carefully with a feather or a hare's paw, I could nevertheless not prevent that the figures, which were destroyed just before, quickly developed again to some extent anew and still wonderfully. Therefore, I painted a piece of black paper with adhesive paste, laid it down on the figures and pressed it on them lightly. So I succeeded in making several copies of the figures. I have presented these six copies to the Royal Society. This new variety of printing was very favorable for me in order to progress further very quickly, because I had neither pleasure nor time to sketch or destroy all the figures.*"

Lichtenberg observed that dust figures appear on the area of the cake of electrophorus where light sparks have gone. According to him, the nature of electricity or the movement of the electric fluid had affected the formation of such figures. Lichtenberg identified two types of figures as star-like and moon-like. Lichtenberg extended his testing for various scenarios to understand the situation. At first, he used different cakes and dusts such as amber, cinnabar, lycopodium, sugar, wheat flour, metal filings, and discovered that fine sulphur or rosin in a linen pouch is best for powdering. Later figures were used by him to find out the polarity of the electricity and an instrument composing a rotating cylinder driven by a clockwork, was proposed to find the atmospheric electricity.

The discovery of Lichtenberg gave the foundation to a lot of researchers who began to find out the true reason that figures were formed as Lichtenberg theory was unable to explain it correctly. In 1779, T.Cavallo identified that during the powder was being shaken in the lining pouch before dusting it over a cake of electrophorus, the particles were electrified. Therefore, the power particles were attracted by the plate. However, his conclusion was not agreed with what Lichtenberg suggested [36]. In 1786, J.A de Lucas used Lichtenberg figures to study creeping discharges marking a remarkable turn in the studies of creeping discharges. Further research were carried out to study the characteristics of Lichtenberg figures. However, still, most of the people focused on producing these figures considering them to be beautiful and to be an interesting phenomenon [38, 42].

In the 19th century, Different experiments to record the creeping discharges using photography, instead of dust figures, were carried by different researchers such as B. Silliman et al. in 1842 [37], Pinaud in 1851 [39], and O.N. Rood in 1862 [43]. Photographic figures could be obtained easily using a dark chamber. However, since the nineteenth century, there was a doubt that the light caused by the discharge or the concentrated electric field had created the traces of the figure [43].

2.2.2 Fundamental Studies on Surface Discharges

In 1917, Max Toepler studied the effect of the polarity and the voltage on creeping discharge development on a dielectric material placed between a high voltage electrode and a ground electrode, and amount of the discharge was quantified using Lichtenberg figures [42, 44]. His research led to open a new chapter in creeping discharge studies and to important discoveries.

In 1928, C. Edward Magnusson used a belt generator as a method to generate impulse waves to produce Lichtenberg figures and further studied the best method to record the figures out of available methods [45]. Creeping discharges of short time intervals were quantified using Lichtenberg figures by Pederson and he carried out further studies to differentiate the characteristics of positive and negative discharges [42, 46]. In 1939, F. H. Merrill and A. Von Hippel investigated the development of Lichtenberg figures, primary figures, spark, black figures and plasma, and the effect of electronegative gases over the surface discharge propagation under impulse voltages. They examined deeply the effect of space charge on the branch formation of the pattern for both polarities. According to their observations, at high pressure values, positive branches were turned in to plasma facilitating the development of sparks. On the other hand, at low pressure values, ghost-like structures appeared on the negative plate. However, as the voltage increased, it sharped the structure of the black figures and changed the pattern to be a primary figure with sparks travelling along the edges of it [47]. The basis required for the research over the next years were provided by these fundamental studies.

In 1954, J.G. Anderson and T.W. Liao investigated the propagation of creeping discharges over Kraft papers immersed in insulating oil using impulse voltages. A probe technique was used to find out the potential of the streamer channels. The optical observation was made through the wall of the test cell by a special arrangement. Under the negative impulse voltages, it was observed that a negative space charge region propagates ahead of the discrete stepped streamers as in the mechanism of natural lightning. However positive impulse waveform had made the pattern and the associated chan-

nel length, branching differ from the case of negative polarity and they showed the characteristics of positive streamers in the air [48].

Sill Lichtenberg figures were demonstrated by making the pattern propagate on a dusted surface with powder and by blowing away the surplus powder. In 1961, A. Morris Thomas identified that Lichtenberg figures could be observed on some surfaces by applying heat. For his experiment, he used a resin film exposed to discharges and a pattern of thread-like grooves appeared as it was being heated gently. It was concluded that if the surface of a material does not have a residual strain, it can not give heat-developed figures. He also discovered that a sequence of alternative polarity leads to the propagation of the discharge and the effect of a discharge of a considered polarity is not cancelled by the subsequent discharge of opposite polarity [49].

In 1963, Essam Nasser studied the effect of the contamination of the solid materials over the discharge phenomena such as arc, streamer and glow, using oscilloscope images and identified the stages of the discharge development [50]. In 1969, he investigated the branching structure of streamers developing between a point and a plane inside air using a photographic film [51]. In 1971, he used voltage pulses applied to the negative point-plane electrode system to observe the development of streamers into spark breakdown and the temporal and spatial properties [52]. These studies were further studied by J. D. Cross et al. in 1972, J. S. Brzoskot et al. in 1975 and Bearnhard in 1975. Bearnhard Gross investigated the characteristics of spark discharge using irradiated samples of methyl-methacrylate placed in a point-plane electrode system [53]. J. D. Cross et al., studied the phenomenon of surface discharges and flashes on borosilicate glass insulators held between steel electrodes under impulse voltages in a vacuum chamber [54].

In 1978, Akihiro Kawashima and Seisaburo Hoh used the camera method with a high-speed film to investigate the characteristics of discharges propagating on seven types of different materials. They found out that the patterns are different from material to material and the pattern appearing voltage depends on the surface resistance of the tested materials [55].

2.2.3 Study of Creeping Discharges over Solid Dielectrics

The research regarding creeping discharges moved on to application-based studies in late 20^{th} century. The main focus of these studies was to analyse creeping discharge development over the solid/liquid and solid/gas interfaces which were used inside capacitors, cables and transformers. Propagation of these discharges on insulating interfaces can damage the insulation system leading to complete failure of the power system components. Therefore it is important to understand the creeping discharge initiation condition, propagation and their characteristics [56].

In 1978, A. H. Sharbaugh, J. C. Devins and S. J. Rzad studied the pre-breakdown mechanism in liquids using a point-plane electrode system. According to their finding, collision ionization occurs in gas or liquid phase prior to the breakdown [57]. In 1982, they studied the velocities of positive streamers in liquids and over solid/liquid interfaces using the same point-plane electrode system. They identified that the velocities do not depend on the instantaneous value of the applied voltage, which was believed until then, but on the rate of rise of the voltage. They suggested that there are two scenarios which determine the propagation velocities. One is that the size of the gap and the rate of rise of the voltage directly affect the velocities of positive streamers. In the other scenario, the velocities are gap independent and rate of rise slightly affects it. The rate of rise and the ionization process decide to which scenario the considered electrode geometry belongs. However, there was a third case where velocities increase exponentially with the applied voltage [58]. S. Ohgaki and Y. Tsunoda investigated the characteristics of positive creeping discharges propagating over acrylic sheets immersed in liquid paraffin, applying negative impulse voltage to the ground electrode of the point-plane electrode system. They observed the tip velocity and the potential are constant with impulse voltage in its rising portion. Based on their observation, a model was proposed in 1994 [59]. In 1993, P. Atten and A. Saker studied fractal characteristics of creping discharges such as final length, mean radius, charge produced., propagating over glass sheets immersed in mineral oil [60]. In 2002, R. Hanaoka et al. investigated the effect of grounded side electrode and surface charging of solid mate-

rial on the creeping discharge characteristics with impulse voltages using three types of sample materials which were immersed in transformer oil. In both positive and negative streamers, the effect of the grounded side electrode on the relationship between the discharge length and the voltage was prominent. They showed the potential gradient of the streamers does not depend on the applied voltage [61].

The research was further extended to analyse the effect of a few factors such as the type of applied voltage, type of insulating material and gas pressure on creeping discharge development. In 2002, A. Beroual and N.K. Bedoui studied the characteristics of creeping discharges propagating over three different samples of solid insulations under AC and DC voltages. Different shapes of discharges for the same experimental conditions were observed indicating the different mode of propagations. They observed that hydrostatic pressure has an effect over the final length, the number of branches and the light emitted. It was also shown that discharge initiating voltage is higher with AC voltage than DC voltages [62]. They further studied the influence of the physiochemical properties such as the geometry of the solid samples over propagation characteristics [63].

In 2005, L. Kebbabi and A. Beroual investigated the characteristics of creeping discharges propagating over three solid materials samples immersed in mineral oil under negative impulse voltages. It was observed that streamers propagate radially and density of branches increases with the increase of sample thickness [64]. Later in 2006, they used optical and electrical investigation to analyse characteristics of creeping discharges under impulse voltages of both polarities. They observed the space charge density depending on the polarity of the applied voltage has an effect over the shape of the discharge pattern and its radial discharge density [1]. In 2008, they studied the effect of the hydrostatic pressure over the discharge length of creeping discharges over three types of material samples under lighting impulse voltages. It was observed that the pressure has an effect on the relationship between final discharge length and the applied voltage irrespective of the polarity of the impulse voltage [65]. Further studies were carried out by them to investigate the capacitive effect of material samples over

creeping discharge propagation under negative impulse voltages. The effect was studied through the permittivity and the thickness of used materials [66]. In 2009, They used a partial discharge detector connected to point-plane electrode system to study the influence of voltage and the kind of material sample on the number of discharge events and their locations on one voltage cycle. It was observed that the voltage affects the total number of discharges recorded during 500 cycles of voltages and the maximum value of apparent electrical charge. On the other hand, the number of discharges corresponding to the negative discharge was higher than that of positive ones irrespective of the sample and the applied voltage [67]. In 2010, A. Beroual et al. studied the development of creeping discharges over solid/gas interfaces under lightning impulse waveforms. Material samples were made of epoxy resin and three types of gases (SF_6, N_2,CO_2) and $SF_6 - CO_2$ mixtures were considered. Discharge lengths corresponding to SF6 gas is shorter than that corresponding to CO_2 and N_2 irrespective of the polarity of the applied voltage. On the other hand, the addition of a small amount of SF_6 into CO_2 or N_2 had reduced the discharge lengths and hence improve the dielectric strength of the composite insulating system [68].

Recently, studies were further extended to analyse the amount of tree formation with alternative insulators such as vegetable oil and nano-composite materials. Viet-Hung Dang and A. Beroual investigated the fractal characteristics of discharge patterns propagating over pressboard immersed in rape-seed oil and mineral oil under lighting impulse waveforms. They observed that creeping discharges in mineral oil are more branched than in rape-seed oil. However, discharge lengths corresponding to mineral oil were shorter than that corresponding to vegetable oil [69]. They further investigated the currents associated with the discharges. It was observed main discharge was followed by a secondary discharge of which current had the opposite polarity of the main discharge. It was due to the electric field distortion by deposited space charges as the pattern propagated [70]. In 2013, Saeed Zohdi et al. investigated the creeping discharge activity over the hardwood timbers under both AC and DC voltages. They showed that the negative discharges make the timber breakdown prior to the breakdown with AC voltages. At the same time, they studied the capacitive effect on the

breakdown time [71]. In 2014, Y. Z. Lv et al, studied the creeping discharge propagation over the mineral oil/press-board interfaces and nanofluid/press board interfaces. They showed that the TiO_2 nano partial can improve both partial discharge inception voltage and reduce the tendency of creeping discharges to propagate up to the flashover point [72]. In the same year, Fares Sadaoui and Abderrahmane Beroual investigated the characteristics of creeping discharges propagating over three different material samples named Bakelite, glass and epoxy resin immersed in gas and gas mixtures under AC voltage. It was observed discharge lengths corresponding to glass and Bakelite are slightly longer than that corresponded to epoxy resin [73]. In 2015, M.A. Douar et al., investigated the influence of perpendicular and parallel electric fields over the creeping discharges propagation over thermoplastic and one-cycloaliphatic filled epoxy resin material samples under lighting impulse voltages. It was observed that the parallel electric field makes the propagation of the discharge stop considerably for all materials compared with the perpendicular electric fields [74]. In 2016, Yuzhen Lv et al. studied the characteristics of creeping discharges over the TiO_2 nanofluid impregnated pressboards under AC voltages. Nanofluid had reduced the permittivity mismatch between the oil and pressboard. Therefore, nano fluid made a higher resistance for creeping discharges to propagate than that of pure oil-impregnated press board [75]. In the same year, X. Zhou et al, investigated the creeping discharge activity on differently aged press board samples immersed in mineral oil under AC voltages. They observed two different discharge patterns as chronic creeping discharge and acute creeping discharge which occurred due to massivelyaged press board samples. They showed that chronic discharges occur in the liquid phase and the pattern cannot propagate up to flash over rapidly. However, multiple discharge mechanisms were involved in the propagation of acute creeping discharges [76]. In 2017, A. Beroual and F. Sadaoui analyzed the partial discharge activity occurred during the creeping discharge propagation over glass material samples immersed different types of gases and gas mixtures under AC voltages. Maximum charge amount produced by positive discharges is higher than that of produced by negative charges irrespective of the type of gas and its pressure [77]. Takeshi Nishikawa et al, studied the behaviour of creeping discharges propagating over press-

board samples immersed in three types of vegetable oils under rectangular impulse voltages. They compared characteristics such as discharge shape, discharge current and the light emitted, which depended on the pulse width and the voltage, with those corresponding to mineral oil [78].

2.3 Numerical Models

Creeping discharges over the surface of insulating materials occur via complicated tree-like patterns. It is important to use mathematical models to simulate the growth of these fractal structures, in order to aid the analysis of experimental creeping discharge patterns, and to provide a theoretical foundation to describe the tortuous nature of creeping discharges and their development.

Sawada et al. used a stochastic model to explain the branch formation of discharge patterns [79]. In their point of view, there is a probability which decides the number of side branches to be born. They tried to simulate discharge patterns by assigning a factor to the tip of the growing pattern. The factor was called as tip priority factor R which define the probability of the main branch to grow further to the probability of a new side branch to be born. This factor could make a significant effect on pattern formation and its shape as a non-equilibrium parameter. The program adopted to simulate the model in a 2d computer simulation as follows:

1. +1 is assigned to the areas with traces of the streamers of already growth discharge pattern, and -1 is assigned to the area surrounding the streamers of the pattern. Remaining sites get the value of -1.

2. Randomly one of the point with a value of -1 is selected and it is linked to the main pattern. Then the areas surrounding the newly formed streamer parts are changed to -1.

3. The probabilities of new sites to be linked to the main pattern are decided by tip

priority factor in the simulation.

It was observed that the pattern become equivalent to the Eden model without the tip priority factor. Three of the patterns that they obtained according to the algorithm are showing in Figure 2.2. The network of one-dimensional lines has made the pattern in two-dimensional space. However, the model cannot explain the physical meaning of actual discharge patterns because the algorithm has neglected the effect of the local electric field at the tip of the discharge pattern so that patterns do not resemble the experimental discharge patterns in shape.

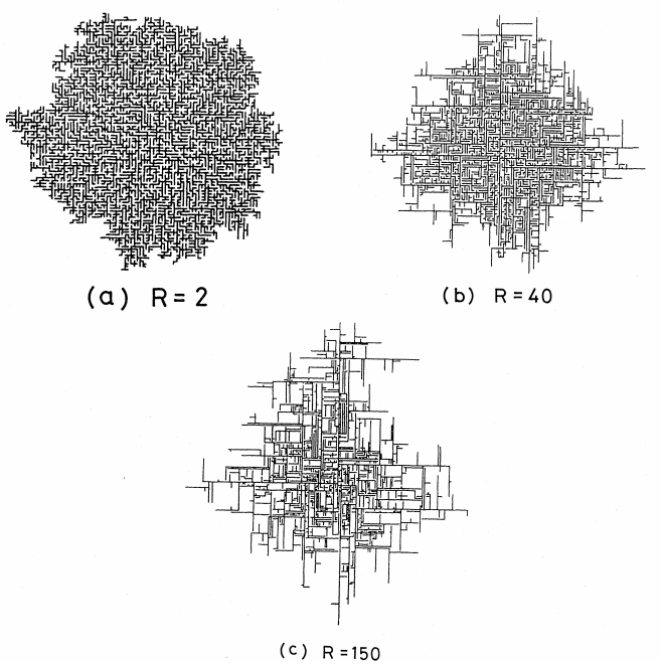

Figure 2.2: Examples of random patterns produced by computer simulations.Tip priority factors are (a) R=2,(b)R=40, and (c)R=150 [79]

In 1984, Niemeyer at el. elaborated the dielectric breakdown model which is also a stochastic model, to explain the point-plane electrode system based experimental surface discharge patterns in compressed SF_6 gas [35]. The algorithm considered the local electric field as the only factor that affects the pattern propagation and computer simulations were carried out in 2-dimensional space. They used a square lattice grid for 2D computer simulations. Centre point of the lattice grid represented one electrode

and other electrode was considered as a circular boundary at a sufficient distance. The algorithm they adopted can be listed as follows.

1. The pattern is shown by the black coloured dots which are connected by lines. At the starting moment, all the grid points except the points which make the boundary and the centre have the potential of zero. Potentials of the centre point and the boundary are one and zero respectively.

2. The growth of the pattern occurs in a stepwise manner in a Laplacian field. Each site having the capability to be linked to the main pattern is indicated by dashed bonds.

3. Then they are subjected to an electric field weighed probability distribution function in which there is a power-law dependence with exponent η to describe the relationship between local field and the probability and one of the points is linked to the main pattern. Later the voltage of the newly link dot is changed to zero. The procedure continues until the pattern touches the boundary.

Without the effect of the probability density function, simulated patterns resembled what was given by the Sawada model. A computer-generated pattern of about 5000 steps based on the rule is shown in figure 2.3. 2-dimensional lines simply connect the grid points without making any crossing points. The simulated patterns obtain by DBM model had the characteristics of the experimental discharge patterns and resembled their shape.

The model proposed by Niemeyer at el. was further studied by Mcleod et al. in ‘1985 [80] and S. Satpathy in 1986 [81]. Mcloed et al. observed the effect of the polarity of the point electrode on the shape of propagating pattern over polyethylene material samples. The patterns had highly ramified branches. however, the streamers tended to propagate toward the ground electrode with a minimum number of side branches with a positive point electrode. Then they tried to carry out simulations to create the patterns to have the same shape as experimental patterns based on the assumption adopted

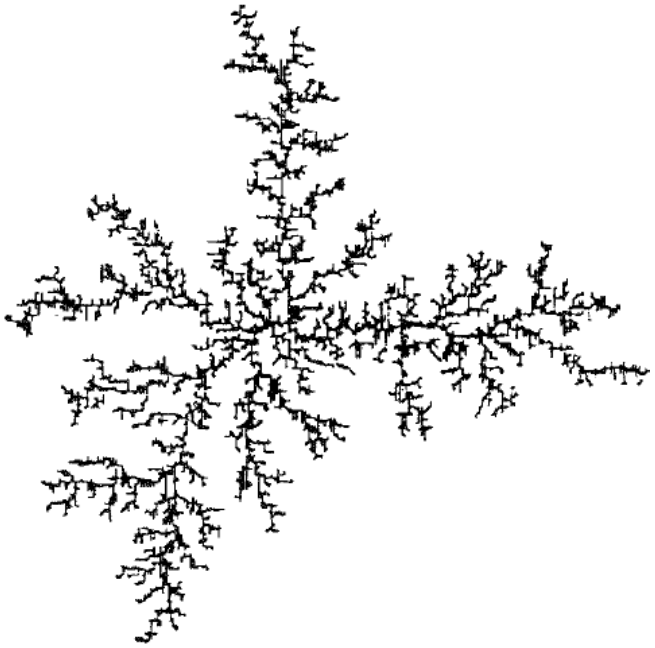

Figure 2.3: Example of computer-generated discharge pattern [35]

in [35]. However, in their case they considered the point electrode to be above the ground plane and varied the exponent η in [35] from 0.5 to 1.5. Figure 2.4a illustrates the propagating pattern when the value of exponent η was 0.5. With a weak electric field dependence on the probability of side branch formation, the growing patterns accentuate the stochastic nature of the breakdown and could be considered to resemble the pattern with negative point electrode. Figure 2.4b illustrates the propagating pattern when the value of η is 1.5. The pattern tends to propagate over the points having the highest local electric field accentuating the deterministic nature of the breakdown and could be considered to resemble the pattern with positive polarity. S. Satpathy tried to extend the dielectric breakdown model(DBM) to simulate 3D-discharge patterns in 3d-laplacian field. The pattern propagation was considered in a cubic lattice inside a spherical surface which made one electrode. The probability of a grid point to be linked to the main pattern was proportional to the local electric field raised to a power η . However, their simulations were limited to integer values of η between one and four. Figure 2.5 shows a pattern obtained by the 3D Laplacian field.

In 1986, H.J Weismann and H.R Zeller generalized DBM model to introduce a break-

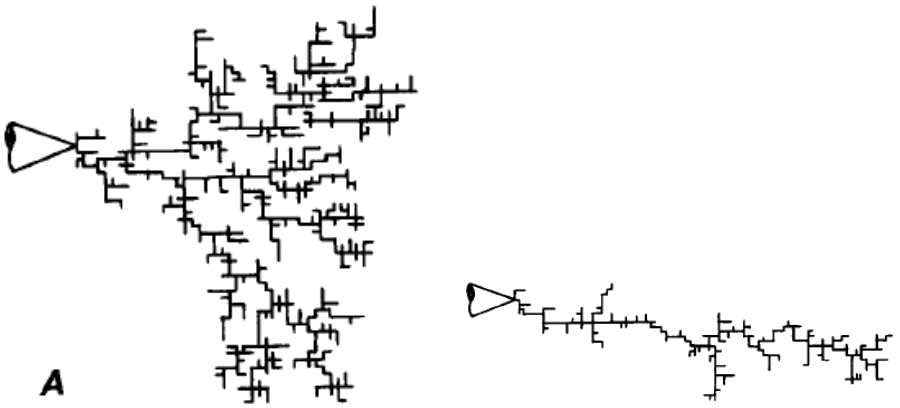

(a) η = 0.5 (b) η =1.5

Figure 2.4: Simulated discharge Pattern [80].

down criterion showing the relationship between stochastic and deterministic aspect of dielectric breakdown [82]. They identified the requirement of the critical electric field F_c for the tip of the propagating patterns to propagate further and considered a potential gradient F_s along the streamer channels. Probability values were assumed to be proportional to the local electric field if the local electric field exceeded critical electric field and else it became zero. Potential of the streamer channels were no longer equal to the potential of the point electrode due to the potential gradient. Figure 2.6 shows a pattern based on the algorithm where the voltage gradient is (5/6) times the critical electric field.

S. Fujimori observed that even though different simulation models had been proposed, none of them was formulated to address the electric breakdown of a particular medium. Therefore, breakdown prevention of them become difficult due to the effect from properties of the medium [83]. With different conditions, actual discharge patterns make various forms. As an example, they observed that voltage pulses can make the pattern to be more tree-shape and clenched fist-like discharge patterns are formed in high pressure SF_6. Therefore, in their work, they concentrated on obtaining pattern information such as geometrical information, instead of understanding the structure of the discharge formation. The proposed model was used to simulate tree shape figures in-

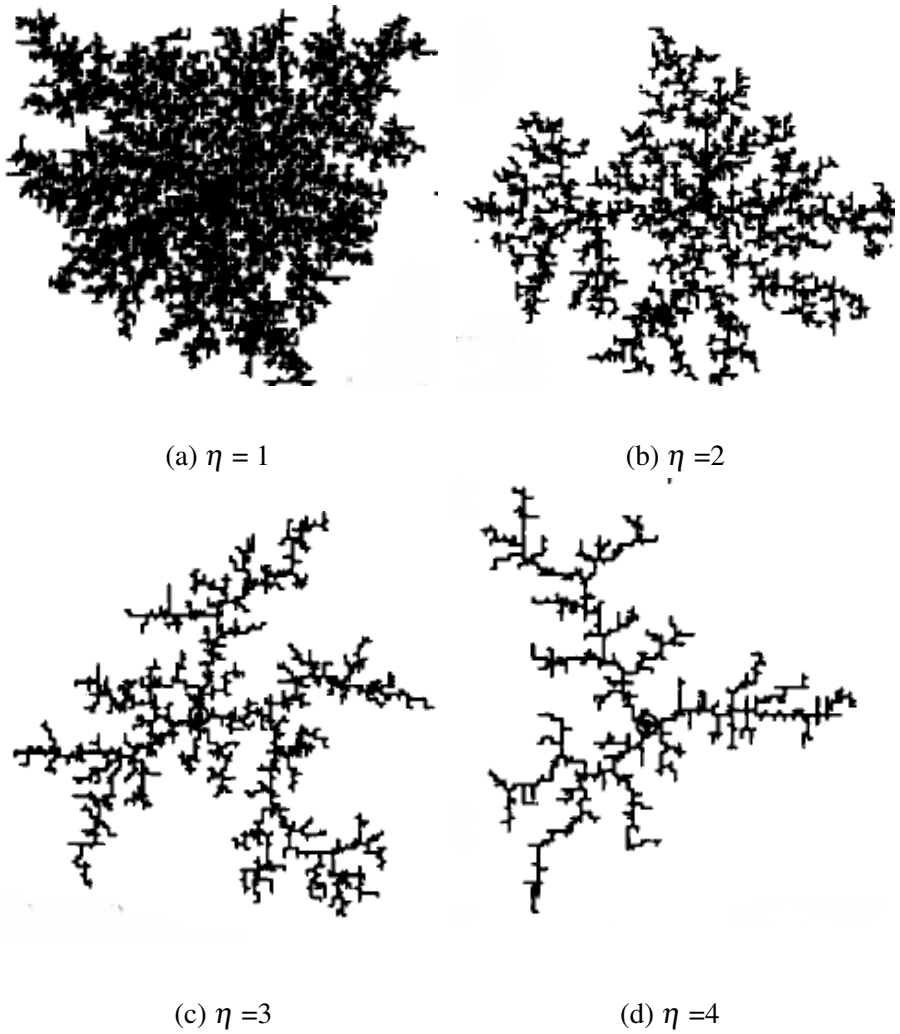

(a) η = 1 (b) η =2

(c) η =3 (d) η =4

Figure 2.5: Typical discharge patterns for a two-dimensional dielectric breakdown under three-dimensional Laplace field [81].

side a point-plane electrode system with a gap distance of 700 and a rotational elliptical coordinate system was considered to calculate the potential of grid points.

In 1990, K. Kudo and S. Maruyama adopted a model to simulate tree-like and bush-like patterns [84]. A two-dimensional square lattice grid was used, in which the origin represented the tip of the point electrode and the ground electrode was modelled as a line at a sufficient distance. The algorithm starts with a particle at a randomly chosen point on a circle of which centre is the origin. The particle is subjected to a random walk until it reaches the origin and then it becomes a part of the growing pattern. This procedure continues until the pattern becomes significantly large. The rule on the

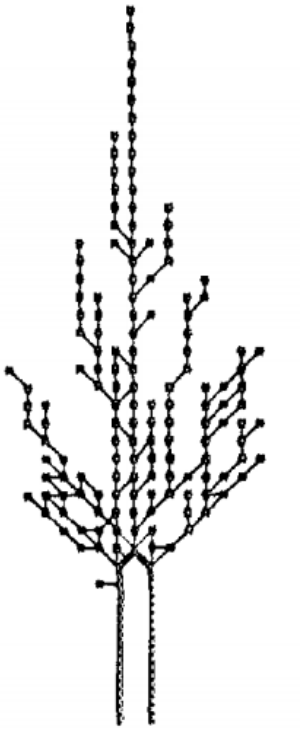

Figure 2.6: Example of a discharge structure with an internal electric field [82].

random walker becomes somewhat different for ball-like tree formation. Figure 2.7a shows an example of a tree produced by the adopted model with the origin is chosen as the tip of the growing pattern. Same model was used to simulate bush like and ball like trees as illustrated in figure2.7b and 2.7c respectively. However, it could not explain the physical meaning of the parameter used in the model.

In 1996, T. Czaszejko tried to adopt a random walk model to explain the propagation of a water tree in 3 dimensions [85]. Simulations were carried out inside a 3-D cube. The tip of the point electrode was placed in the middle of the cube and the bottom surface of the cube represented the ground electrode. A random seed initiated from the tip of the point electrode and jumped from one grid point to another at a time until it landed on the propagating pattern. From the point on which the random seed landed, a new branch propagated toward one of the neighbouring nodes. This procedure was continued until the tree pattern became sufficiently large. Figure 2.8 shows an example of a water tree based on a random walk model. However, still, it was not clear whether

(a) Tree-like tree (b) Bush-like tree (c) Ball-like tree

Figure 2.7: Trees produced by random walk simulations [84].

the patterns of water tree had the characteristics of surface discharge patterns and the simulating models adopted for electrical trees could be used for water trees.

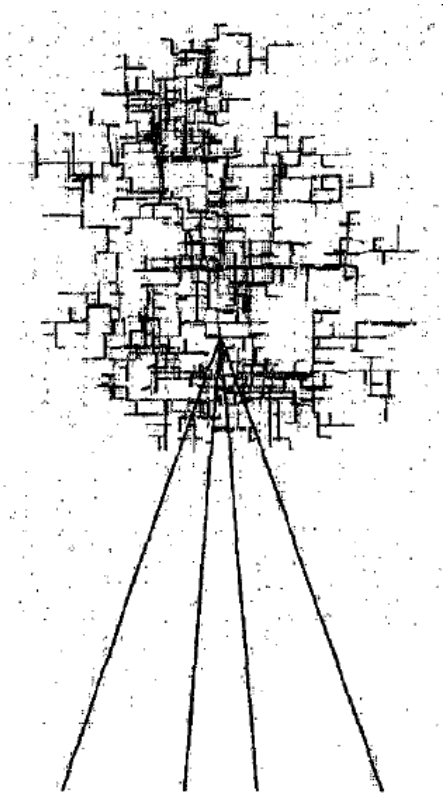

Figure 2.8: Computer simulated tree containing 1500 branches [85].

DBM model produces tree patterns to have the same characteristics of the experimental pattern. DBM model lacks a proper physical justification. This had prompted the requirement of a model based on a quantifiable physical mechanism. In 2000, L A Dissado et al. introduced a discharge avalanche model based on the deterministic properties instead of stochastic properties to explain electrical breakdown mechanism in solids [86]. They considered that the streamer channels are hallowed gas-filled tubes and the electric field created by the discharge produce a local electron avalanche. Space charges would cause the local electric field to fluctuate in time and space so that the damage done by the discharge avalanche also change. Simulations were carried out inside a poison field taking the local electric field fluctuation to be a random variable. Figure 2.9 shows an example of a tree pattern based on discharge avalanche model.

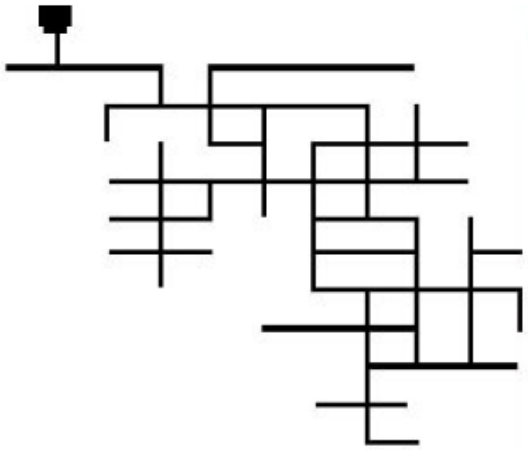

Figure 2.9: Simulated tree pattern based on discharge avalanche model [86].

Exiting proposed models were used for further studies on surface discharges by H. Uehara et al., in 2005 [87] and Dulan Amarasinghe et al. in 2007 [88]. H. Uehara et al. tried to propose a model to include the concept of time into tree simulations. In order to explain the concept in their simulations, two models were used. One model considered that the number of times the random number used in the simulation was generated as the time. Other one depended on the amount of degraded volume due to tree formation. It was observed that the temporal propagation of the simulated discharge is similar to that of experimental discharges patterns. Dulan Amarasinghe et al. studied the effect of cell configuration on the lighting and surface discharges using the model proposed

in [35]. According to the characteristics of discharges given by cross configuration, diagonal configuration and space filling configuration, they concluded that chosen cell configuration has an effect on the fractal characteristics of simulated discharges.

There are no further studies reported about simulation of creeping discharges because studies have gradually progressed into experimental patterns-based researches instead of simulated patterns as none of the models still had been able to account the effect from properties of the medium.

2.4 Fractal Analysis

2.4.1 Fractal Geometry

Most of the objects in nature are irregular and complicated and for the creating of such objects, complex functions are being used in computer graphics. However, it is not possible to describe them by using classical geometry and its figures such as spheres, lines and polygons. Therefore, there should be a method to describe such complicated patterns. In 1918, French mathematician Gaston Julia used a complex function to study its iteration process deeply and introduced a Julia set for which the function does not diverge and the finding made a turning point in the field of fractal geometry. In 1979, Mandelbrot gave a set similar to Julia set and both of them used a complex equation such as $f_c(Z) = Z_n + C$, to generate these sets. Their finding and sets led to a wide area of researches due to their complexity in nature. Until the fractals were discovered in 1970, it had passed through lot of findings such as the Cantor set by George Cantor in 1872, Sierpinski Gasket by Wallow Sierpinski in 1916, Koch Curves by Helge Von Koch in 1904, Levy C curve by Paul Pierre Levy in 1938. Generally, fractals can be categorized into two as regular fractals and random fractals. Structures having an exact copy of each other with different sizes make regular fractals. Koth snowflake shown in figure 2.10 can be considered as an example where small triangles are added to the sides of a large triangle to an infinite degree. Most of the structures in nature can be

considered as random fractals where small-scale structure may differ in detail and this type is the one which influenced Mandelbrot to give the name *'fractus'* in Latin word which means a broken stone with an irregular surface [89, 90].

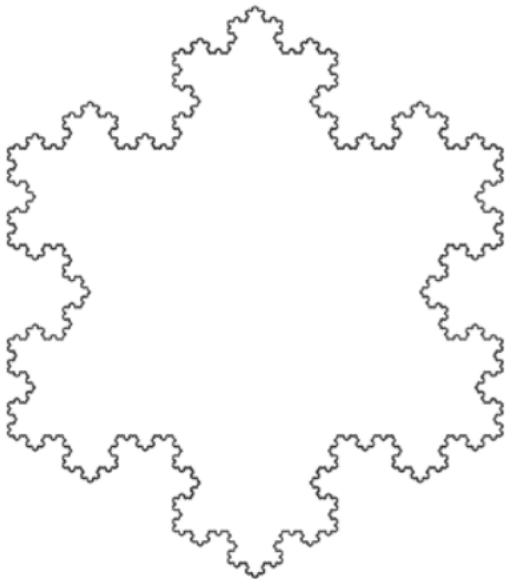

Figure 2.10: Koch Snowflake

2.4.1.1 Properties of fractals

Even if fractal structures are magnified, it will make the same complicated figure with the infinite amount of details. Basically, fractals have four main properties [89].

1. Self-similarity.
2. Fractional dimension.
3. Fractals are non-differentiable.
4. Fractal has infinite length, yet they enclose the finite area.

The main characteristic of every fractal is self-similar nature. Upon magnification of the fractal pattern, it is possible to find out parts which look like the whole pattern.

Every little leaf of the fern leaf shown in figure 2.11 has the same shape as the whole fern leaf. Even if the small leaf is magnified again, the result is the same. So, it makes the perfect selfsimilarity. However, if the structure is not perfectly self-similar, it is called approximate self-similar.

Figure 2.11: Fern leaf

2.4.2 Fractal Behaviour of Creeping Discharges

Horton and Strahler studied the shape of the bifurcation system of streams of a river and proposed the Horton law concerning the order of them. Order of the source stream is one. Two first order streams meet at a point and make a second order stream. when two second-order stream have joined each other, a third order stream is formed. Likewise, two streams having two equal orders make a streamer with one order higher. If the joining streams have unequal orders, then newly form stream gets the order of higher order stream. Figure 2.12 shows a bifurcation system of streams of a river where the highest order is six. Horton law satisfies the power law equation given by [91].

$$N_k = R_b^{x-k} \tag{2.1}$$

Where N_k is the number of streams of order k, R_k is the bifurcation ratio, and x is the highest order within the stream network. wherever the law is applicable to, the plot of log N_k Vs. Log R_b becomes a straight line [91].

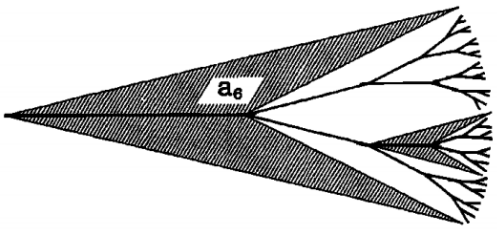

Figure 2.12: Diagram of a Horton system [91].

In 1982, Mandelbrot had shown that stream system shows the fractal characteristics and estimated its dimension. In 1998, Katsutoshi Kudo studied the adoption of the branching structure of the discharges to the Hortons law. Electrical tree formation was studied using the samples of polymethyl-methacrylate and polycarbonate under a point-plane electrode system for impulse voltage. A microscope was used to extract the pattern and it was drawn in a two-dimensional geometry. Figure 2.13 shows the relation between the logarithm of number of branches and the branch order in PMMA. The curve has become a straight line confirming that experimental tree patterns follow the Horton law. They used computer simulation to develop patterns of electrical tree formation and observed that simulated patterns also followed the Hortons law. Therefore, it was concluded that the branching structure of both experimental and simulated the discharges are related to static and random properties showing fractal properties [92].

2.4.3 Fractal Analysis Methods

2.4.3.1 Fractal dimension

Dimension identifies the way the object feels the space. Dimensions of a point, a line, a square and a cube are 0, 1, 2 and 3 respectively. Such dimensions are called Euclidian

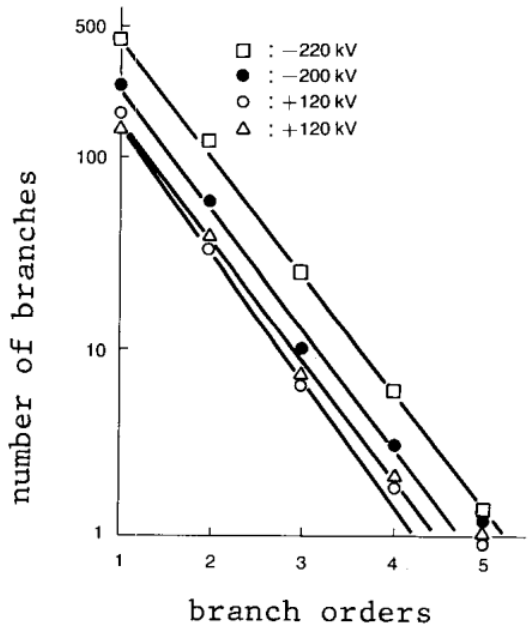

Figure 2.13: Relationship between the number of branches and the branch orders for PMMA [92].

dimension. Likewise, fractals have fractal dimensions.

2.4.3.2 Final discharge length

When it comes to creeping discharges, the discharge may have several main streamers starting from its starting point. Then there may be side branches starting from main streamers. Discharge morphology depends on different factors such as electric field distribution. As an example, under mineral oil, negative streamers tend to propagate radially while positive streamers are more concentrated around its initiation point with more ramified branches having different discharge lengths [1]. Therefore, each streamer may have different total discharge lengths. what we define as the final discharge length is the maximum discharge length out of all the streamers that the pattern has and it assesses the voltage required to get a discharge of a particular length.

2.4.3.3 Radial discharge length

Once a creeping discharge initiate, it can propagate up to the flashover point depending on the electric field distribution. Number of streamers propagating toward the boundary and their length may depend on several factors such as the structure of the solid insulator. When it comes to the experimental investigation based on point-plane electrode geometry, what identifies the flashover is the moment a streamer touches the plane electrode via the edge of the solid material as it makes a conduction path between two electrodes. what we define as radial discharge length is the maximum radial extension that the discharge pattern makes from its initiation point. It can assess the voltage required for the flashover.

2.4.4 Fractal Dimension Estimation Methods

2.4.4.1 Similarity method

When a line is magnified by a factor of 2, it will result in 2 identical line segments. Likewise, upon the magnification of a square and a cube by the same factor, the results will be identical 4 squares and identical 8 cubes respectively. Equation 2.2 can be used to find out the dimension of the fractal pattern.

$$D = \frac{\log N}{\log e} \tag{2.2}$$

Where e, D, N are the magnification, number of identical shapes and the dimension, respectively.

To Calculate dimensions, take a look at the fractal, called the Koch Snowflake shown in figure 2.14. The idea behind calculating the fractal dimension is that every part of the snowflake has the same dimension as the whole pattern. As an example, any piece of a square has the dimension of 2. Therefore, if it is possible to find out the dimension of a

segment which builds the snowflake, then snowflake has the same dimension. Middle third of each line of the triangle is replaced by two lines with a rotation of 60 degrees and those two lines have the same length as the removed line part of the triangle as shown in figure 2.15. Thus, it is cleared that four identical line have been formed due to this transformation and each part is one-third of the original. Therefore, it can be concluded that each line has made four similar copies having a scaling factor of 3. So, the dimension of the snowflake turns to be, [89]

$$D = \frac{\log 4}{\log 3} = 1.2618$$

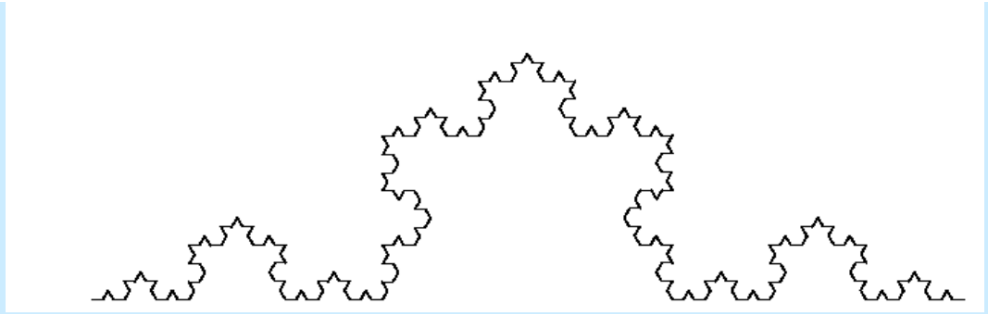

Figure 2.14: Koch Curve

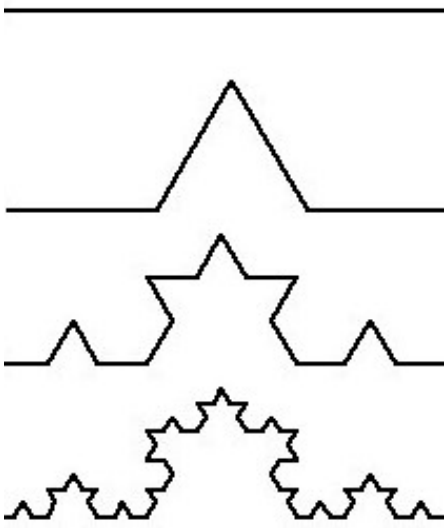

Figure 2.15: Koch Curve

2.4.4.2 Changing coarse-graining level

This method is one of the common method used to calculate the dimension of fractal patterns and often called as box counting method. The idea behind box counting goes back to the 1980 and the method had been called using different names such as capacity dimension, kolmogorov entropy and entropy dimension [93]. A most common basic shape such as a circle or square is used to cover the figure completely in which fractal pattern exists. Then the number of boxes that cover the fractal pattern is counted. The relationship between the number of covering boxes N(r)and the box side length r to determine the fractal dimension D_f is given by [91]

$$N(r) \sim r^{-D_f} \tag{2.3}$$

To find out the dimension the logarithm of N(r) is plotted against the logarithm of the box side length. If the pattern holds the fractal characteristics, then the resultant curve should be a straight line and the slope of the curve gives the fractal dimension [91,94].

2.4.4.3 Fractal measure relation

This method can be implemented by different techniques.

- Total length of the streamers L inside a circular area of the fractal pattern is measured. The relationship between L and the radius of the circular domain R to calculate the fractal dimension D is given by [94],

$$L(r) \sim R^D \tag{2.4}$$

- Number of mass points M(r) inside a circle is measured by varying its radius r according to the relationship [91],

$$M(r) \sim r^{D_f} \tag{2.5}$$

where D_f is the fractal dimension.

- If the fractal pattern consists of filamentary branches as in creeping discharges, then the relationship between the number of branches m(r) that cut the circle constructed on the pattern and the radius r is given by [91],

$$m(r) \sim r^{D_f - 1} \tag{2.6}$$

where D_f is the fractal dimension.

2.4.4.4 Correlation function

Fractal dimension can be extracted from correlation integral using different techniques. However, the idea depends on a pairwise distance algorithm. The correlation integral algorithm introduced in 1983 by Grassberger and Procaccia is used to define the correlation dimension for a given dataset [95]. Let $X_1, X_2, X_3, ..X_n$ be the mass points occupied by pattern and r be any positive number. Then correlation integral is given by

$$C(r) = \lim_{x \to \infty} \frac{2}{n(n-1)} \sum_{i=1}^{n} \sum_{j=i+1}^{n} (\left\| x_j - x_i \right) \| \leq r) \tag{2.7}$$

Where I(.) indicates one or zero and $\left\| x_j - x_i \right\|$ donates the distance between data points x_i and x_j.

Therefore, the correlation dimension is given by

$$D = \lim_{r \to 0} \frac{\ln C(r)}{\ln r} \tag{2.8}$$

The slope of the linear part of the curve of logarithm of ln(C(r)) against logarithm of ln(r) gives the fractal dimension D [96].

2.4.5 Studies about Fractal Analysis of Creeping Discharges

2.4.5.1 Simulated patterns

In 1982, Y. Sawada et al. introduced the 2-dimensional stochastic model to simulate the creeping discharge propagation subjected to tip priority factor R. The self-similarity nature of the pattern they discussed, was terminated at a finite scale. To determine the fractal dimension, the lines consisting the patterns were considered to have an infinitesimal width and the minimum number of balls N of diameter η to cover the circumference of the pattern was counted. Fractal dimension was defined as the tangent of the inclination of the line graph shown in figure 2.16. They identified the existence of two dimensions for each pattern [79].

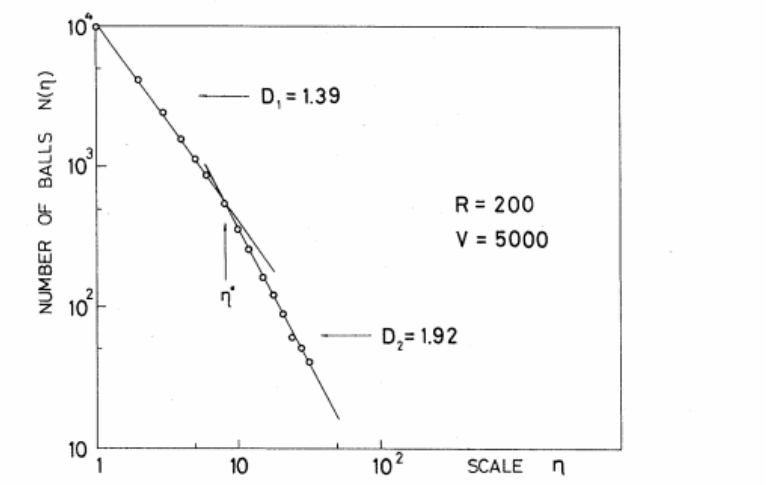

Figure 2.16: Dependence of the ball number N on the diameter of the ball η [79].

In 1984, L. Niemeyer et al showed that the DBM model is able to simulate experimental discharge patterns and their fractal properties were studied in a computer simulation. They constructed a circle of a certain radius and plotted the number of discharge point inside it as a function of the logarithm of the radius. The gradient of the plot

Table 2.1: Dependence of dimension D on the exponent η [35].

η	D
0	2
0.5	1.89±0.01
1	1.75±0.01
2	1.6

gave rise to the dimension. They further studied the effect of the value of exponent η of probability distribution function in [35]. Table 2.1 shows the values they obtained on the exponent. In 1985, R.D. McLeod et al extended the simulation on the DBM model and identified the inverse relationship between the exponent η and the associated fractal dimension [80]. In 1986, 3d-laplacian field was used to simulate the 3D-discharge patterns by S. Satpathy [81]. To determine the associate fractal dimension, he considered the linear potion of the plot of total number of discharge bond enclosed by a sphere of radius. Least square fit provided a fractal dimension of 1.93 for the pattern corresponding to the exponent η of one.

K. Kudo and S. Maruyama studied the regularity of treelike and bush like patterns of two-dimension and three-dimension to find out the associate fractal dimension. Their studies revealed that tree patterns given by their model have fractal properties and fractal dimension depends on the type of patterns [84]. In 2007, Dulan Amarasinghe and Upul Sonnadara used the model proposed by Niemeyer et al. to simulate creeping discharges as well as lightning discharges. They used several methods to estimate the fractal dimensions such as Correlation Function, Sandbox method, Box Counting method. However, they pointed out the value of the dimension depends on the estimation method [88].

2.4.5.2 Experimental patterns

In 1984, S. Ohgaki and Y. Tsunoda investigated the growth characteristics of positive surface discharges propagating over acrylic samples of different thickness values immersed in liquid paraffin. It was observed that final discharge length increases with the

applied voltage for every thickness case [59].

In 1993, P. Atten and A. Saker generated discharge patterns propagating on glass material samples immersed in transformer oil. A linear variation final discharge length and final mean radius were found for both polarities [60].

In 2002, R. Hanaoka et al investigated the fractal properties of the streamers travelling over oil immersed solid material with a grounded side electrode under lightning impulse voltages. Surface charging polarity of the streamers and the position of the side electrode affected the final discharge length. However, the discharge length increased with the applied voltage irrespective of the side electrode and the polarity of the voltage [61].

In 2002, A. Beroual and N.K. Bedoui investigated the influence of the hydrostatic pressure on the final discharge length of creeping discharges under DC and AC voltages. It was observed that discharge length increases quasi-linearly with the applied voltage for whatever the polarity of the voltage and it reduces with the increase in pressure [62]. In 2011, A. Beroual et al. confirmed the same linearity of discharge length of discharge pattern propagating over three type of solid material samples immersed in transformer oil under AC voltage [63, 65, 97].

In 2010, A. Beroual at el. made a fractal analysis on the creeping discharge pattern travelling on epoxy material samples immersed in SF_6, CO_2, N_2 gases and $SF_6 - CO_2$ gas mixtures. Final discharge length corresponds to the SF6 was shorter than that corresponding to CO2 or N2 irrespective of the polarity of the applied voltage. It was observed the electronegative gases reduces the discharge lengths [68]. They extended their studies over polytetrafluoroethylene (PTFE) material samples filled with different kinds of micro-mineral fillers [98].

In 2005 L. Kebbabil and A. Beroual investigated the influence of three type of insulating material and their thickness on the fractal characteristics of creeping discharges under impulse voltages. Fractal dimension calculated by box counting method depended on the nature of the solid material and their thickness. It was observed that when the

thickness decreases, density and the fractal dimension increases. They believed that there is a relationship between the fractal dimension and the physical parameter of the material [64]. In 2006, they studied the effect of the material and their thickness of the considered three materials over the discharge lengths and the radial density of branches using optical observation [1, 66].

In 2011, A. Beroual and Viet-Hung Dang used box counting method to calculate the fractal dimension of creeping discharge patterns propagating over mineral oil and rape-seed oil impregnated press-board samples under lightning impulse voltage. Dimensions corresponding to mineral oil was higher than that corresponding to rape-seed oil. Therefore, it was concluded that it has a relationship between the fractal dimension and the physiochemical parameters of total insulating structure [69]. They showed that final discharge length increases quasi-linearly with the applied voltage and discharge length is greater with the press-board/ rape-seed oil interface than the other case [70].

In 2011, A. Beroual and M-L. Coulibaly investigated discharge propagation on PTFE, glass and epoxy resin immersed in Sulphur hexafluoride(SF_6) under positive impulse voltage. When the gas pressure was increased, stopping lengths, branch densities and associate fractal dimension values decreased [99].

In 2016, A. Beroual analyzed the fractal characteristics of creeping discharges propagating over solid/liquid and solid/gas interfaces under positive DC and impulse voltages, in term of fractal dimension. It was observed that the fractal dimension is higher with lightning impulse voltages than DC voltages [100]. This thesis is focused on classifying insulating materials according to the amount of tree formation on different kinds of solid/liquid interfaces under a divergent electric field. The study is mainly focused on creeping discharges propagating on nano silica-based epoxy composite immersed in insulating oil.

CHAPTER 3

FRACTAL ANALYSIS OF CREEPING DISCHARGE

3.1 Introduction

Creeping discharges propagating over different kind of solid/liquid interfaces has been the focus of many research work in the recent past [71–73, 75]. Identifying the characteristics of these discharges is very useful for design optimizations of HV apparatus. The shape of these discharge consists of radial ramified branches similar to Lichtenberg figures [94]. Fractal geometry has made it possible to classify random patterns similar to creeping discharges [91]. This chapter discusses the methods used in the current study to analyse creeping discharge patterns and their adaption. The chapter also discusses the processing program used to calculate the fractal dimension of the creeping discharges.

3.2 Fractal Dimension

Several methods can be adopted to calculate the fractal dimension of creeping discharges and in this thesis, box counting method is used for the analysis. Researchers in the past have used this method for the analysis purposes of surface discharges in their findings [69, 94, 100].

3.2.1 Box Counting Method

This method determines the number of boxes required to cover a fractal pattern completely. However, the dimension given by box counting method is somewhat lower than that given by other methods such as correlation function and fractal measure relation, because it does not consider the density of fractal points and therefore there is no way to weight the boxes according to the mass of the patterns inside them [101].

The relationship between the number of covering boxes N(l) and the side length(l), determining the fractal dimension D is given by [94],

$$N(l) \sim l^{-D} \tag{3.1}$$

then,

$$D = -\lim_{l \to 0} \frac{\log N(l))}{\log l} \tag{3.2}$$

3.2.2 Processing Program

The original image shown in figure 3.1a is converted into a binary image as illustrated in figure 3.1b using a MATLAB based application. Therefore prior to the conversion process, all the traces of the discharge are extracted using Adobe Photoshop CC software. Then a MATLAB code is applied to the binary image which generates a grid of square boxes over the image. While changing the side length of the boxes at each step, the number of boxes having any parts of the discharge pattern is counted. The developed program is shown in Appendix B. Figure 3.2a and 3.2b show the binary images covered by squares of side length l = 36 pixels and l = 88 pixels, respectively. The slope of the log-log plot of the number of boxes Vs. box size gives the fractal dimension as shown in figure 3.3.

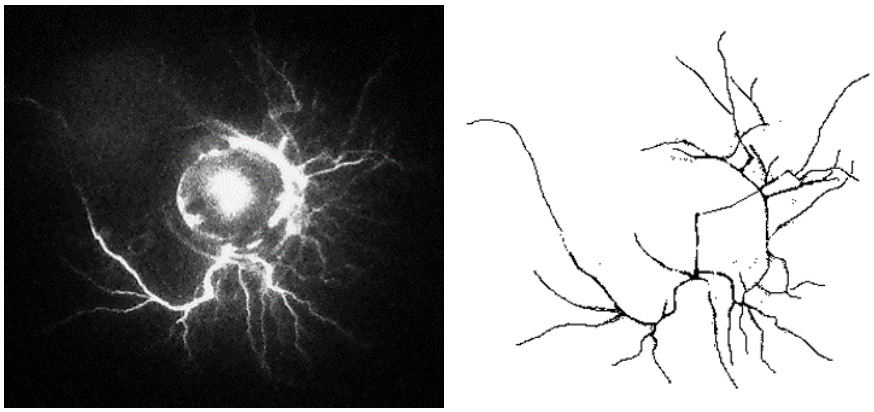

(a) Original image (b) Binary image

Figure 3.1: Application of box counting method

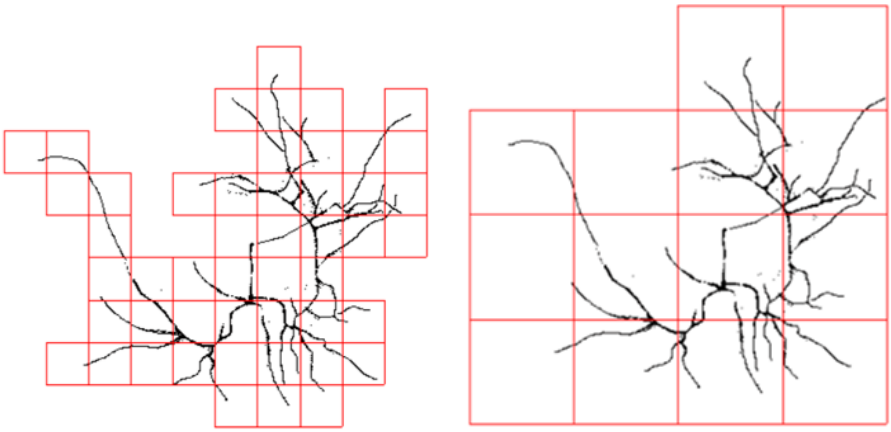

(a) squares of side l = 36 pixels (b) squares of side l = 88 pixels

Figure 3.2: Application of box counting method

3.3 Discharge Length

3.3.1 Radial Discharge Length

A circle is constructed over the binary image taking its centre to be the discharge initiating point, increasing its radius from zero to onward as shown in figure 3.4. The radius of the circle becomes radial discharge length at the moment in which none of the streamers cut the circle.

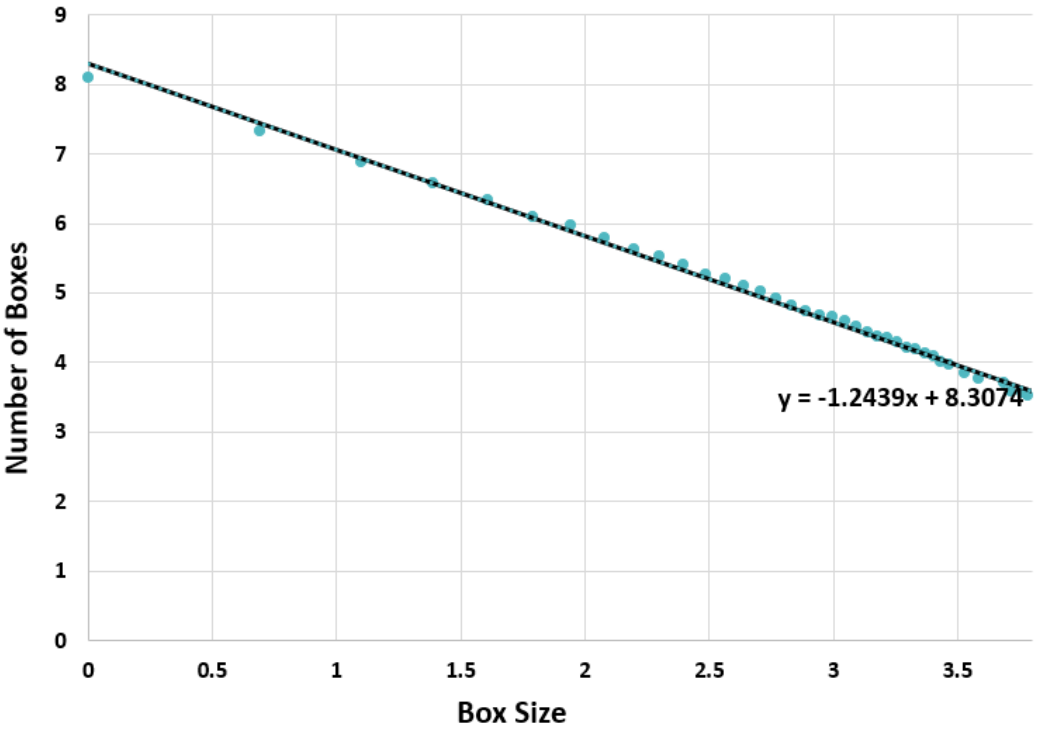

Figure 3.3: Total number of boxes N versus the side length l of the boxes obtained from the analysis of an example of a discharge

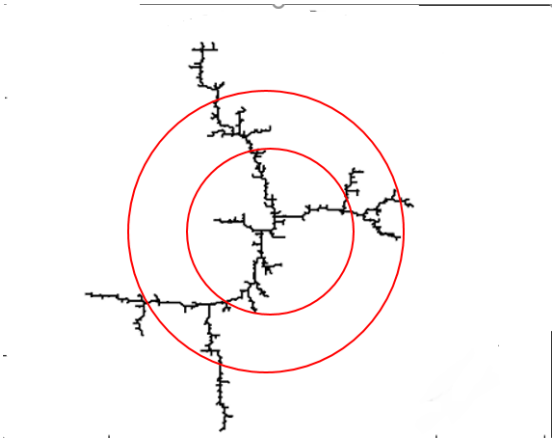

Figure 3.4: Radial discharge length measurement

3.3.2 Final Discharge Length

Creeping discharge pattern may have few main streamers starting from its initial point. Red coloured path in figure 3.5 shows the propagation of one streamer out of all stream-

ers. Discharge length of that streamer is the length of the red coloured path. The maximum discharge length out of all streamers that the pattern has, become final discharge length.

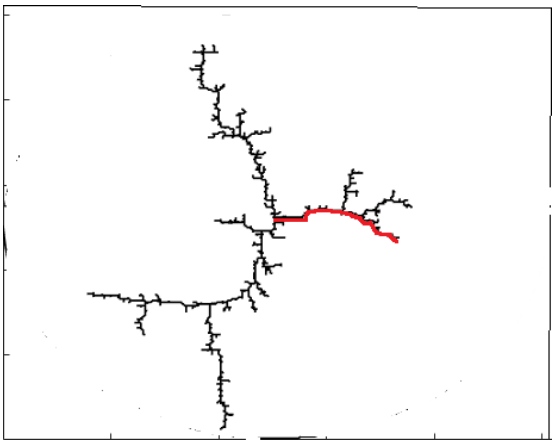

Figure 3.5: Application of final discharge length

3.4 Conclusions

In this chapter, three types of the fractal analysis method are adopted to analyse creeping discharge patterns.

Commercially available software such as MATLAB and Adobe Photoshop are used to extract all the traces of actual creeping discharge pattern which propagate over solid/liquid interfaces, and to convert them into binary images. The developed MATLAB program can implement box counting method on the fractal pattern and generate the variation of the number of boxes with the box size. The curve corresponding to the box counting method become a straight line if the considered pattern holds random characteristics and the gradient gives the fractal dimension. Final discharge length which corresponds to the maximum discharge length of a streamer, is higher than that of radial discharge length which corresponds the maximum radial length of a streamer.

CHAPTER 4

EFFECT OF TYPE OF SOLID MATERIAL ON CREEPING DISCHARGE PROPAGATION

4.1 Introduction

The streamer propagation over solid/liquid insulating interfaces is influenced by the presence of the pressboard and other kind of insulating materials. It has been shown that the kind of solid insulating material and the characteristics of the composite insulation system have a significant impact on the discharge initiation and its propagation [102, 103]. As an example, consider the electric field distribution in a system without a solid insulating barrier as shown in figure 4.1a, where electric field vectors are in the direction of the streamer. However, if there is a solid barrier parallel to the direction to the streamer as in figure 4.1b, electric field vectors are no longer in the same direction and the maximum electric field is towards the insulating surface with a higher value than that without a barrier [104].

This chapter analyses the experimental studies on the propagation patterns of creeping discharges on solid dielectric materials; glass, acyclic, pure epoxy, and nano-composite and their fractal characteristics in a divergent electric field under ac stress. The optical observation is used to study the creeping discharge characteristics from different aspects such as discharge lengths and fractal dimensions.

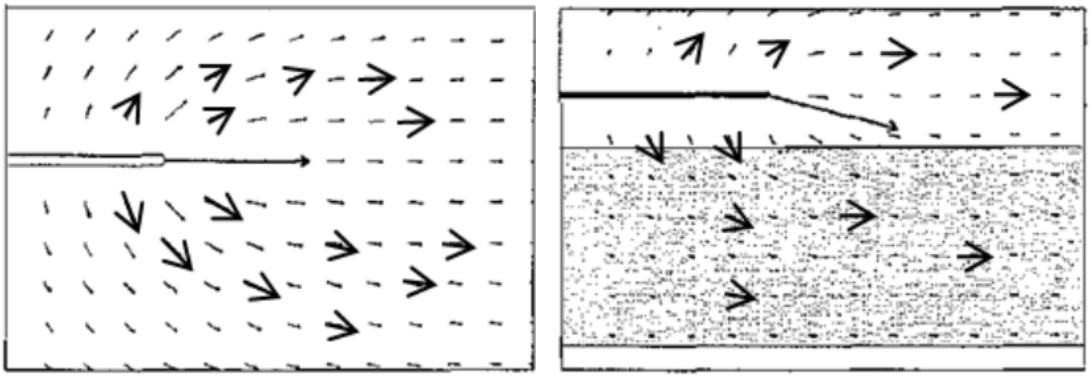

(a) In the air. (b) Along an insulating surface.

Figure 4.1: Vector plots of the electric field distribution for a propagating streamer [104].

4.2 Sample Preparation

Flat square shaped solid material samples of side length 9 cm and 3 mm thick are used for the study. Basically, four kinds of solid materials; glass, acyclic, pure epoxy and silica/epoxy nano-composite are used to analyze the creeping discharge propagation over the solid/liquid interface. A type of copra coconut oil is selected as the dielectric medium. More details about the manufacturing process of coconut oil can be found in chapter 6. Prepared glass and acrylic samples of 3mm thickness are used for the experiment, and epoxy and nano-composite epoxy samples are prepared using the facilities available at the Department of Material Science and Engineering, University of Moratuwa, Sri Lanka. Silica/epoxy samples are prepared to have 1% filler loading. Sample preparation of pure Epoxy and Epoxy Nano-composites are discussed in detail in the next section.

4.2.1 Material Used

4.2.1.1 Host material

Epoxy resin has been selected as the base polymer in the study. There are epoxy resins being used for different purposes such as moulding, coating and paint. The resin category which is used for moulding purpose is called as Cycloaliphatic Epoxy Resins. The epoxy consists of diglycidyl ether of bisphenol-A (DGEBA) type Epon®Resin 828. The curing agent is Modified Cyclo-aliphatic Amine Adduct type 3388. The chemical structure of epoxy is shown in figure 4.2. The considered epoxy type has a lower viscosity compared to other types and commonly used in high voltage industry.

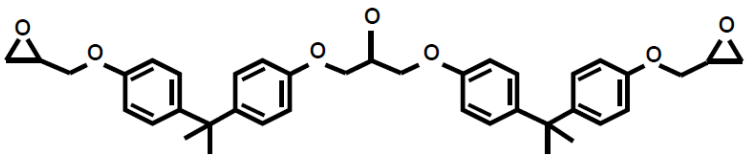

Figure 4.2: Chemical structure of bisphenol-A type epoxy resin

4.2.1.2 Filler material

Several nano-filler materials are being used in industry such as aluminium oxide, silicon dioxide, magnesium oxide and zinc oxide [105, 106]. Effect of silicon dioxide fillers on the properties of epoxy based nano-composites has been the focus of many studies that were carried out recently [107–109]. Silicon dioxide (SiO_2) can be identified as the most common silicon compound. It is resistive to alteration of chemical structure. Therefore, SiO_2 is chosen as the filler material of the epoxy-based nano-composite and the particle size of SiO_2 powder is 50 nm.

4.2.2 Synthesis of Epoxy Samples

In this study, both pure epoxy and nano-composite material samples are synthesized. The fabrication process of nano-composite samples consists of several steps.

- Measuring process of epoxy, hardener and nano-fillers.
- Sonication.
- Ethanol evaporation.
- Mechanical mixing process.
- Curing process.

A block diagram representing the synthesis procedure of nano-composite material is shown in figure 4.3. For this research, samples having silicon dioxide nano compositions (weight to weight) of 1 % are prepared. As the first step, required volumes of epoxy and curing agents are measured using a pipette and measuring cylinders. Sonication is a process used to disperse the agglomerate filler particles in a medium (ethanol). Mechanical mixing process mixes the epoxy and the filler medium making the fillers transfer into the epoxy. Evaporation process removes the ethanol remaining in the mixture. Finally, in the mechanical process, it mixes the medium after curing agent is added to the mixture.

Steps that should be followed in the fabrication process of pure epoxy are listed as follows:

- Measuring process of epoxy, hardener.
- Mechanical mixing process.
- Curing process.

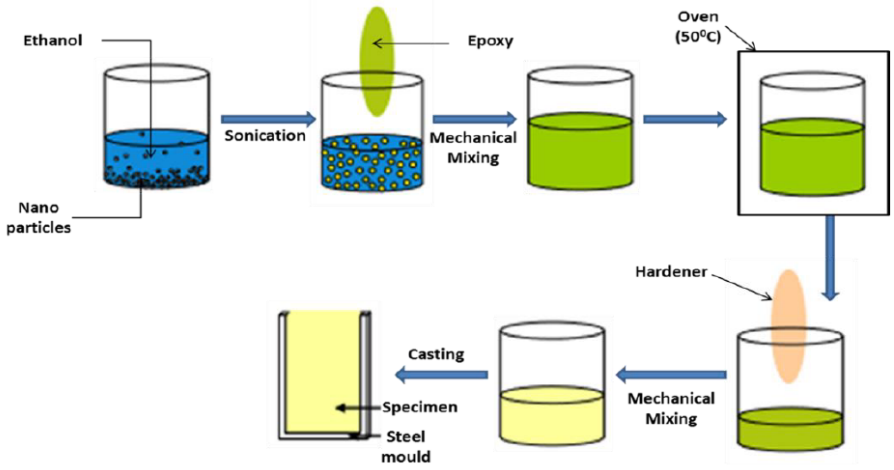

Figure 4.3: Fabrication process of nano composite material [106].

However, the fabrication process of pure epoxy consists of simple mechanical mixing of the measured volumes of epoxy and curing agents.

4.2.2.1 Mould designing

A mould is required for the casting of nano-composite and pure epoxy samples, and it would decide the thickness and the dimensions of the samples. The moulds are prepared with clear flat glass sheets with different thickness according to the requirement of the samples as shown in figure 4.4. The area of the cavity is designed to produce the samples of 9 cm $\times$ 9 cm as they are going to be tested samples for creeping discharge test. Smooth nature of the glass surface helps to eject the samples from the moulds very easily.

4.2.2.2 Measuring process of epoxy, hardener and nano-fillers

As stated in the data-sheets of the suppliers, epoxy resin and the curing agent should be mixed in 3:2 volume ratios. Generally, amount of the nano-fillers are decided based on the weight of nano-filler to the weight of epoxy resin. Required filler mass (m) can be calculated, using the equation 4.1.

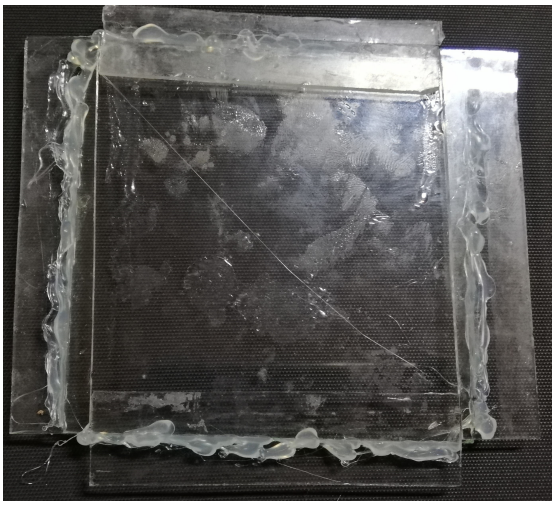

Figure 4.4: Design mould.

$$\frac{m}{m+M} = \frac{w}{100} \tag{4.1}$$

where w and M are filler weight ratio and the weight of the epoxy mass respectively.

$$m = \frac{mw}{100 - wM} \tag{4.2}$$

Figure 4.5 shows the usage of microbalance to measure the weight of epoxy volumes.

4.2.2.3 Dispersion of particles

Any agglomerated particles can be broken into their original form by submerging the measured nano filers inside a medium. Sonication is used to disperse the SiO_2 nanoparticles in ethanol (C_2H_5OH) breaking up existing agglomerates. Methanol or distilled water can be used as an alternative solvent instead of ethanol. Boiling points of methanol, ethanol and water are 64.7 ^{0}C, 78.4 ^{0}C and 100 ^{0}C respectively. Lower boiling point makes the solvent to evaporate more easily in the next step of the synthesis [106]. However, methanol is not environment-friendly like other two solvents. Therefore, ethanol is selected for the study instead of methanol. Ten millilitre volume

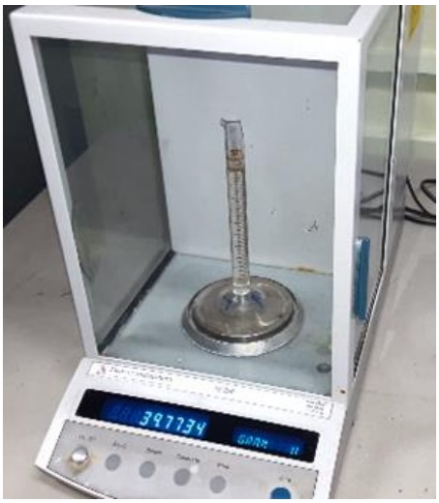

Figure 4.5: Balance for the measurement of epoxy resin weight.

of ethanol and measured nano-fillers are put into a beaker. Then the particles in the medium are manually shaken for few seconds. Afterwards, the beaker is submerged in the ultrasonic water bath for 30 minutes as shown in figure 4.6. The temperature is set to the minimum value that the instrument is capable to control the temperature of the water.

Figure 4.6: Dispersion of nano-particles inside the ultrasonic water bath.

4.2.2.4 Mixing

The measured epoxy resin is added to the ethanol and nano-particle mixture, and mixed well for a period of 20 minutes using a glass rod in order to transfer the nano-particles

into the resin. Ethanol and nano-filler mixture can be mixed with curing agent instead of epoxy resin. However, the properties of the agent might be affected by humidity due to its sensitivity and it can affect the dielectric properties and mechanical properties of the sample [110]. Therefore, the mixing should be carried out with the epoxy. The solution of epoxy resin and nano-filler with ethanol is kept in an air-cooled oven for approximately 2 hours at 50 ^{0}C to evaporate the solvent. Subsequently, the measured curing agent should be added to the mixture and it is stirred using a glass rod for a period of 20 minutes. However, the agent should not be added until the temperature of epoxy and nano-filler mixture come to room temperature because the temperature affects the time taken by the sample to become solidified.

4.2.2.5 Curing Process

A very thin layer of silicone oil must be applied on the surface of the cavity of the mould as it acts as a lubricant and makes it easy to eject the samples from the mounds. Then the mixture can be poured carefully into the mould cavity to minimize the formation of bubbles. After curing final composite inside the cavity for 4 days at room temperature, the sample should be removed from the mould and post-cured around 2 weeks at room temperature. Figures 4.7a and 4.7b show two samples of pure epoxy and 1 % silicon oxide nano-composite respectively.

4.3 Experimental Setup

In the current study, a point-plane electrode system-based test apparatus is adopted in order to initiate creeping discharges and compare their propagating characteristics on different solid/liquid interfaces. Electric fields generated by needle plane electrode systems are usually selected by researchers to experimentally investigate the creeping discharge development where the discharge initiates from the needle tip and the tangential field component drives the propagation as inside actual high voltage appa-

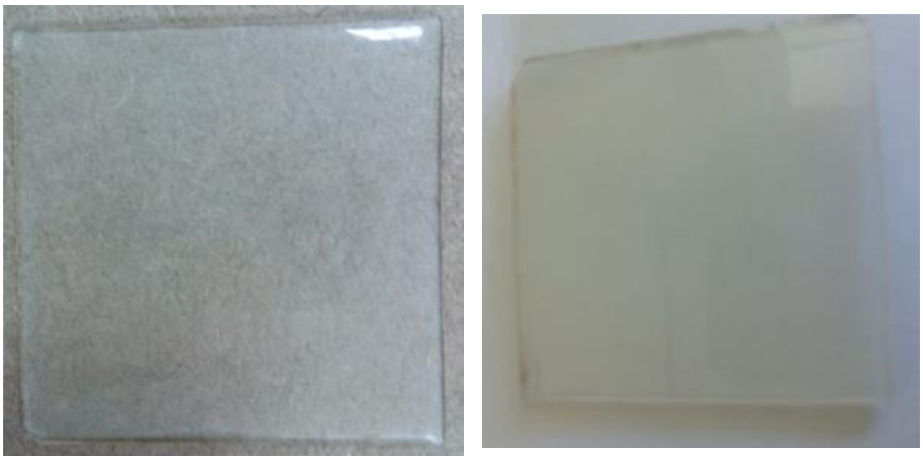

(a) Pure epoxy sample (b) 1% Nano-composite sample

Figure 4.7: Prepared samples

ratus [111–113]. During the manufacturing process of HV apparatus, liquid impurities are minimized using filtering processes. However, the long-time operation may cause the local electric field concentrations due to bubbles, moistures etc. These enhanced fields can initiate a discharge. Once the discharge starts, it tries to propagate in the direction of the uniform electric field and penetrates solid dielectrics. Instead, it may propagate on the solid/liquid interface where the electric field is divergent. This explains why needle-plane electrodes were used to study and compare creeping discharge characteristics.

Figures 4.8 and 4.9 show the schematic view of the test cell, and the actual test apparatus respectively. The test cell consists of a hollow cylindrical core of 100 mm high and 130 mm inner diameter, made of clear acrylic to visualize the discharge, and a square shape brass plate as its lower cover. The test cell is mounted on an apparatus made of wood. The test cell has the point-plane electrode arrangement. The vertical point electrode is held using a movable bearing system so that vertical electrode could be moved vertically, and the lower cover is ground electrode itself. The point electrode made of tungsten has a diameter of 1 mm and the tip of it has a hemispherical end. The field between two electrodes is supposed to be a divergent one. The gap between the two electrodes could be varied from zero to 20 mm. Thin flat insulating material samples

are maintained horizontally between two electrodes. Then samples are immersed in insulating liquid by filling the test cell with an oil. A CCD camera with a high frame rate connected to a high-performance video card is mounted over the test cell and the integrated images taken by it are used for the optical observation of the discharge.

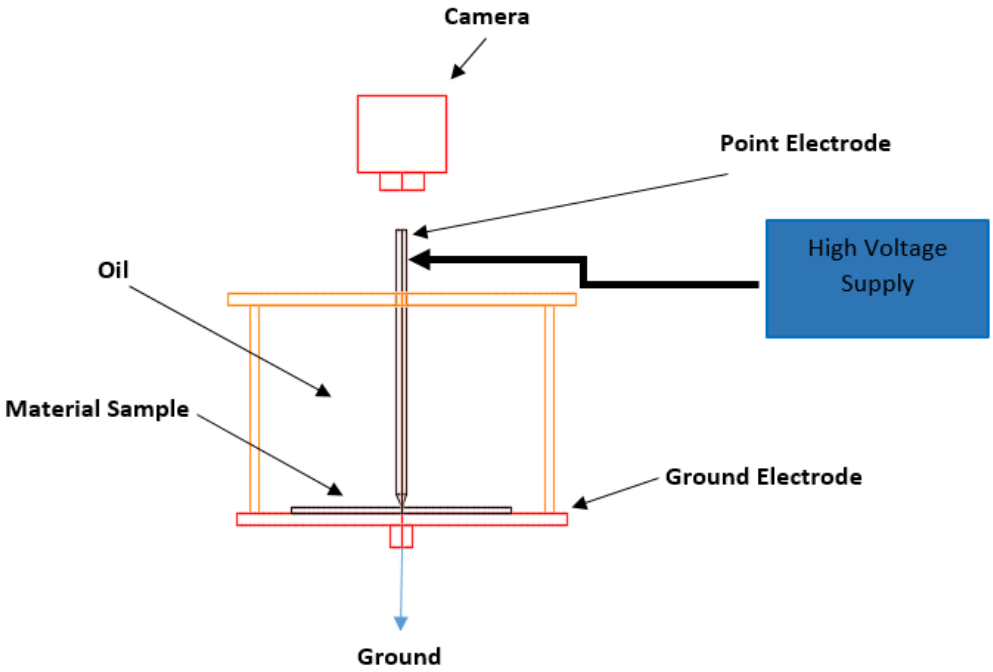

Figure 4.8: Model of the test setup

The plane electrode is grounded and the point electrode is energized by a partial discharge (PD) free HVAC test transformer.

It was observed that with an AC supply, the propagating pattern changes rapidly due to the natural phase reversal of the power supply. With the high-speed CCD camera and the video card connected to it, one can take optical figures very fast at its maximum rate. However, it cannot be predicted at which angle of the AC cycle, their maximum extension occurs because even at zero crossing point there are discharges due to space charge effect [2]. In the study, the pattern which has the maximum extension can be identified using a software after loading all the available photos recorded in 3 seconds for each voltage measurement.

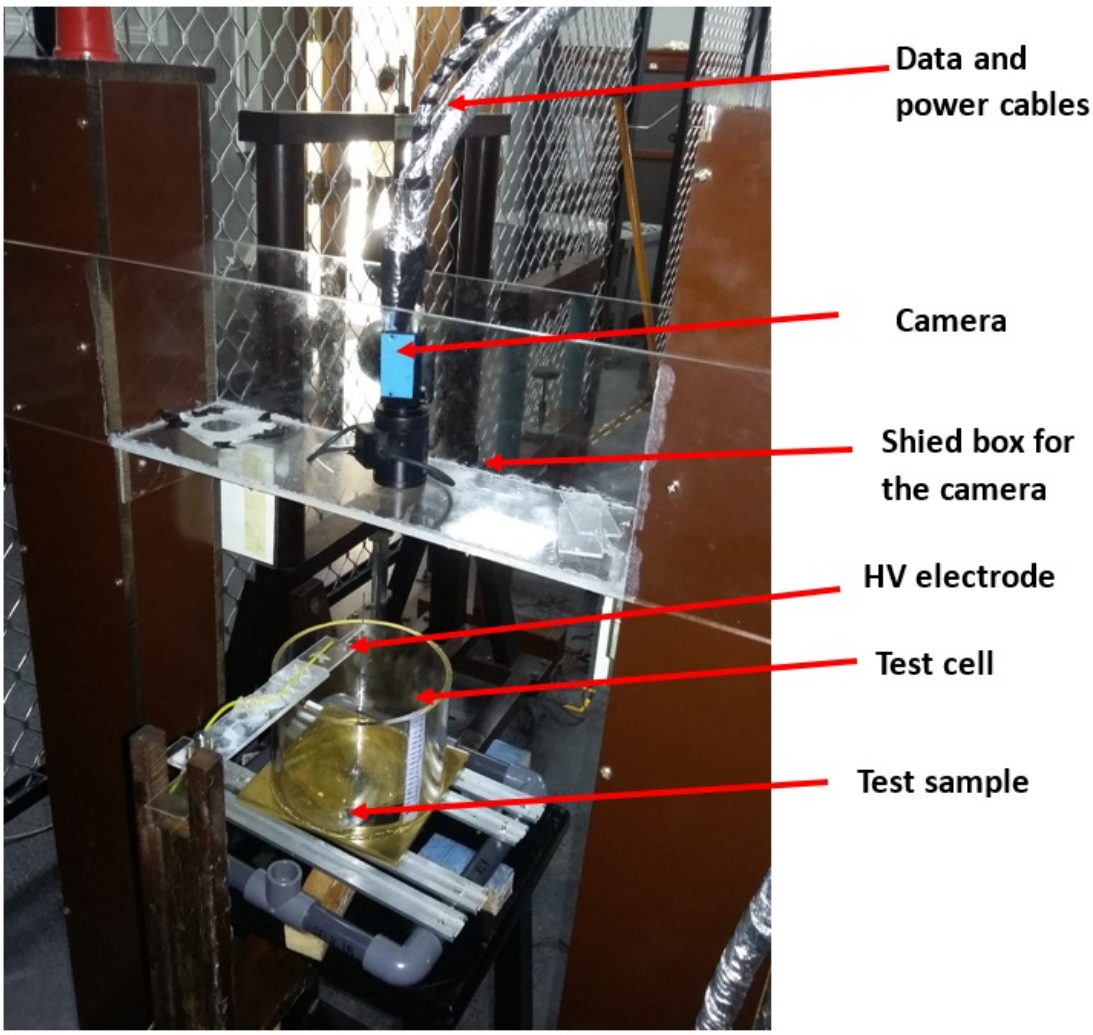

Figure 4.9: Experimental setup

4.4 Procedure

The experimental setup based on a point-plane electrode system is used. The test cell is filled with coconut oil and square shaped material samples discussed in section 4.2 are immersed between two electrodes in such a way, point electrode nearly touch the surface of the samples. If the flash-over or the complete dielectric breakdown is observed, the test cell is filled with new oil in order to maintain the condition of oil used in the experiment. The oil volume is kept constant throughout the testing procedure.

4.5 Results

Creeping discharges under an alternative voltage do not always propagate radially with this point plane arrangement. Electric field distortion by space charges on the insulators is considered to be the main reason for such an orientation [114]. Creeping discharge characteristics such as light intensity, number of main streamers, and branches and amount of ramification, depend on the type of solid material type.

Figures 4.10 - 4.13 show the development of discharge patterns propagating over acyclic, glass, epoxy and nano-composite material samples respectively. Size of the discharge patterns increases when the applied voltage is increased. The thickness and the brightness of the channels reduce along the streamers. The shape of the discharges on glass/oil interface is different than what was observed on other considered interfaces. It accounts for luminosity, number of main streamers and amount of ramification. On this material, it is noted that the patterns have more ramified branches and luminous points. These luminous points have made that streamers cannot be identified separately or defined very well just by naked eye. Other than that, discharge patterns propagating over glass surface tends to propagate radially compared to other cases where curved streamer can be observed. It may due to the electro-hydrodynamic motion of oil in the vicinity of the point. Therefore, streamers try to follow these contours. Patterns propagating over acyclic/oil interface show similar characteristics as the patterns on epoxy /oil interfaces. However, the amount of ramifications is weak and the branches are thinner. Patterns propagating over pure epoxy and nano-composite samples show the characteristics of lightning discharges with a main single streamer. The area of ionization around the tip of the point electrode seems to be higher with epoxy-based materials. The light emitted by the patterns propagating over acyclic and epoxy-based materials are not intensive at the initial stage of development compared to that of glasses. However, as the voltage increases, the amount of ionization seems to exceed that of glass.

Final discharge length and radial discharge length increase quasi-linearly with the volt-

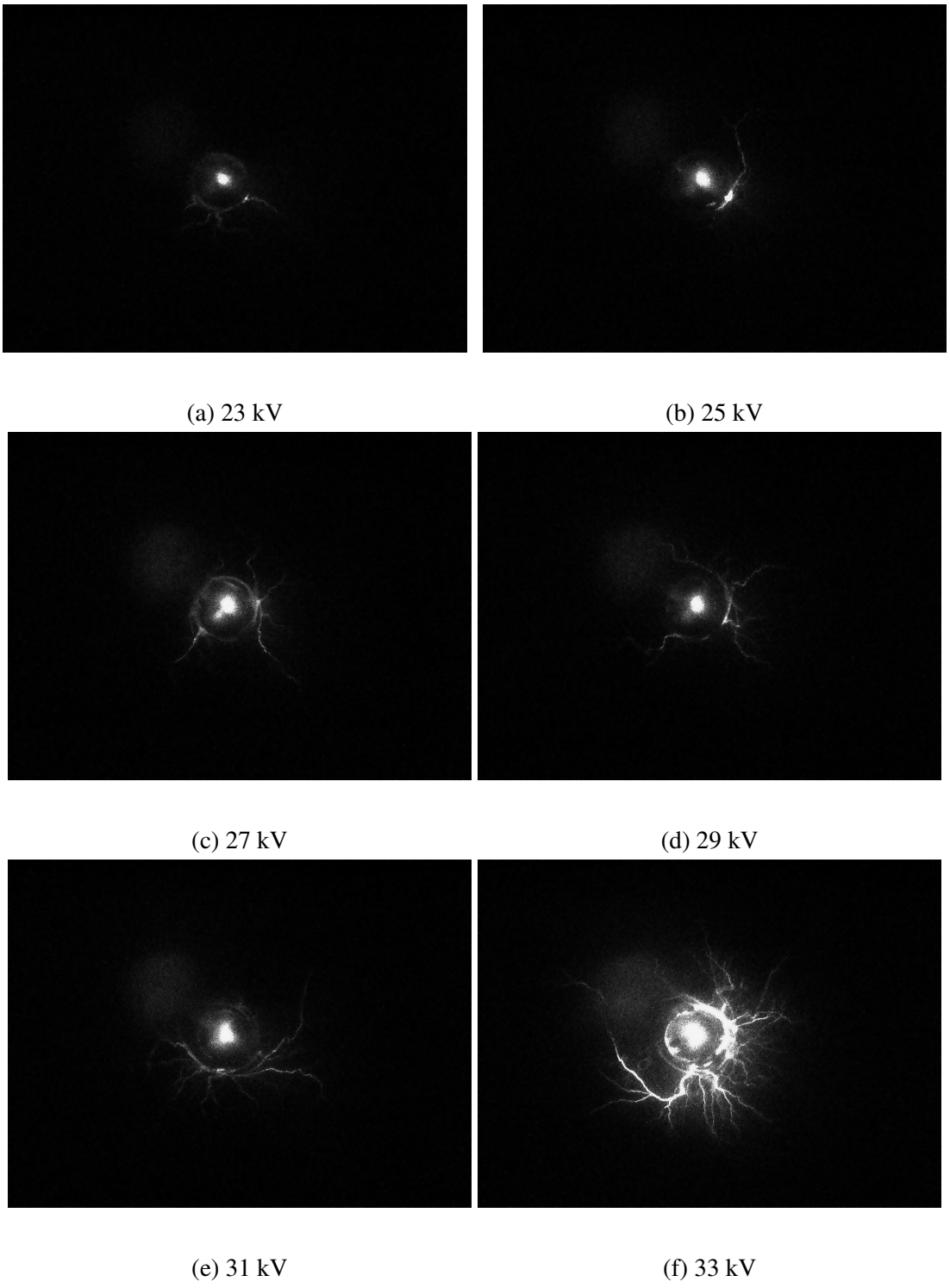

(a) 23 kV (b) 25 kV

(c) 27 kV (d) 29 kV

(e) 31 kV (f) 33 kV

Figure 4.10: Stages of creeping discharge development on an acrylic surface.

age as shown in figures 4.14 and 4.15 respectively. It should be noted that each discharge length value presented in the thesis is an average value measurement taken from four solid dielectric samples. Similar quasi-linearity was stated in other stud-

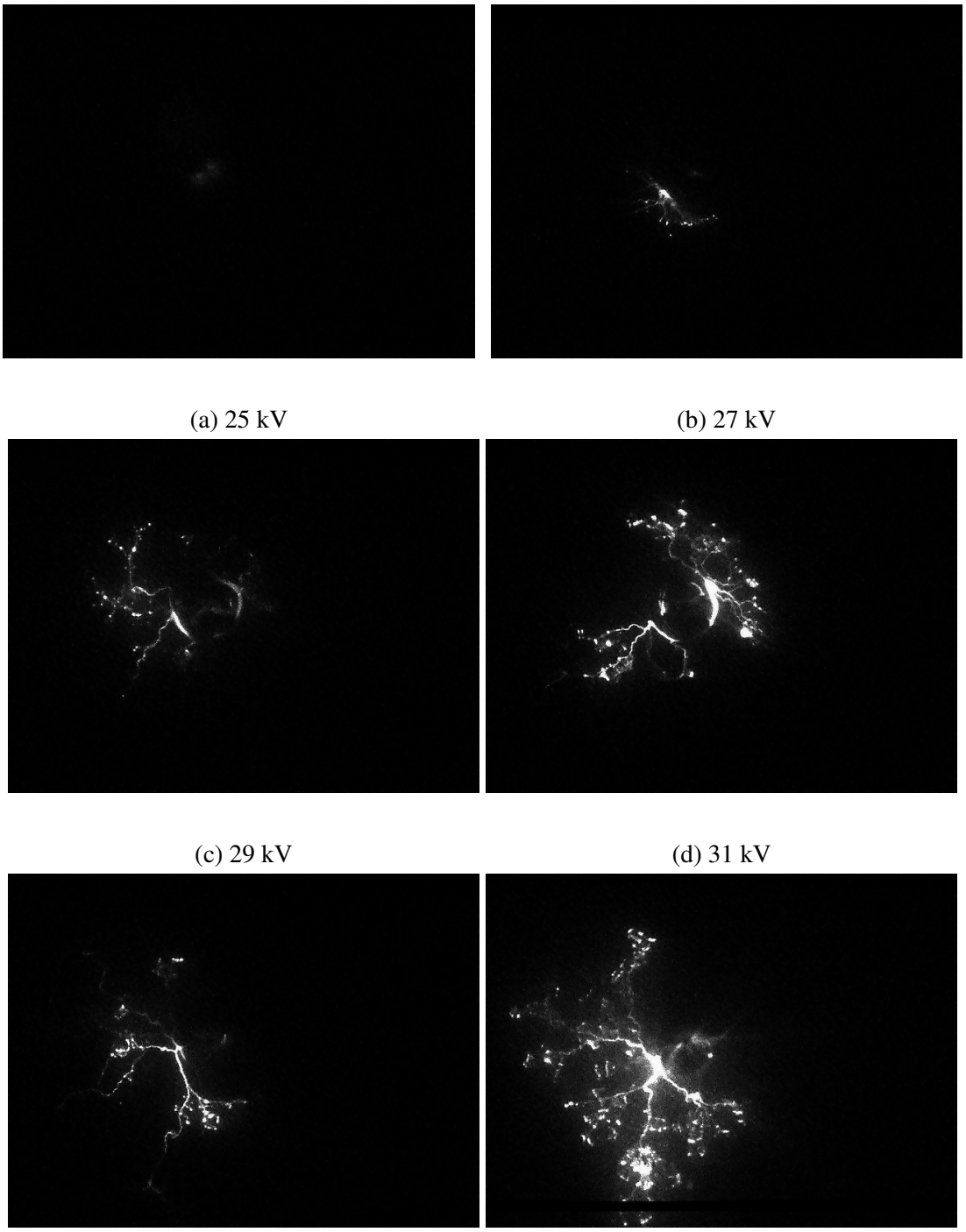

(a) 25 kV (b) 27 kV

(c) 29 kV (d) 31 kV

(e) 33 kV (f) 35 kV

Figure 4.11: Stages of creeping discharge development on a glass surface.

ies [97,99,100]. It increases with the dielectric constant of the solid dielectric material sample according to the permittivity values given in table 4.1. For a given value of the voltage, discharge lengths are higher with nano-composite than that of other three

(a) 23 kV (b) 25 kV

(c) 27 kV (d) 29 kV

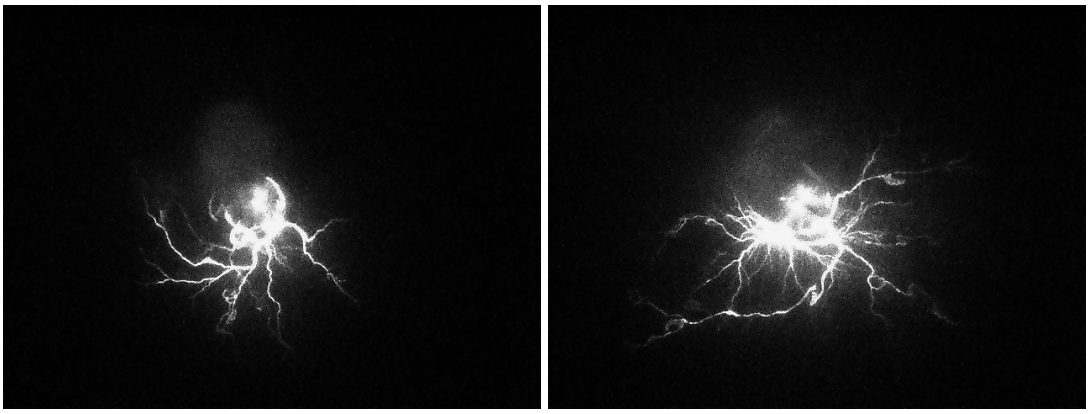

(e) 31 kV (f) 33 kV

Figure 4.12: Stages of creeping discharge development on an epoxy surface.

samples. The observation that the dielectric constant of insulator greatly influences the creeping discharge propagation and associated discharge length indicates that the capacitive effect plays an important role in the mechanisms of creeping discharges.

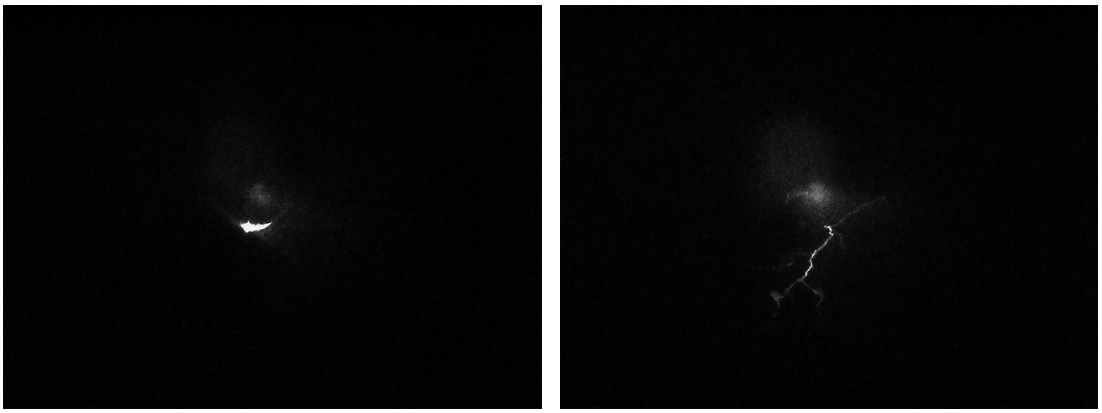

(a) 23 kV (b) 25 kV

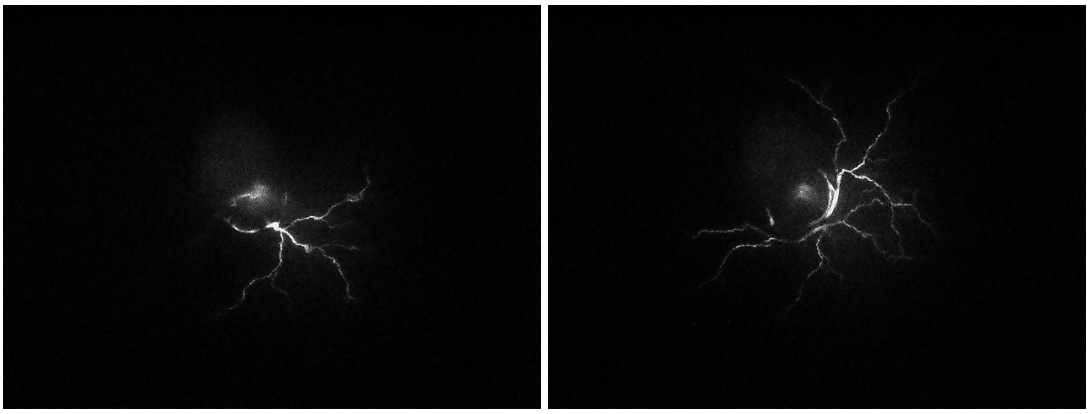

(c) 27 kV (d) 29 kV

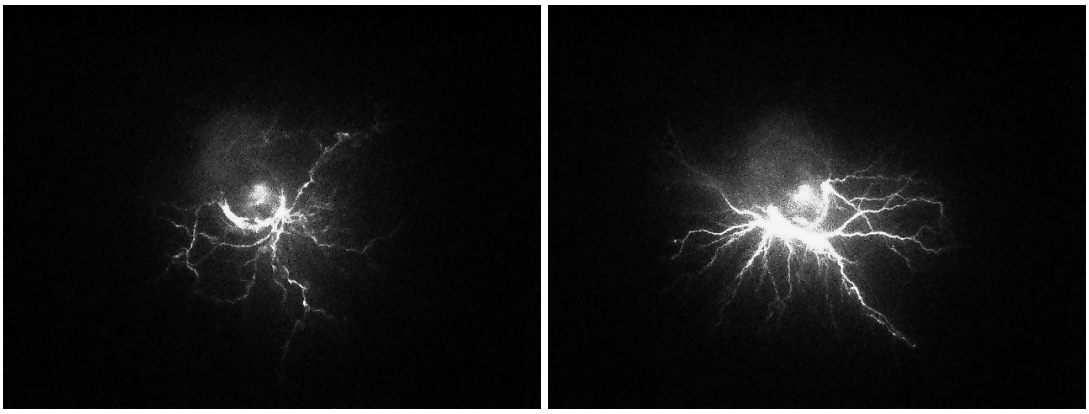

(e) 31 kV (f) 33 kV

Figure 4.13: Stages of creeping discharge development on a nano-composite surface.

However, it can be observed that the dielectric constant is not the only fact that governs the propagating characteristics as the curve corresponds to glass material sample seems to cut other curves. Fractal dimension given by the patterns propagating over

glass surface is higher than the other surface, which can be explained by the high amount of ramification.

Table 4.1: Dielectric properties of solid material samples

	Acrylic	Epoxy	Nano-composite	Glass
Dielectric breakdown voltage(kV/mm)	41	36.3	38.9	32
Dielectric constant	4.5	4.89	5.25	5
Fractal dimension	1.244	1.263	1.259	1.30

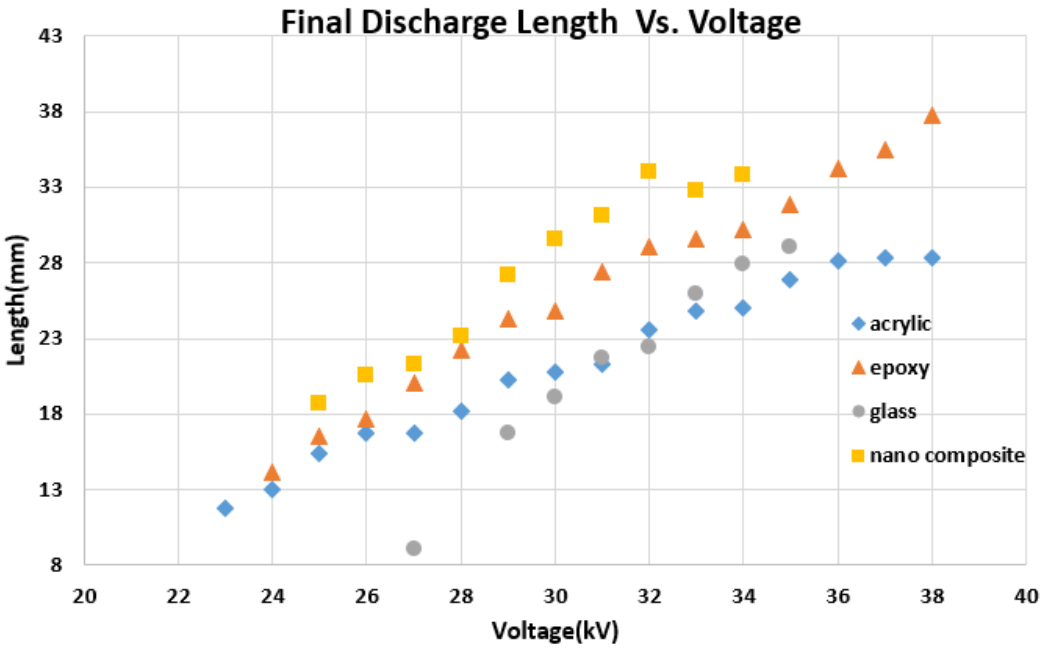

Figure 4.14: Variation of the final discharge length of the creeping discharges propagating over the solid samples versus the applied AC voltage.

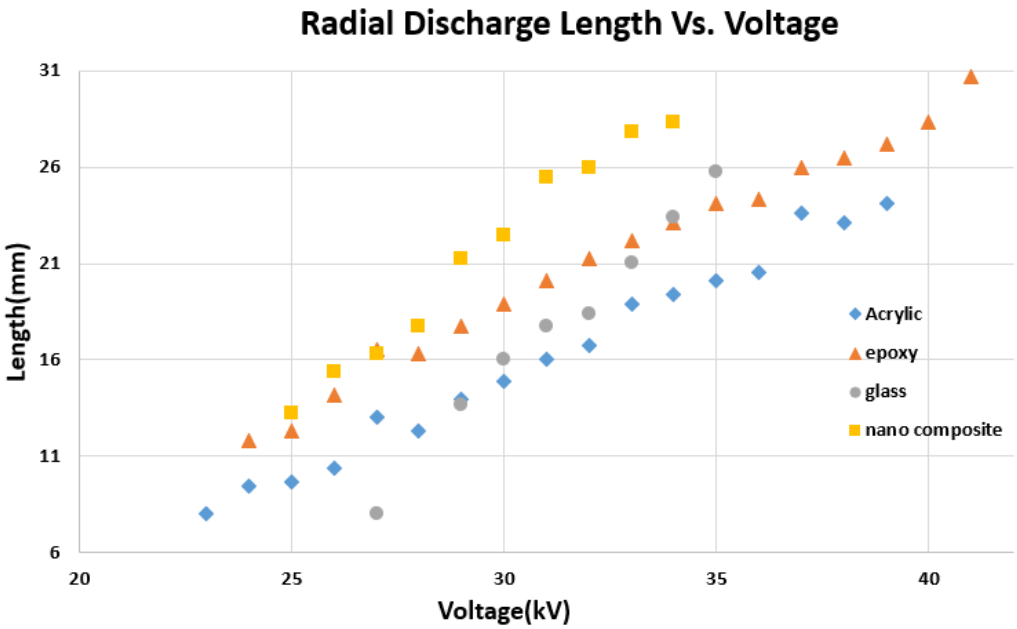

Figure 4.15: Variation of the radial discharge length of the creeping discharges propagating over the solid samples versus the applied AC voltage.

4.6 Promotion Effect of Solid Material on Discharges

The most possible reasons for the promotion effect of the considered solid insulation materials on discharges would be the influence of hetero-charges [115, 116], electron emission from the surface of the material, the permittivity of the material and residual bubbles [115, 117] left by previous discharges on the subsequent ones.

4.6.1 Space Charges

Once a surface of a solid material is charged with space charges it takes some time for charges to dissipate. The dissipation time depends on the characteristics of the material such as surface conductivity.

When the electrode is positively charged, electrons around the electrode, generated by the ionization process accelerate toward the point electrode while positive ions move toward the electric field of decreasing intensity. Due to the mobility difference of ions,

it leaves behind radial positive space charges. Local electric filed between this charge layer and the point electrode will reduce. However, the field becomes concentrated near these charge layers and new avalanches strike into newly formed channels. Space charge distribution is shown in figure 4.16.

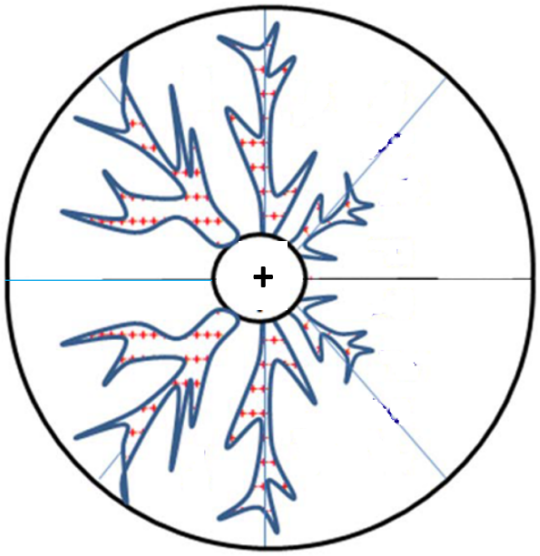

Figure 4.16: Surface charge distribution with the positive electrode

When the point electrode is negatively charged, positive irons around the cathode accelerate toward the point electrode or electric field of increasing intensity. However, the effect of the mass is more influencing on the mobility of the ions than the intensity of the electric field. Therefore, it will leave behind a positive space charge layer around the point electrode and it increases the local electric field between the charge layer and the point electrode. It will weaken the radial electric field and create a tangential one spreading the ionization all over the surface. Corresponding space charge distribution is shown in figure 4.17.

However, the current study does not consider just a half cycle of the AC power supply. Therefore, the effect of both home-space charges and hetero-space charges which promote the development of subsequent discharge should be considered in this scenario.

In the considered test apparatus where a point-plane electrode system exists, when the supply voltage is in its positive half cycle, electrons generated due to ionization will

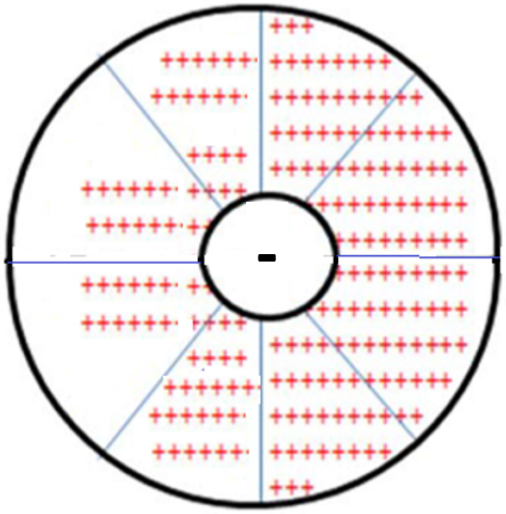

Figure 4.17: Surface discharge distribution with the negative electrode.

be attracted toward the tip of the point electrode while positive charges move away from it. However, due to the mobility difference between positive iron and electrons, even after the discharge, there may be positive charges left by the discharge over the solid/liquid interface. These charges will distort the electric field created by the point electrode which has the same polarity by shielding it. Therefore, local electric field is reduced between the needle tip and these homo-space charges. It prevents the next discharge that may occur in the same cycle of the supply voltage. The deposited space charges may last until the negative cycle of the supply voltage. When the phase reversal of the applied voltage occurs, deposited positive charges will increase the local electric field as the hetero-space charges and assist the development of the negative discharge. Amount of this memory effect to keep hetero-charges depends on the type of the material.

4.6.2 Bubble Generation

Intensive joule heating raises the dielectric liquid to a supercritical state and then vaporizes the liquid within a short time. Streamer channel involves low-density channels. It has been shown that the energy required to vaporize the liquid near the point electrode

is approximately equal to the energy dissipated during the charge injection [118]. The charge injection process occurs in random several sites of point electrode and forms the low-density regions which are called as streamers. This low-density region leads the growth of secondary streamers which depends on the field enhanced ionization of the liquid [119].

Several experimental findings have shown that the inner pressure of these filaments is higher than the external pressure at the beginning of their gas phase growth. The low-density channels take some time to expand and get their inner pressure equal to the surrounding medium. The expansion time depends on the decay times of streamers into bubbles [120]. Studies about boiling liquid have shown that thermodynamic parameters affect the liquid to gas phase transition and the expansion of the streamers. As the low-density channels expand in the liquid due to high internal pressure, both temperature and the pressure decrease to the steady-state boiling conditions. As the temperature reaches the ambient value, vapour condensates and finally streamer channels disappear bursting-up to bubbles and generating shock waves [121].

Even after one discharge propagates and its channels burst up, there may be residual low-density channel or bubbles left over the surface. They can promote the initiation and propagation of subsequent discharges. In some cases, the solid surface prevents the expansion of some streamer channels and keep the residual channels over it. Then they will facilitate the development of new discharge [115, 117].

Solid surface can oppose the spatial propagation of some streamers preventing the space charge going into the liquid. Therefore, more charges will remain on the solid surface after the discharge. As the voltage increases, more charges or current move inside streamer filaments and more residual charges can reside on the surface. Therefore, the effect of space charges become significant.

4.6.3 Surface Roughness

Positive streamers mainly propagate inside the dielectric liquid. However negative streamers propagate on the interface closer to the solid surfaces. Therefore, surface profile affects the negative streamers than the positive streamers. Smooth surface makes the discharge length of the streamer shorter and a smaller resistance for the streamers to burn the surface of the solid surface especially when the power supply is in its negative half cycle [122, 123]. Considered materials have different surface profiles. However, the surface of the prepared glass samples have more smoother surfaces and surface profile become prominent in discharge propagating on glass/oil interface.

4.6.4 Effect of Relative Permittivity

The capacitance of the solid insulation affects the discharge inception voltage [124]. If the flat solid material sample is modelled as a parallel plate capacitor, the permittivity influences the capacitance according to the equation 4.3.

$$C = \frac{\varepsilon A}{d} \tag{4.3}$$

where ε=permittivity of the material, d=thickness of the material, A= surface area

The increase in the capacitance of the solid material sample enhances the electric field at the tip of the point electrode. Enhanced electric field makes the discharge propagate more on the surface of the material. Therefore, as the material relative permittivity increases, it increases the tendency of creeping discharges to propagate. Figures 4.18a and 4.18b show the electric field distribution at the tip of a needle-plane electrode system in COMSOL Multiphysics based FEM respectively. The corresponding simulated model is shown in Appendix A. The simulation results confirm that the tangential electric field component increases upon the increment of the relative permittivity of the solid material.

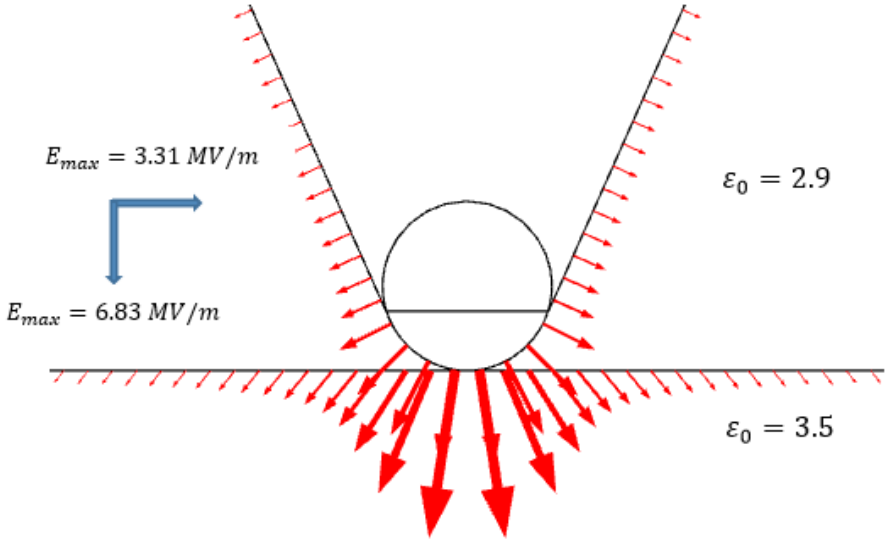

(a) $\varepsilon_0 = 3.5$

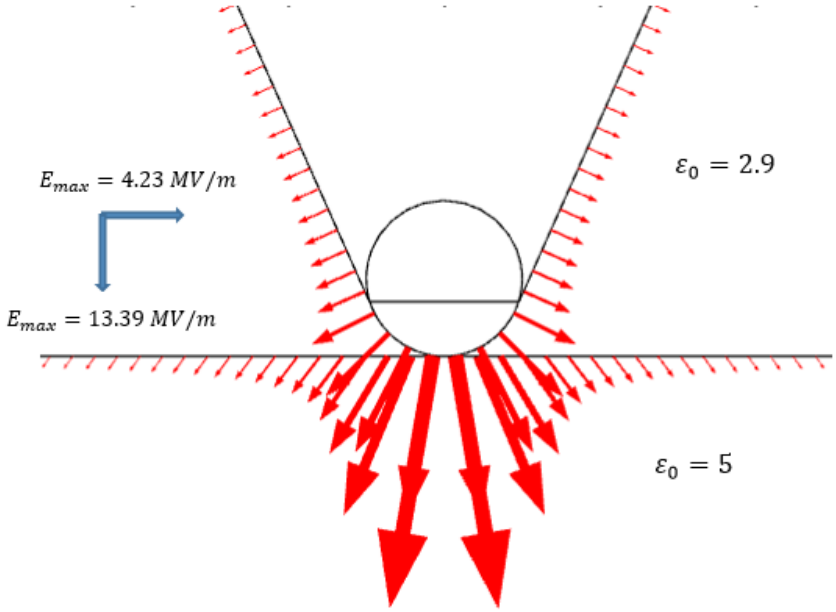

(b) $\varepsilon_0 = 5$

Figure 4.18: Example of electric field distribution obtained using COMSOL package for a structure consisting of solid samples immersed in oil, for a voltage of 1 kV and a solid thickness of 3 mm

4.6.4.1 Effect of nano-particles

The permittivity value of the epoxy composite material depends on the bulk polarization mechanism. The amount of opposition made on the mobility of di-pole group in nano-based epoxy materials, governs the permittivity of the final product. According to past studies, experimental results, as well as simulations have shown that nano-particles reduce the mobility of polymer chains. Strong bonding between charged nano-particles and polymer chains leads to a formation of highly immobile polymer nano-layer closer to the surface of nano-particles. Therefore, it can be expected that mobility of polymer chains which are interacting with these immobile nano-particles are limited [125] and can change the relative permittivity of epoxy samples. The effect of considered nano particles on the creeping discharge propagation will be discussed in section 4.7 in detail.

4.6.5 Effect of Electron Emission from the Surface Layer

Under an intensive electric field, space charges such as electrons and positive ions are emitted from the surface of the material due to molecular ionization and ionic dissociation [126]. During the creeping discharge propagation, space charges generated from the avalanche can excite the surface of the solid material and emitted new electrons from the surface can lead to the generation of a new avalanche. This newly generated avalanche can again excite the surface of the material. This phenomenon continues facilitating discharge propagation.

4.6.5.1 Effect of nano-particles

Nano filers can reduce the electron emission, which assists the discharge initiation and propagation, from the surface of the composite. Deep and shallow electron traps introduced by the nano-fillers can restrain the emission of excited electrons from the surface of the nano-composite material surface as shown in figure 4.19. Therefore,

the influence of the electron emission from the surface of the nano material on the discharge avalanche generation is minimized. It can affect the discharge lengths, fractal dimension and number of branches.

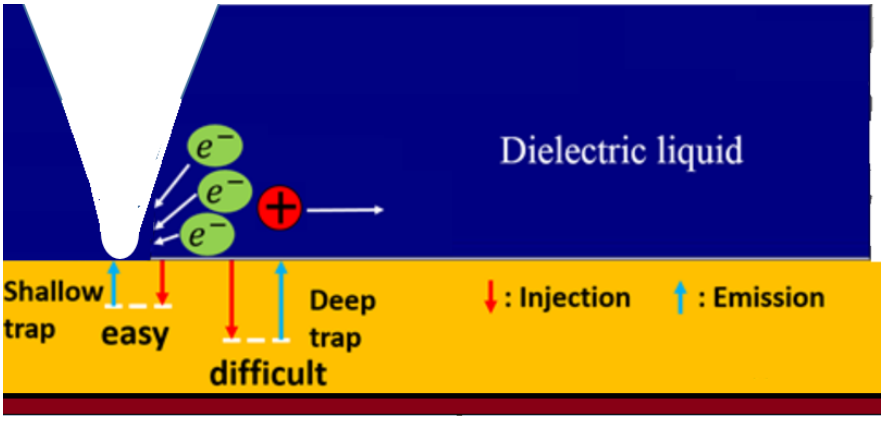

Figure 4.19: Effect of nano-particles on electron emission [25].

4.7 Discussion

The pattern propagating over glass/coconut oil interface has more ramified branches. Previous studies have shown that negative discharges propagating under vegetable oils have the same characteristics of what were observed on glass/coconut oil surface [127]. Therefore patterns propagating over glass/oil surface show the characteristics of negative streamers than positive ones. On the other hand, the voltage does not have a significant effect on the brightness of the streamers. However, the intensity of the steamers is lower on other interfaces at low voltage values. The surface of the glass material can be considered to be smooth than other interfaces. The surface profile of epoxy and nano-composite samples have been influenced by the moulds and the injecting procedure. As explained in section 4.6, the discharge tries to creep on smooth surfaces without just sliding over the interface, leading to an intensive glow. Since the negative streamers propagate closer to the solid/liquid surface, it can be expected that negative streamers are the ones which creep the surface showing the characteristics of negative streamers. To confirm the concept, same material samples are used for testing

purpose again unless they have been punched. However, the discharge initiates at a low voltage on the glass surface and propagates more easily leading to complete flashover confirming that discharge propagates on the creeped traces of the previous discharge.

Gaseous channels increase their volume as the inner pressure inside them is higher than the external pressure and expansion time may depend on few factors such as hydrostatic pressure, and decay rate of streamers. On the other hand, more charge moves inside streamers as the instantaneous voltage increases with AC voltages. That amount reduces along the streamers with the propagation of side branches. This phenomenon can cause the thickness of the streamers to increase as the patterns grow and reduce along the channels as they are created as channels segments in different time intervals.

Nano-particles has increased the relative permittivity of the epoxy material as shown in table 4.1. It should be noted that the relative perimittivy values given in table 4.1 are calculated by measuring the capacitance of samples. The reason may be the usage of significantly large nano-particles around 50 nm. Figures 4.20 and 4.21 show the variation of the relative permittivity of nano-composite upon the filler loading and upon filler size respectively. When the particle size increases, the relative permittivity of nano-composite is enhanced than that of epoxy samples. Reason is that fillers with large particles increase the mobility of epoxy chains [25]. Toshikatsu Tanaka et al., have explained the effect of the size and the loading of the filler on the permittivity using a concept where electron traps exist inside shell, interface and core quantum dots (QDs), in a core-shell structure embedded in the polymer matrix [128, 129].

According to figures 4.14 and 4.15, it seems that the effect of capacitive effect over the pattern propagation on the nano-composite material samples hence associated discharge lengths, is significant than other factors such as the amount of electron emission. It seems that the rate of increase of the discharge length with the applied voltage (gradient of the quasi-linear curves) depends on the surface profile as observed in other studies [65]. However, its effect seems to be more significant on glass/oil interface.

Fractal dimension is more related to the amount of ramification. When the dimension

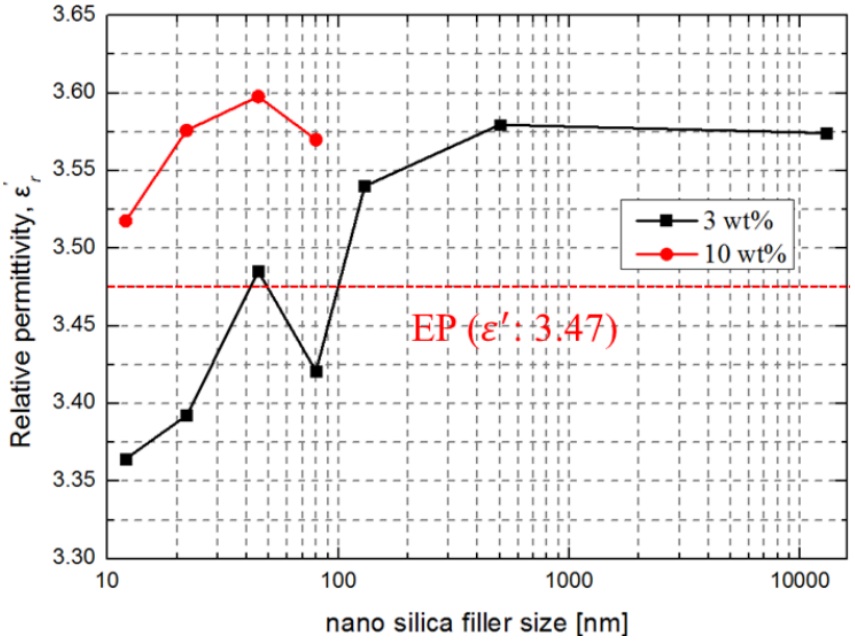

Figure 4.20: Relative permittivity at 100 kHz as a function of nano silica size for different filler loading [25].

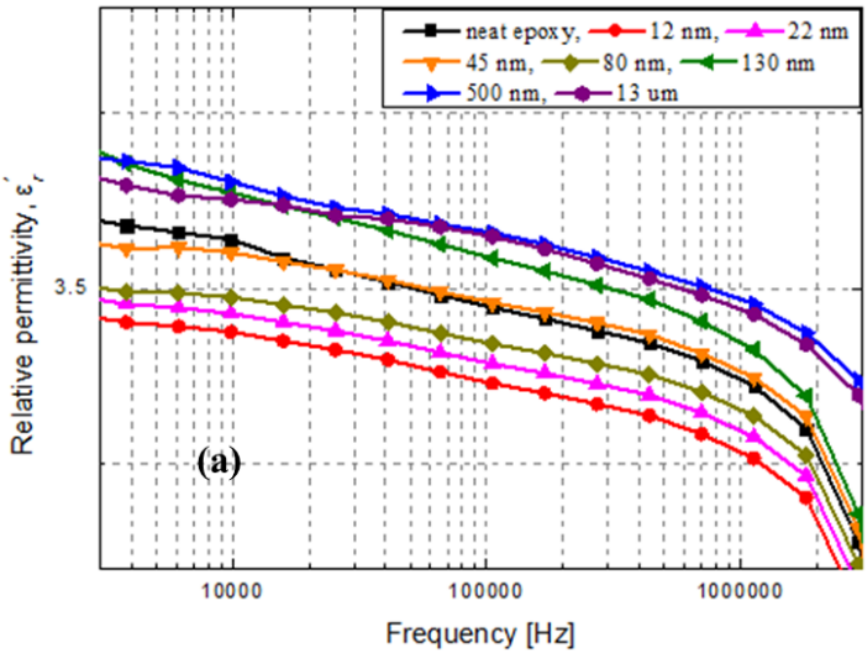

Figure 4.21: Frequency dependence of Relative permittivity with different nano silica sizes with keeping the filler loading 3 wt % [25].

related to acrylic and epoxy material are compared, it is obvious when the relative permittivity increases dimension increases. Similar observations have been made in

previous studies [130]. More ramified branches associated with glass/oil interface as observed have increased the fractal dimension than other three cases. However, nano-particles have decreased the amount of ramification on the epoxy interfaces slightly.

Breakdown strength of epoxy materials has been increased slightly by nano-particles. The behaviour of nano-fillers is somewhat different even though micro-particles decrease the breakdown strength acting as the centre of charge concentration. Interfacial area of nano-particle is considerably higher and their inter-particle distance is quite small. Therefore, they act as barriers to the flow of current through the composite increasing the breakdown strength. However, it seems that the amount of surface discharge propagation does not depend on the dielectric breakdown voltage of solid material.

4.8 Conclusions

In this chapter, experiments are carried out with a high-speed image recorder to investigate creeping discharges along surfaces of glass, acrylic, pure epoxy and nano-composite epoxy samples under an AC divergent field.

Silicon dioxide nano-particles with 1% concentration are used to increase the dielectric properties of the epoxy material. Indeed, according to experimental test results, it increases the dielectric breakdown voltage of epoxy by 7%. However, the particles size are not sufficient to reduce the mobility of polymer chains. Therefore, the relative permittivity of the nano-composite is higher than that of pure epoxy. Combining past studies on nano materials and the current study, it can be concluded that the particle size should be lower to increase the dielectric especially creeping discharge performance significantly. However further studies should be carried out with different filler sizes to determine the required particle size.

Radial discharge length and final discharge length increases quasi-linearly with the applied voltage. It can be shown the dielectric constant of the solid material affects

discharge lengths of creeping discharges. The rate of rise of discharge length with the applied voltage reduces as the dielectric constant reduces except the cases of glass material. According to the propagation patterns and discharge length curves corresponding to the glass material it can be concluded that the surface profile has a significant effect on discharge propagation. Smooth surface that glass samples had made the discharge creep the surface more while reducing discharge lengths.

According to the discharge length results correspond to the nano-composite material, it can be concluded that even though surface electron emission which facilitates more discharges is reduced by the nano-particles, the capacitive effect is more significant in discharge propagation.

CHAPTER 5

EFFECT OF MATERIAL THICKNESS AND OIL LEVEL ON CREEPING DISCHARGE PROPAGATION

5.1 Introduction

At the design stage of an insulating structure, it is important to attend to the weakest point of the insulation; the solid/liquid insulations. Once the electric field over the solid/liquid interface reaches the level necessary for molecular ionization in which positive ions and electrons will be extracted from neutral molecules, streamers initiate. Sustaining over-excitation can make the creeping discharge run-through the interface leading the complete flashover. Therefore, it is required to keep the electric field on the surface of the solid insulation at a minimum value to minimize the propagation of creeping discharges [131].

The influence of the geometry of solid insulating materials on the inception voltage of creeping discharges over clean and polluted has been studied by many researchers. Different empirical relationships have been introduced to find the incepting voltage during the designing stage of high voltage apparatus depending on the capacitance of insulators [25]. These studies are mainly focused on the analysis of the discharge length to find out data required for the dimension of high voltage apparatus under impulse voltages, which may be the main reason for discharge initiation. The capacitance of the insulation system is one of the main reason, which affects the creeping discharge inception and hence propagation characteristics as discussed in chapter 4. Therefore, physiochemical properties such as surface profile and the dimension of the

solid materials can be changed in the effort of the minimization of the creeping discharge propagation.

On the other hand, engineers have done many studies to understand the creeping discharge propagation mechanism in an effort to reduce the likelihood of breakdown. Most of the work had focused on the formation of streamers which are low-density conductive gaseous channels that are formed in the liquid closer to the interface [132–135].

This chapter describes the experimental creeping discharge patterns propagating on solid dielectric materials; glass, acyclic, pure epoxy upon the variation of thickness and on glass material samples upon the variation of the oil level. As discussed in chapter 4 material samples are immersed in copra type coconut oil and results on the discharge shape, streamer extension, as a function of the voltage have been presented using the optical observation.

5.2 Procedure

The same experimental setup based on a point-plane electrode system is used. The test cell is filled with coconut oil. The first part of the experiment is focusing on the effect of material thickness on the pattern propagation. Therefore, the samples prepared in chapter 4 with three different thickness of 2 mm, 3 mm and 5 mm are used for the study. The oil volume is kept constant throughout the testing procedure. Later Square shaped glass samples having a thickness of 3 mm and a side length of 9 cm are used to find the effect of the oil level on the creeping discharge formation. Four oil levels are considered for the study as listed in table 5.1.

Table 5.1: Considered oil levels

	Level 1	Level 2	Level 3	Level 4
Oil height (mm)	10	20	35	50
Oil volume(ml)	154.86	307.72	548.51	769.3

The distance between the electrodes is changed according to the thickness of material samples in such a way, the point electrode nearly touches the surface of the samples. If the flash-over or the complete dielectric breakdowns are observed, the test cell is filled with new oil. Material samples are changed with new ones if the flash-over or the complete dielectric breakdown occur. A stir is used to disperse the by-product throughout the liquid after each flash-over or the breakdown.

5.3 Influence of Thickness of Material

Figures 5.1 - 5.3 show the influence of the thickness of the material on the development of discharge patterns propagating over acyclic, epoxy and glass material samples respectively. The thickness of the material affects the development of the creeping discharges over solid/oil interface. It accounts for luminosity, number of main streamers, amount of ramification, discharge length and the shape. Obviously, the size and the brightness of the discharge patterns decrease when the thickness of the material is increased.

Figures 5.4 - 5.6 show the influence of the thickness of material on the discharge length of discharge patterns propagating over acyclic, epoxy and glass material samples respectively. The thickness of the solid insulating samples also influences the final discharge length and radial discharge length of creeping discharges. They increase quasi-linearly with the applied voltage for whatever the thickness of the solid sample. When the thickness of the material increases associated discharge length decreases. Researchers who investigated the geometry of the insulator on discharge development have seen a similar effect [66]. The results confirm the effect of capacitive mechanism on the development of creeping discharge.

Figure 5.7 shows the variation of fractal dimension with the thickness for the three considered solid material samples. It can be observed that the dimension decreases quasi-linearly as the thickness of the insulator decreases. A similar effect was seen by

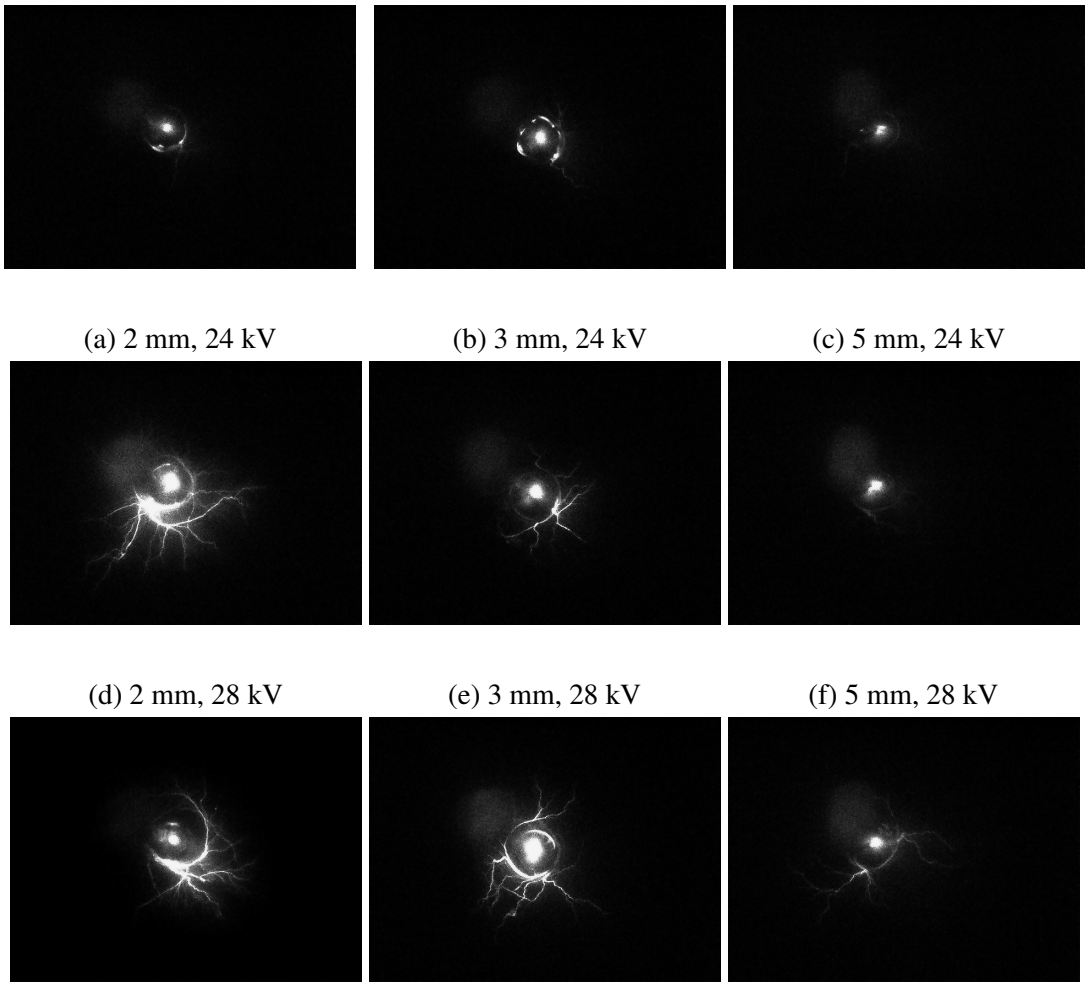

(a) 2 mm, 24 kV (b) 3 mm, 24 kV (c) 5 mm, 24 kV

(d) 2 mm, 28 kV (e) 3 mm, 28 kV (f) 5 mm, 28 kV

(g) 2 mm,32 kV (h) 3 mm, 32 kV (i) 5 mm, 32 kV

Figure 5.1: Stages of creeping discharge development on acrylic surface

Beroual et al, in 2007 [130].

5.4 Influence of Oil Level

The oil level above the solid/liquid interface significantly affects the creeping discharge patterns and their ramifications. Figures 5.8 - 5.10 show the variation of the propagating patterns upon the oil level for 18 kV, 23 kV and 26 kV respectively. When the oil level increases, the size, the number of branches and the emitted light amount decrease. When the oil level is 5 cm, the electric field is unable to initiate at least a streamer upon

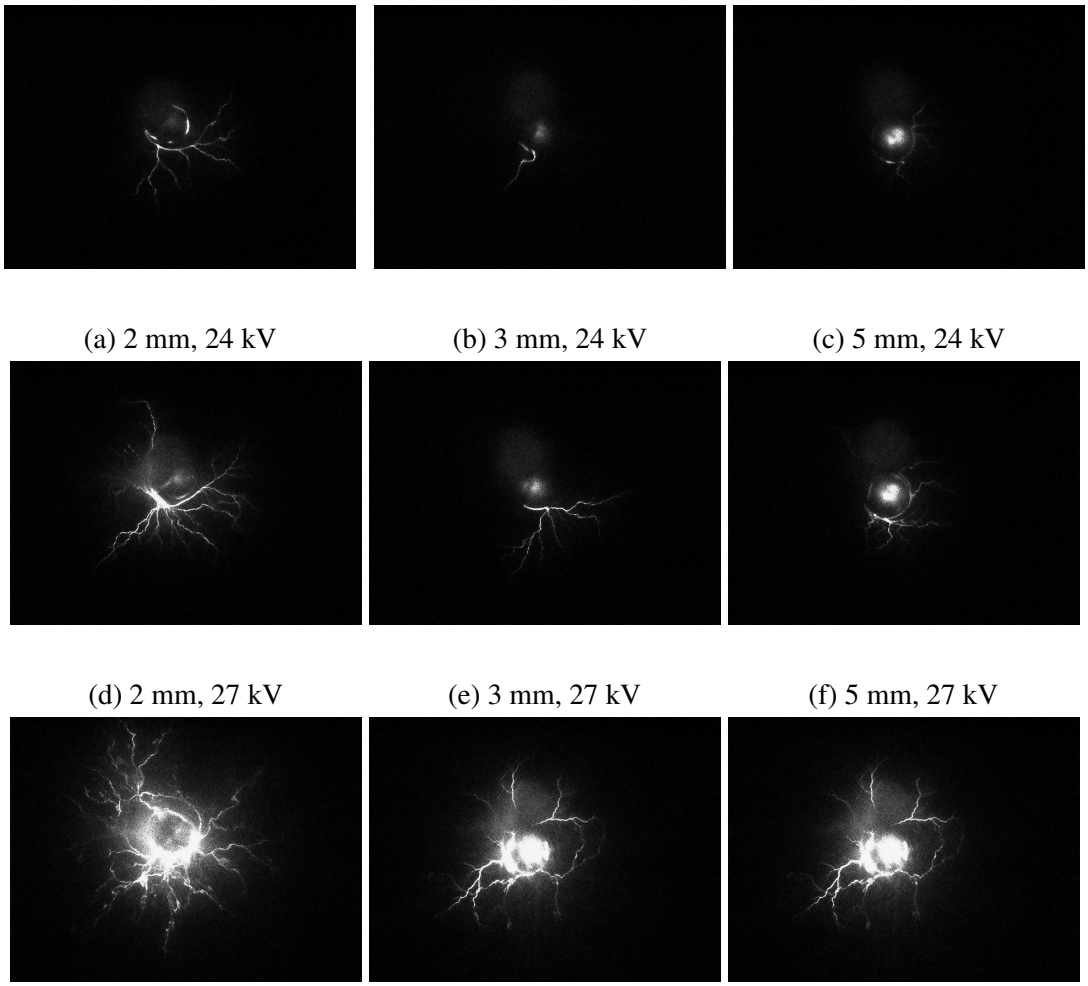

(a) 2 mm, 24 kV (b) 3 mm, 24 kV (c) 5 mm, 24 kV

(d) 2 mm, 27 kV (e) 3 mm, 27 kV (f) 5 mm, 27 kV

(g) 2 mm, 32 kV (h) 3 mm, 32 kV (i) 5 mm, 32 kV

Figure 5.2: Stages of creeping discharge development on epoxy surface

the increasing voltage. A similar effect due to hydrostatic pressure had been shown in previous works [28, 62, 63]. According to their finding, low-density gaseous channels had been affected by the hydrostatic pressure. However, we can expect in our study that the oil level indirectly affects the pressure on the solid/liquid interfaces and therefore, on the gaseous mechanism.

However, when the oil level was lower, an interesting phenomenon can be observed. The electric field generated by point electrode makes a significant force on the oil and creates an oil-free circular region (circular contour around the electrode point) around the tip of the electrode. Discharge propagation is limited to this boundary and it oc-

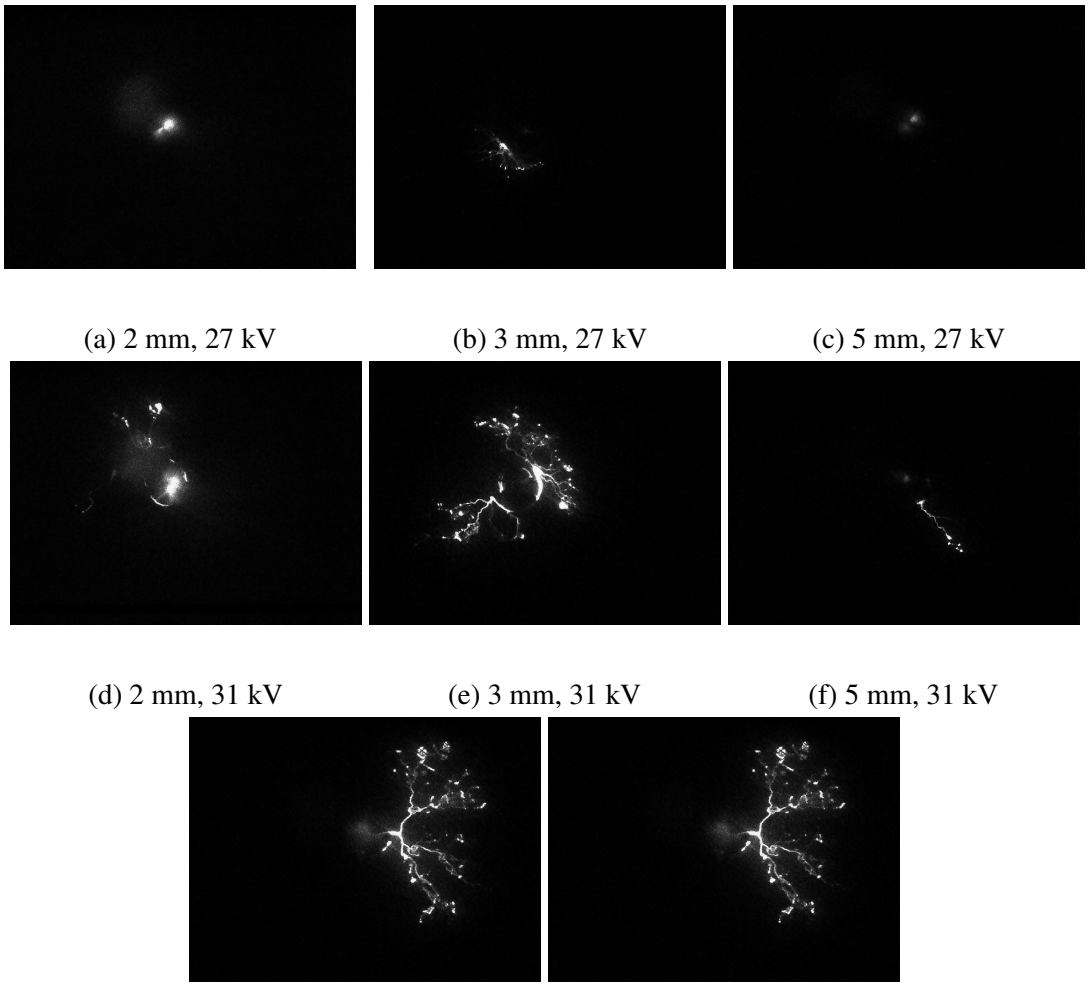

(a) 2 mm, 27 kV (b) 3 mm, 27 kV (c) 5 mm, 27 kV

(d) 2 mm, 31 kV (e) 3 mm, 31 kV (f) 5 mm, 31 kV

(g) 3 mm, 35 kV (h) 5 mm, 35 kV

Figure 5.3: Stages of creeping discharge development on glass surface

curs over the solid surface and inside a thin oil layer. Once a streamer of the discharge reaches oil boundary, it propagates along the boundary as shown in figures 5.8a - 5.10a. Characteristics of the streamers and its ramification are considerably different than that of streamers propagate over solid/liquid interface. Streamer channels are thicker and emitted light is too significantly high. The reason may be that streamer propagation occur inside a thin oil layer and the atmospheric pressure is the only thing which could make a pressure and an effect on the volume and the size of the streamer channels. Space charges and ionization are more concentrated around the tip of the point electrode leading to a glow over the area closed to the point electrode.

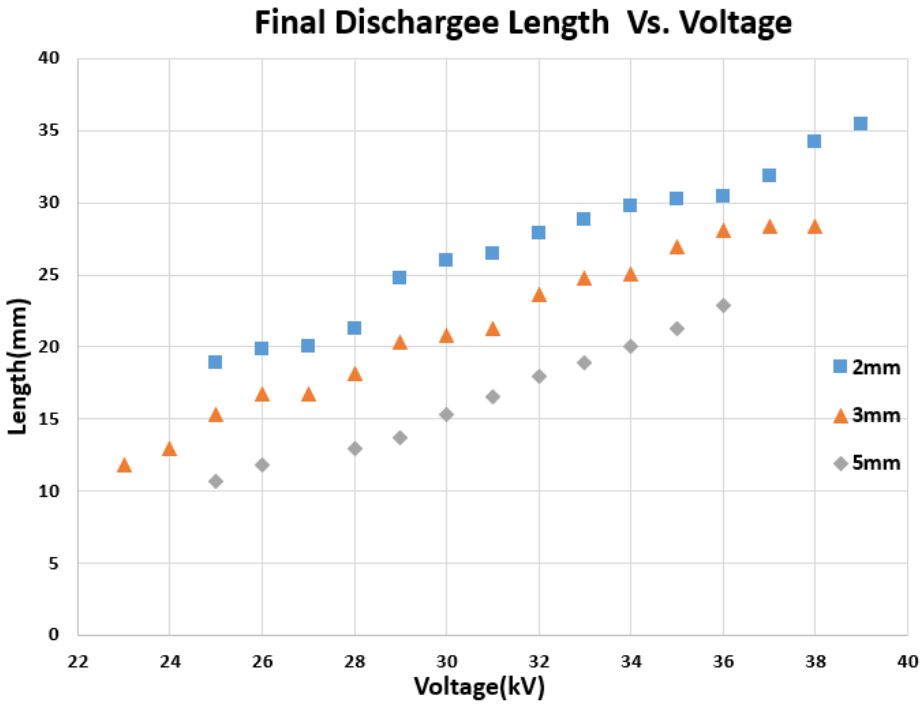

(a) Final discharge length

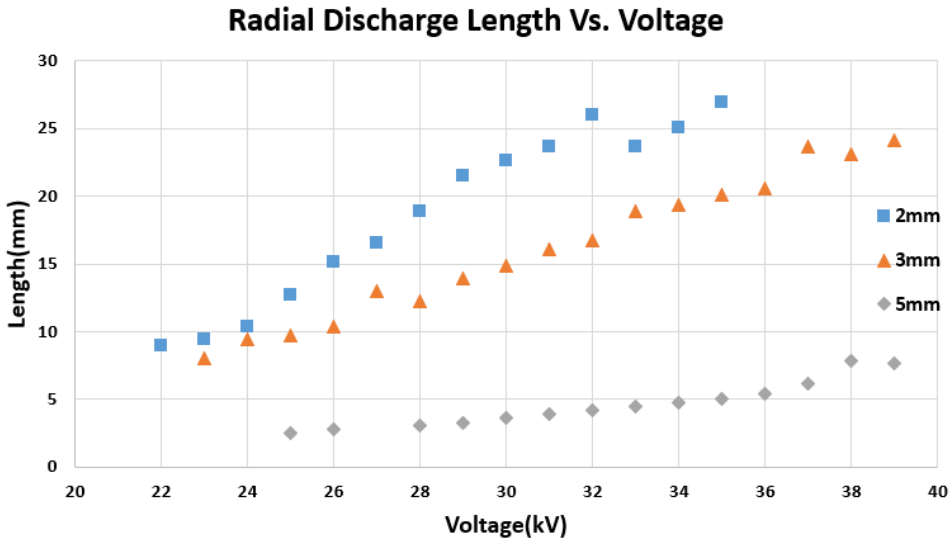

(b) Radial discharge length

Figure 5.4: Variation of the discharge lengths of the creeping discharges propagating over the acrylic samples versus the applied AC voltage for different thickness.

The radial discharge and final discharge length of creeping discharges are reduced when the oil level is increased as shown in figure 5.11 and figure 5.12 respectively.

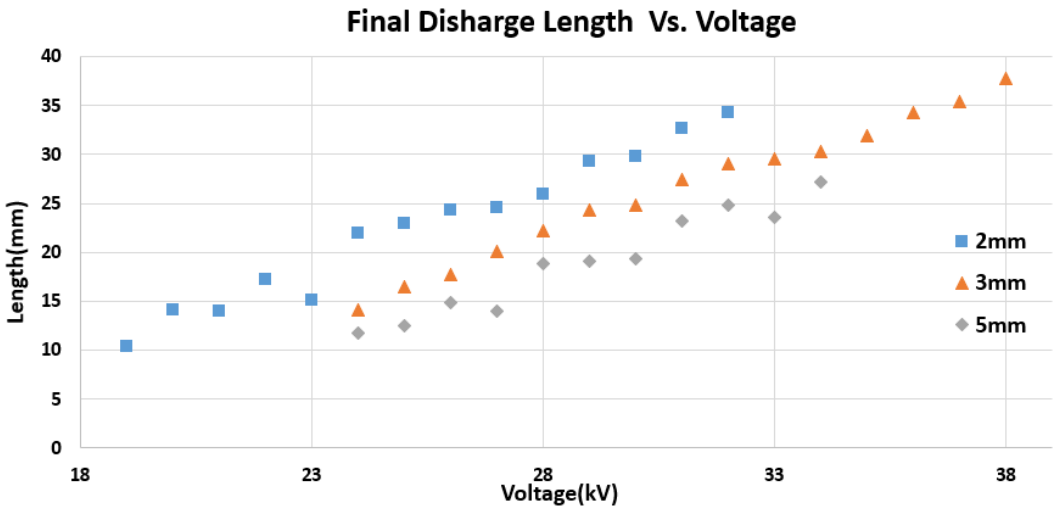

(a) Final discharge length

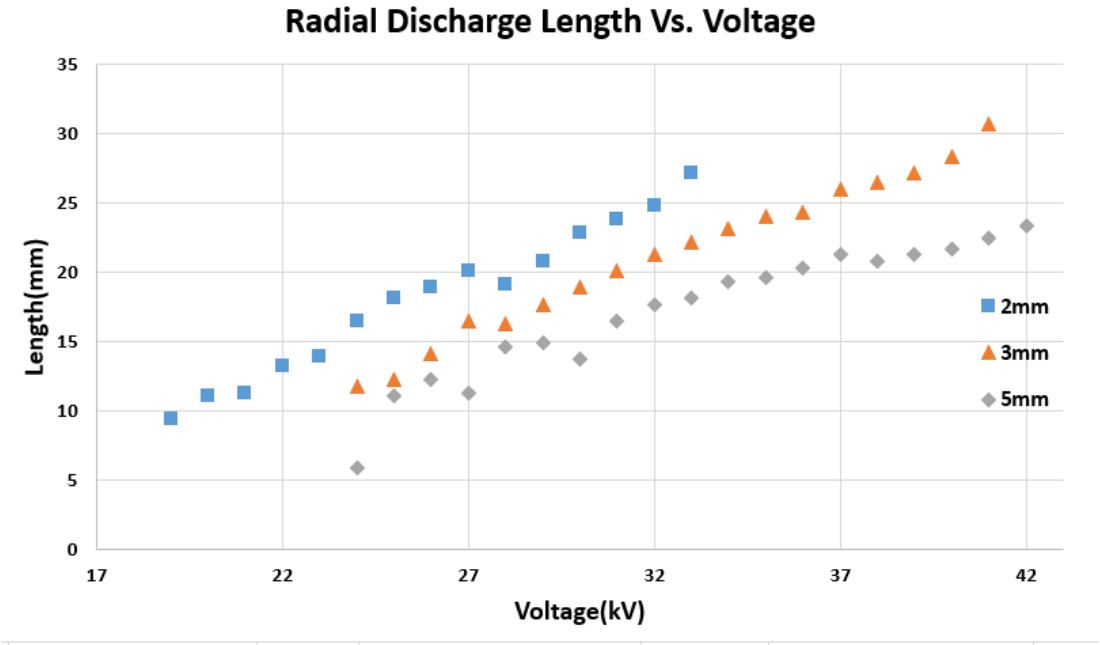

(b) Radial discharge length

Figure 5.5: Variation of the discharge lengths of the creeping discharges propagating over the epoxy samples versus the applied AC voltage for different thickness.

According to the plot of fractal dimension D versus oil level for insulators of 3 mm thickness shown in figure 5.13, it can be observed that the dimension decreases when the oil level increases.

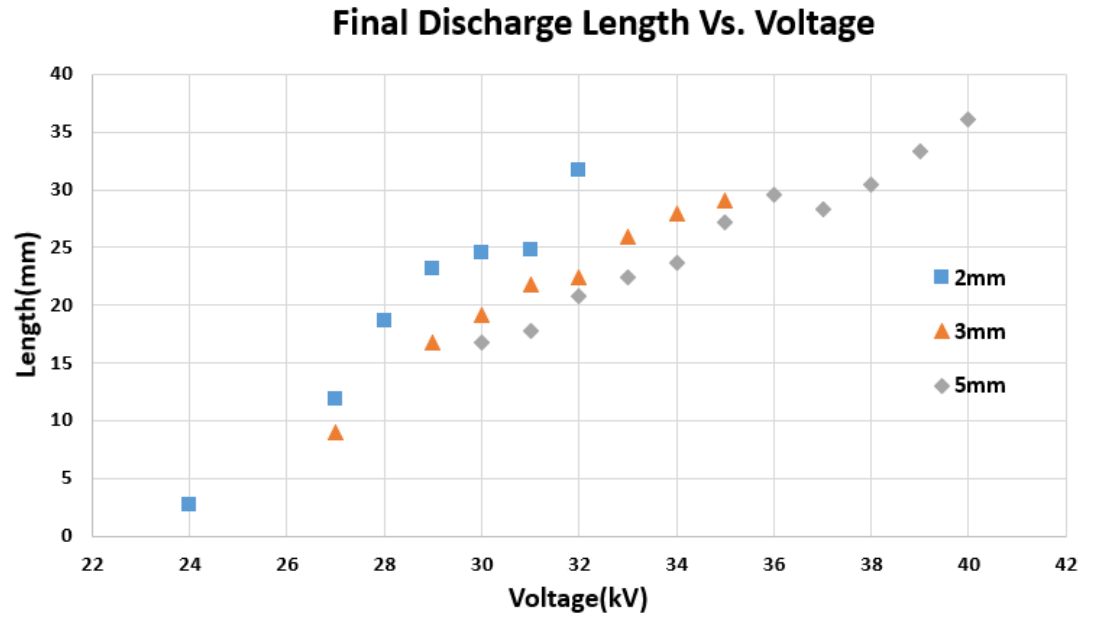

(a) Final discharge length

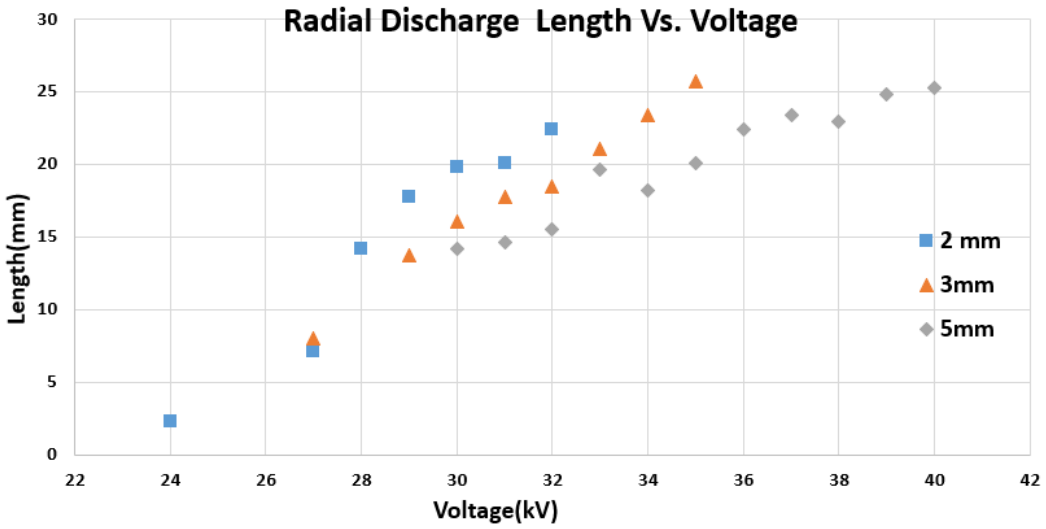

(b) Radial discharge length

Figure 5.6: Variation of the discharge lengths of the creeping discharges propagating over the glass samples versus the applied AC voltage for different thickness.

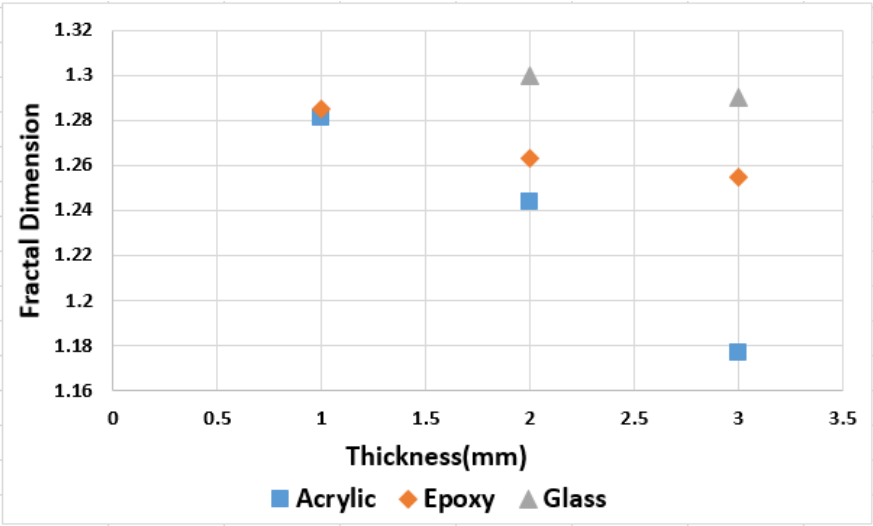

Figure 5.7: Fractal dimension D versus the insulator thickness e

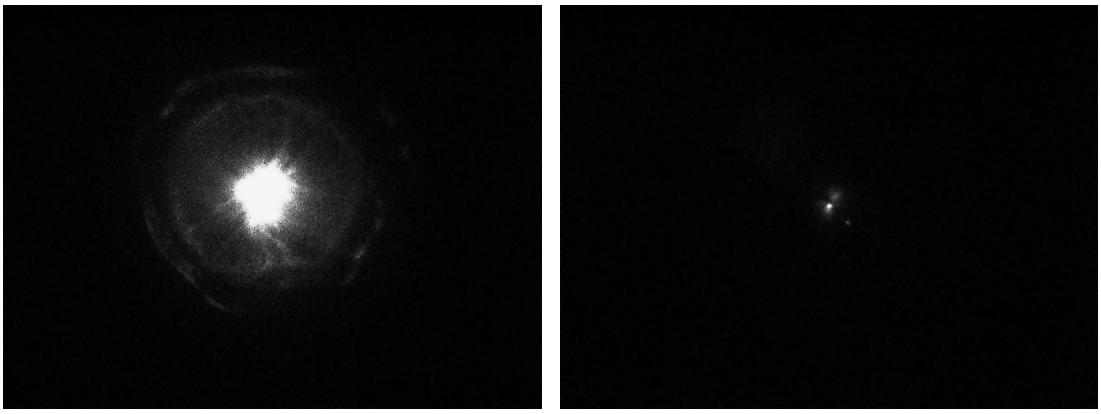

(a) Level 1

(b) Level 2

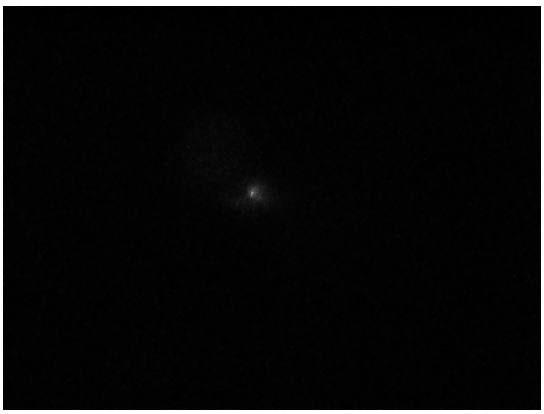

(c) Level 3

(d) Level 4

Figure 5.8: Oil level on creeping discharge development under 18 kV

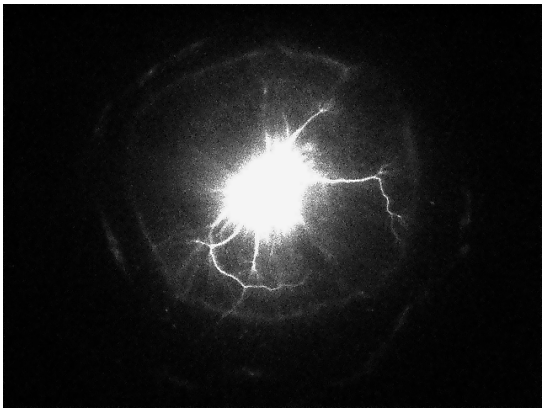

(a) Level 1

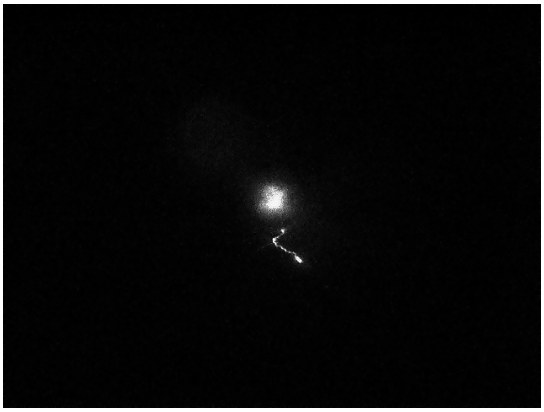

(b) Level 2

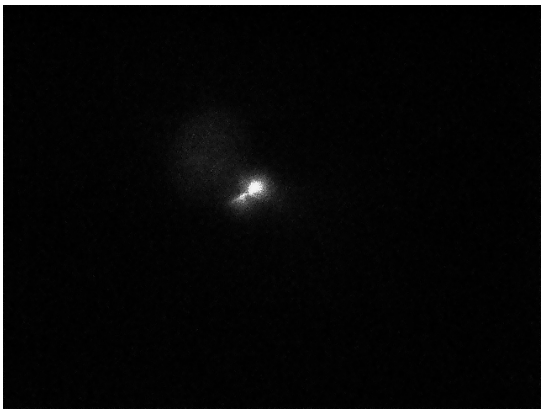

(c) Level 3

(d) Level 4

Figure 5.9: Oil level on creeping discharge development under 23 kV

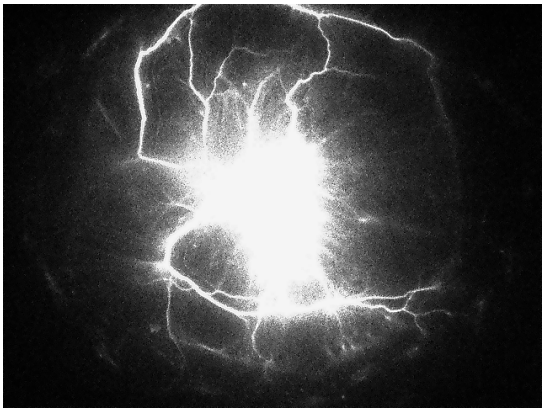

(a) Level 1

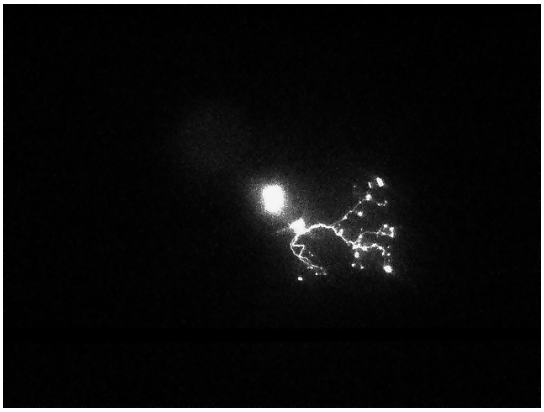

(b) Level 2

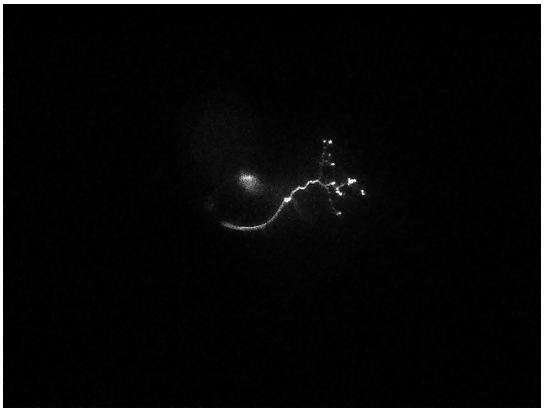

(c) Level 3

(d) Level 4

Figure 5.10: Oil level on creeping discharge development under 26 kV

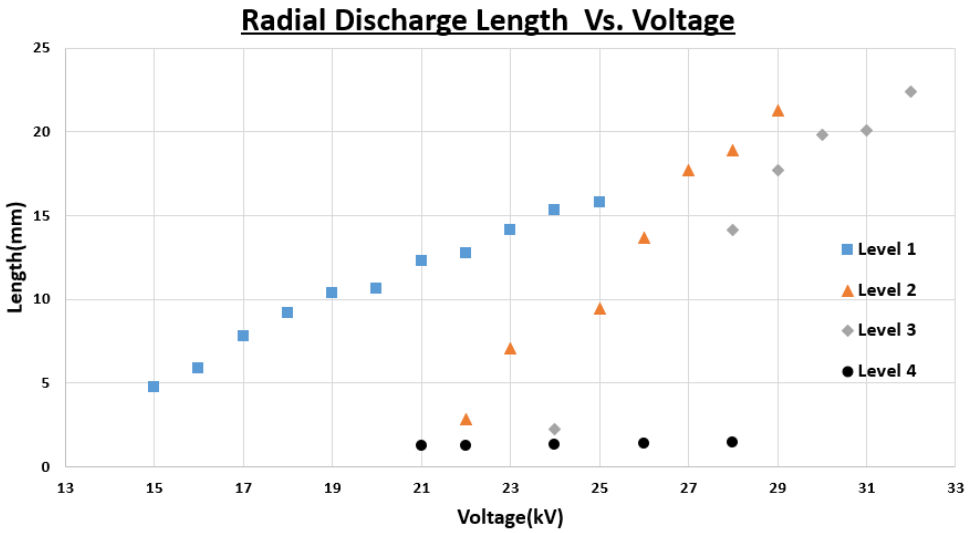

Figure 5.11: Variation of the radial discharge length of the creeping discharges propagating over the solid samples versus the applied AC voltage for different oil levels.

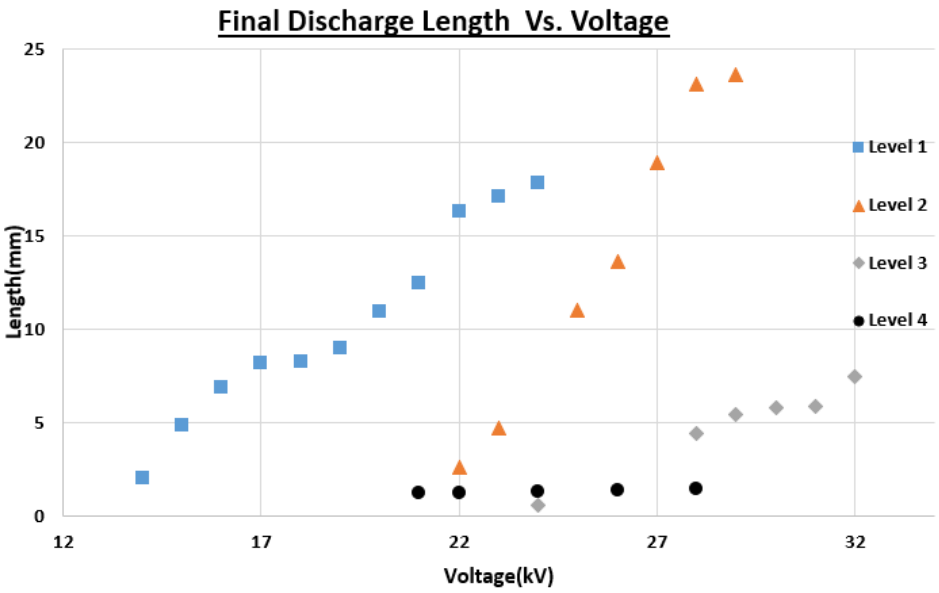

Figure 5.12: Variation of the final discharge length of the creeping discharges propagating over the solid samples versus the applied AC voltage for different oil levels.

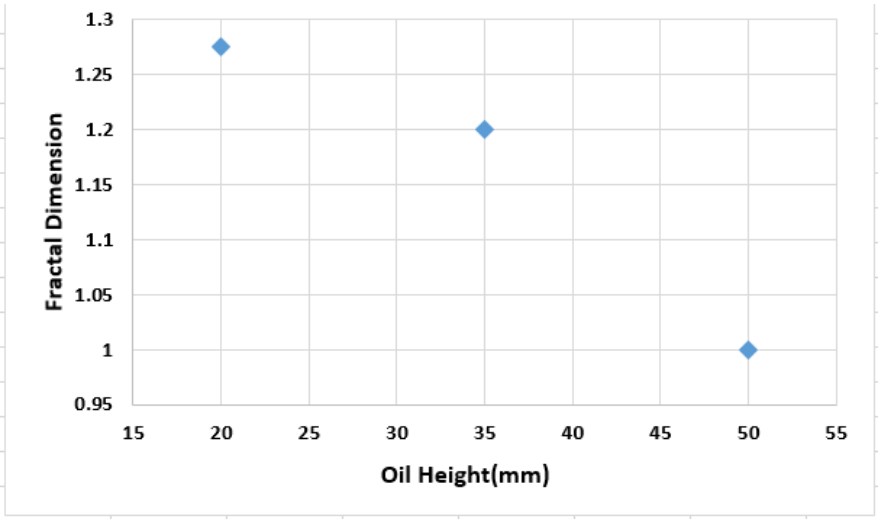

Figure 5.13: Fractal dimension D versus oil height for glass insulator materials; the insulator thickness being e = 3 mm.

5.5 Discussion

In general, the inherent capacitance of the solid insulation affects the discharge inception voltage [124]. If the flat solid material sample is modelled as a parallel plate capacitor, obviously the thickness influences the capacitance according to the equation 5.1.

$$C = \frac{\varepsilon A}{d} \tag{5.1}$$

where ε=permittivity of the material, d=thickness of the material, A= surface area

Increase in the capacitance of the solid material sample enhances the electric field at the tip of the point electrode. Creeping discharges can be initiated at a lower voltage with such an enhanced field and they tend to propagate more on the surface of the material because of the electrostatic energy stored in the material increases. As the material becomes thicker, it reduces the tendency of creeping discharges to propagate. Therefore, it can be seen that when the amount of charges that an insulation material stores decreases associated fractal dimension and discharge length decrease. The experimental observation that the amount of tree formation of the pattern decreases upon the increment of the thickness of the insulation material confirms that the tree formation is well correlated with the fractal dimension.

Figures 5.14a and 5.14b show the electric field distribution at the tip of a needle-plane electrode system over a 2 mm thick material and a 10 mm thick material respectively. It should be noted that a 10 mm thick material is considered instead of 3 mm or 5 mm to show a significant variation of electric field at the tip of the point electrode with the increment of the thickness of the solid material sample. The simulation result confirms that the tangential electric field component decreases upon the increase of the thickness of the solid material.

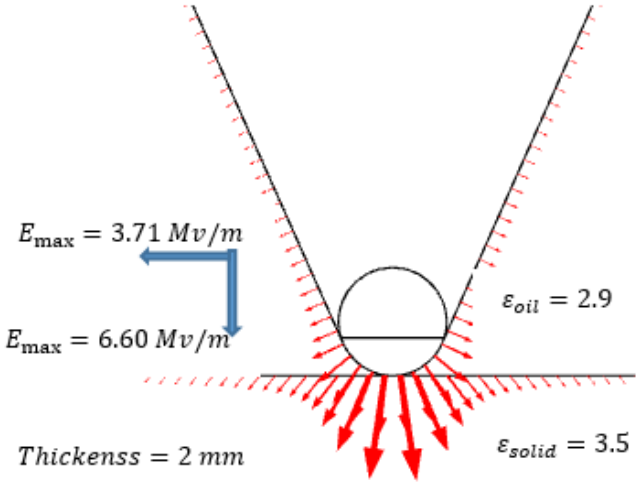

(a) Thickness= 2 mm

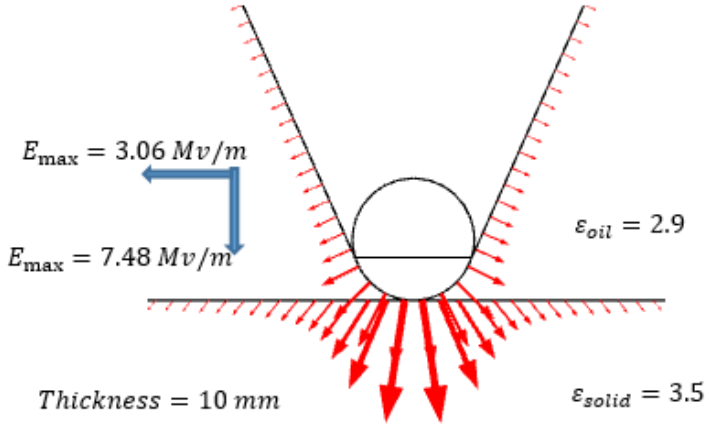

(b) Thickness =10 mm

Figure 5.14: Example of electric field distribution obtained using COMSOL package at the tip of point electrode for a voltage U = 1 kV

Dielectric liquids under intensive electric field lead to the phenomenon called mass transfer/electrohydrodynamic motion which can be explained by several properties of the liquid. Coconut oil is a natural ester with long alkyl groups which are made of long chains of carbon atoms and they do not carry an electric charge. Therefore, these molecules are said to be non-polar. However, applied electric field makes the molecules stretch and re-orient inducing a dipole moment. These dipoles are formed as clusters where space charges act as centres of them. As the space charges move

towards a particular direction depending on the charge of iron, automatically dipoles will be drawn in the same direction. This mechanism has caused liquid oil to fall and rise [136].

Tangential electric field governs propagating characteristics of creeping discharges over dielectric materials [137]. The variation of the tangential electric field at the tip of the point electrode was obtained for the modelled apparatus upon the oil level as shown in figure 5.15. The plane electrode was grounded and voltage of 1 kV was applied to the point electrode. It can be seen that the high oil levels do not have any significant effect on the variation of the tangential electric field. However, the corresponding tangential field is gradually enhancing as the level decreases and suddenly jumping to a higher value in absence of the oil. Therefore, we can expect that the effect of the mass transfer is more prominent as the oil level decreases. The fall of oil level around the point electrode upon the electric field is negligible and cannot be clearly observed when the oil level increases. However, as the level of the filled oil is lower, fall of oil level around the electrode is more and clearly visible as it makes an oil-free region around the electrode. However, there is a electro hydrodynamic motion of the thin oil layer in the vicinity of the point electrode and it causes small circular contour around it concentrating more space charges inside it. That may be the reason for the intensive glow around the point electrode at oil level 1. A similar effect had been observed in [63].

According to the simulation results illustrated in figure 5.15, it can be expected that beyond the oil height of 20mm (around 15-20 mm), the effect of the tangent electric field over the variation of the discharge characteristic is negligible. Therefore, it can be expected that effect of the pressure on the interface has become more prominent. Table 5.2 shows the variation of the pressure on the interface generated due to the mass of the oil.

There are three theories which can be used to explain the effect of pressure on the propagation characteristics.

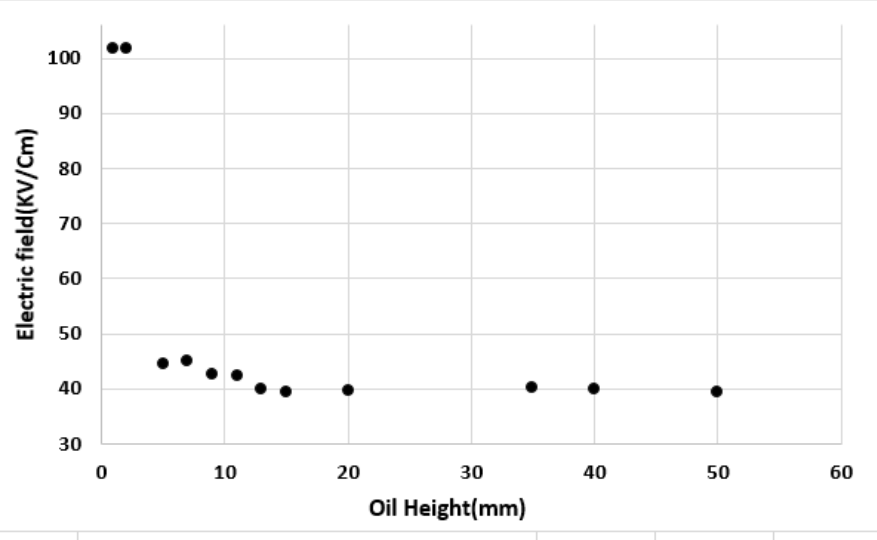

Figure 5.15: Tangential Electric field at the tip of the point electrode

Table 5.2: Hydrostatic pressure on the solid/liquid interface

	Level 1	Level 2	Level 3	Level 4
Oil height (cm)	1	2	3.5	5
Pressure (excluding atmospheric pressure) (Pa)	99	144	212	280

1. Intensive joule heating injected by electrodes within a short time vaporizes the liquid and the streamer formation occurs in term of low-density gaseous channels [133, 138]. The relationship between the energy required and the hydrostatic pressure holds a linear variation. Hence the as the external pressure increases, it prevents the vaporization and the streamer formation [133].

2. The pressure can affect the volume and the lifetime of gas bubbles generated by the collapse of streamers. As the pressure increases, bubbles shrink considerably [134]. It will reduce the promotional effect on the initiation and propagation of subsequent discharges.

3. It is shown that the mean electric field within filaments is greatly affected by hydrostatic pressure. Even if the streamers are supposed to propagate to a particular length under the given pressure condition, it is not possible if the propagating filaments break into a series of gas bubbles. At low-pressure values, streamers stop

due to their voltage drop along the streamers instead of the collapse of streamers [135].

The final discharge length and radial discharge length curves seem to increase quasi-linear with the applied voltage as discussed in chapter 4 and 5. Such a variation on final discharge length was observed for different hydrostatic pressure values by Beroual et al in 2002, 2003 and in 2008 under AC, DC and impulse voltages [28, 62, 63].

Table 5.3: Information of discharge length curves

	Final Discharge Length				Radial Discharge Length			
	Level 1	Level 2	Level 3	Level 4	Level 1	Level 2	Level 3	Level 4
Slope	1.523	3.25	0.8098	0.033	1.1021	2.6196	2.5475	0.033
R square value	0.9653	0.9825	0.9653	0.9717	0.9856	0.9771	0.9679	0.9717

Table 5.3 shows few details about the slope of discharge length curves and associated R-square value considering their quasi-linearity. Being the R square value of each curve closer to 1, it confirms their quasi-linearity. Their rate of rise of discharge length with the applied voltage seems to depend on the oil level. A Similar effect has been shown in [66] with the hydrostatic pressure of the liquid. The rate of rise of each curve become weaker as the oil level increases except the curve corresponds to level 1. The rate of rise of the curves corresponds to the level 1 is lower than than that corresponds to level 2. This phenomenon can occur due to the following reasons.

1. The boundary or contour made by the fall of oil level opposes the pattern propagation.
2. Pattern propagation occurs over the oil-free (just a thin oil layer) solid surface.
3. The electric field strength at the tip of the point electrode is significantly enhanced.

5.6 Conclusions

In this chapter, experiments are carried out to analyse the dependency of the geometrical properties of the solid dielectric material and the oil level on the creeping discharge propagation under AC divergent electric field. The high speed camera was just to capture the output Therefore, three material samples; glass, acrylic and pure epoxy, of three different thickness of 2 mm, 3 mm and 5 mm have been considered to the effect of the thickness on creeping discharge propagation. Quasi-linearly of the discharge length with the applied voltage is observed for whatever the thickness of considered material samples and the increase in material thickness, decreases electric field at the triple junction where the two dielectric material meet. At the same time with the increase of the capacitance of the solid material, it increases the amount of charges that the dielectric material can store on its surface. Therefore, as the thickness of the material increases, corresponding discharge lengths decreases. Amount of ramification of discharge branches also shows a similar characteristic with the thickness of the material according to the fractal dimension values.

It can be observed that size, brightness, discharge length reduces as the oil level increases. It can be concluded that as the oil level increases the effect of the pressure on the soil/liquid interface generated by the mass of the oil become prominent on the creeping discharge propagation.

Three different ways that the external pressure can act on low-density channel formation and promotional effect are identified. They are used to explain the fact that as the oil level increases, associated discharge length and fractal dimension decrease. The curve corresponding to the discharge length Vs. voltage shows a quasi-linear variation and rate of rise with the voltage seems to depend on the oil level. However, as the oil is lower, mass transfer/electro-hydrodynamic motion leads to an interesting phenomenon as the tangential electric field on the interface at the tip of the point electrode is enhanced.

CHAPTER 6

EFFECT OF OIL TYPE ON CREEPING DISCHARGE PROPAGATION

6.1 Introduction

Insulating system is the most vital part of the high voltage equipment such as capacitors, circuit breakers and transformers. Conventionally, the composite insulation systems consisting of mineral oil and the oil-impregnated cellulose products have been used inside transformers. The usage of petroleum-based oil has some disadvantages such as their poor biodegradability, toxicity and exhaustion of mineral resources. Environment-friendly vegetable oils are considered to be a substitute for mineral oil and many research work has been carried out in order to determine dielectric breakdown strength and partial discharge inception of such oils [139].

Solid/liquid interface inside oil-filled high voltage apparatus is the weakest point of an asset as it facilitates surface discharges due to permittivity difference of liquid and solid. When it comes to liquid /press-board insulation system, the electric field is distributed more evenly between vegetable oil and pressboards as the dielectric constant of pressboard and esters are closed to each other [140]. To keep the required level of insulation, the designer should know the creeping discharge phenomenon under different vegetable oil/solid interfaces.

This chapter investigates the behaviour of AC creeping discharges in vegetable-based insulating oils named; virgin type coconut oil, copra type coconut oil, sunflower oil,

soybean oil and the results on the discharge shape, streamer extension, as a function of the voltage have been presented using the optical observation.

6.2 Alternative Natural Ester Oils

6.2.0.1 Sunflower Oil

Refined sunflower oil is more popular due to its high ratio of polyunsaturated-to-saturated fatty acids, good storage stability, low viscosity and bland flavour. Therefore it has become one of the most popular cooking oil in the world. Crude sunflower oil is obtained from properly cleaned seeds [141]. Mechanical pressing can be used to extract around half to three-quarters of the available oil. Solvent extraction is implemented later to extract the remaining oil [142]. The fatty acid composition of sunflower oil depends on the sunflower plant genotype and the environmental conditions such as temperature and light. Breeding efforts have been taken to introduce new hybrid types so that the fatty acid concentration can be varied to archive higher degree of oxidative stability. Depending on the fatty acid concentration there are few types of sunflower oil such as high linoleic, mid-oleic, high-oleic and high stearic [143].

6.2.0.2 Soybean Oil

The origin of soybean is considered as China. Nowadays soybean oil has become one of the important oil in the world. However, their growth has been limited to a selected few courtiers such as India, China. Two methods are being used to extract soybean oil [144]. The traditional method uses mechanical press machines to squeeze oil out from the seeds. The chemical method uses solvents to extract oil [145]. Even though the yielded oil quantity of mechanical method is lower than that of the mechanical method, it produces natural and healthier oil.

6.2.0.3 Coconut Oil

Coconut oil is a natural ester and available in tropical countries like in India and Sri Lanka [146]. Coconut oil is somewhat different from other vegetable oil as it has about 90% of saturated fatty acids. Therefore, its stability in air, thermal conductivity and melting point are higher than other oils. Depending on the manufacturing processes, coconut oil can be categorized into three categories as RBD type oil, virgin coconut oil and copra oil. Virgin coconut oil is obtained from the kernel of the fresh and mature coconuts through mechanical or natural methods where heat may be used without subjecting the oil to an alternation or transformation. Copra oil extraction method known as dry method uses dried and heated meat extracted from the coconut shell and they are crushed or dissolved with solvent producing coconut oil and a high-protein mash [31]. The manufacturing process of coconut oil does not affect its fatty acid profile, even though free fatty acid content changes. When the amount of free fatty acid is indexed as the percentage of lauric acid, percentages of the RBD coconut oil, virgin coconut and copra coconut oil are 0.02 %, 0.13 % and 1.41 % respectively [31].

6.3 Sample Preparation

Commercially available ready-made oils were select for the study. Sample 1 is a type of virgin coconut oil and a cold press method is being used to extract the oil from white scraped coconut. Sample 2 is a type of copra type coconut oil. The moisture content of the coconut meat is reduced below 6% to produce copra. A mechanical method is used to expel the cooked copra to extract oil [31]. Sample 3 is extracted from the seed of soybean. Sample 4 is a type of sunflower oil and extracted from the seeds of the sunflower. The colour of the sample is light and it is rich with essential vitamin E.

6.4 Procedure

The same experimental setup used in previous work is used. Square shaped glass samples having a thickness of 5 mm and a side length of 9 cm are used to find the effect of the type of oil on the creeping discharge formation. The test cell is filled with new oil if the flashover or the complete dielectric breakdowns is observed, to make an accurate comparison among oils.

6.5 Results

Type of dielectric liquid significantly affects the creeping discharge patterns and its ramifications. Figures 6.1 - 6.4 show propagating patterns corresponding considered samples under four different voltages of 22 kV, 26 kV, 30 kV and 36 kV. When the type of the liquid changes the size and the number of branches of the pattern and the emitted light amount varies.

The ramification and the characteristics of the negative streamers that was observed with copra type of coconut oil cannot be observed with other type of oils. However virgin coconut oil seems to preserve the luminous point at some part of the streamers which are observed with copra coconut oil. Even though traces of the channels of the discharge patterns taken by the optical observation cannot be well defined with copra type coconut oil, it has become possible with other considered oils. Sunflower oil and soybean oil facilitate more discharges increasing their discharge length than coconut oils.

As observed in other cases, glass samples were punched due to the direct electric field between the tip of the point electrode and the plane electrode before the pattern propagates up to its flashover point. However, the breakdown voltage of the samples depends on the type of the dielectric liquid.

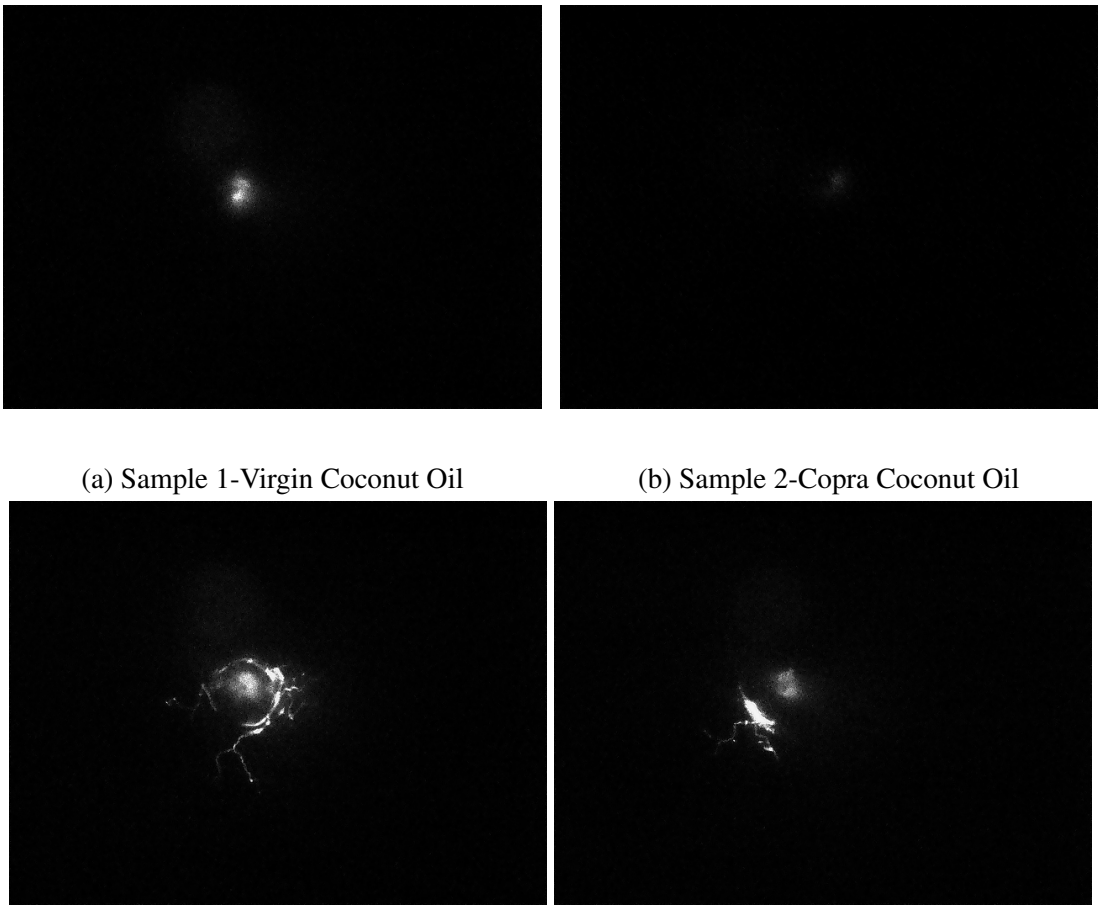

(a) Sample 1-Virgin Coconut Oil

(b) Sample 2-Copra Coconut Oil

(c) Sample 3-Soybean Oil

(d) Sample 4-Sunflower Oil

Figure 6.1: Type of dielectric liquid on creeping discharge development under 22 kV

Figures 6.5 and 6.6 show the variation of radial discharge length versus applied voltage and final discharge length versus applied voltage receptively. Sunflower oil and soybean oil make longer discharges than coconut oils. That is evident according to the patterns given by optical observation. Table 6.1 shows the variation of fraction dimension of the pattern propagating over considered oil/glass interfaces. fractal dimension with copra coconut oil is slightly higher than other cases owing to its higher order ramification. Dimensions correspond to soybean and sunflower oil are nearly equal.

Table 6.1: Variation of Fractal Dimension with the type of oil

Oil type	Virgin coconut oil	Copra coconut oil	Soybean oil	Sunflower oil
Fractal Dimension	1.254	1.32	1.209	1.203

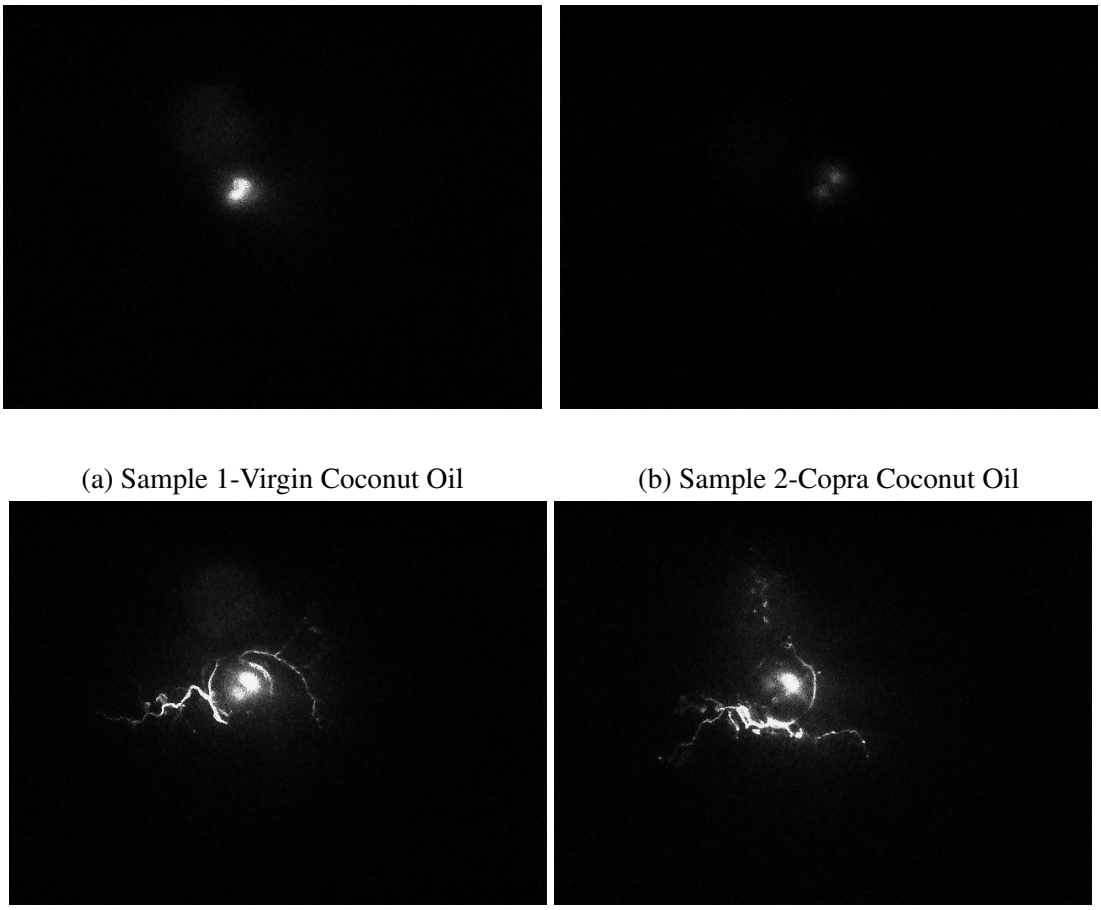

(a) Sample 1-Virgin Coconut Oil

(b) Sample 2-Copra Coconut Oil

(c) Sample 3-Soybean Oil

(d) Sample 4-Sunflower Oil

Figure 6.2: Type of dielectric liquid on creeping discharge development under 26 kV

6.6 Discussion

Breakdown voltages as seen in Table 6.2 were found out according to IEC 60156 standard test method at room temperature of 26 ^{0}C at University of Moratuwa, Sri Lanka, in which sphere gaps of 2.5 mm distance were used. It can be seen that the effect of the dielectric liquid on the size of the discharge pattern and the dielectric breakdown voltage can be explained by considering the permittivity mismatch between solid and liquid dielectrics. Permittivity difference affects the electric field strength at the tip of the point electrode [1]. Therefore, as the mismatch increases, both tangential and direct component of the electric field increase, facilitating more discharges and decreasing the dielectric breakdown voltage of the solid material sample.

(a) Sample 1-Virgin Coconut Oil

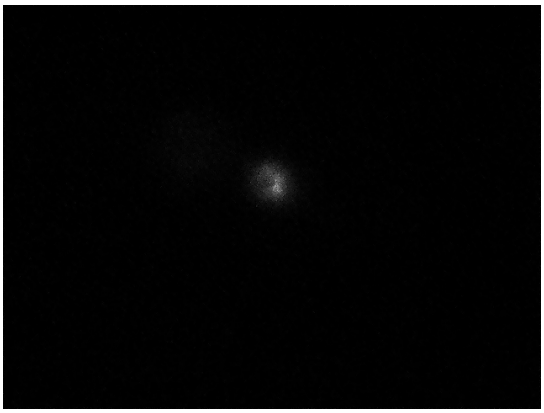

(b) Sample 2-Copra Coconut Oil

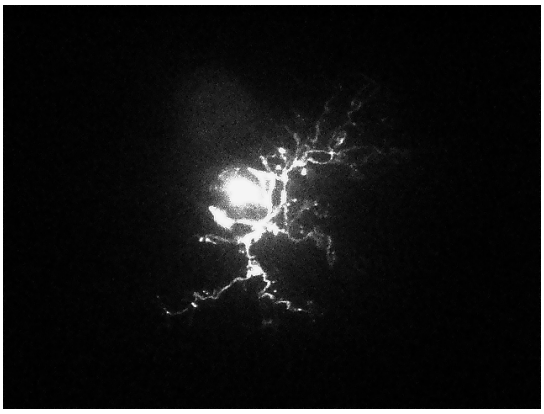

(c) Sample 3-Soybean Oil

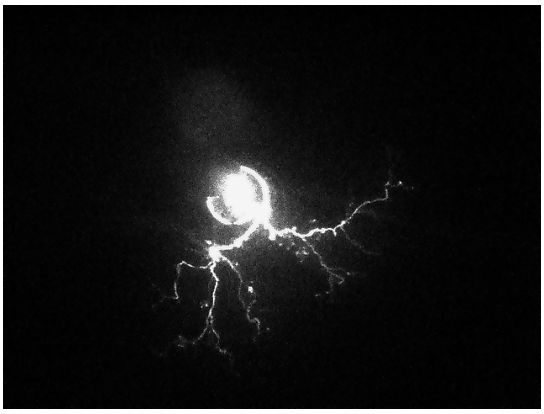

(d) Sample 4-Sunflower Oil

Figure 6.3: Type of dielectric liquid on creeping discharge development under 30 kV

(a) Sample 1-Virgin Coconut Oil

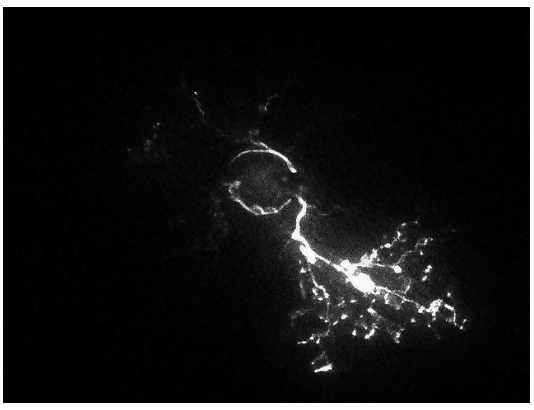

(b) Sample 2-Copra Coconut Oil

Figure 6.4: Type of dielectric liquid on creeping discharge development under 36 kV

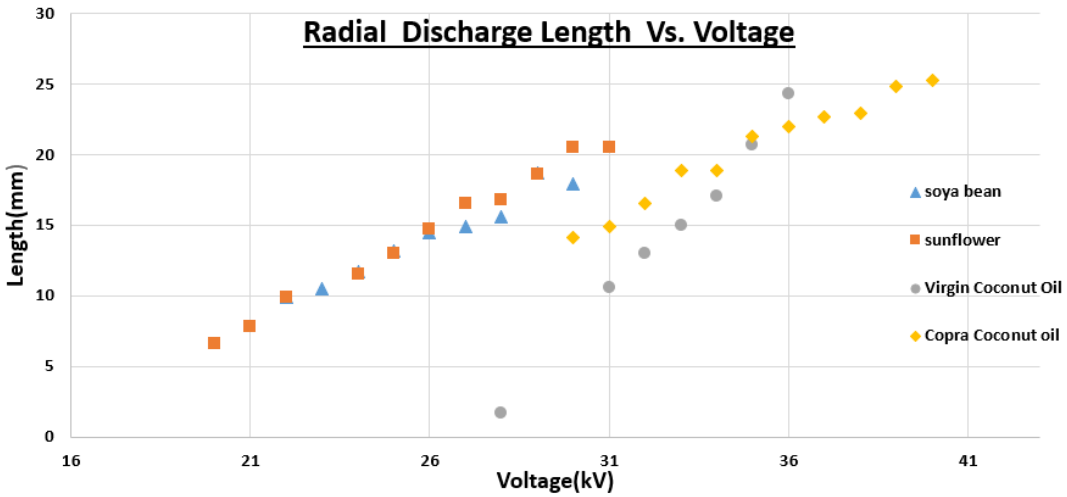

Figure 6.5: Variation of the radial discharge length of the creeping discharges propagating over the solid samples versus the applied AC voltage for different oil samples.

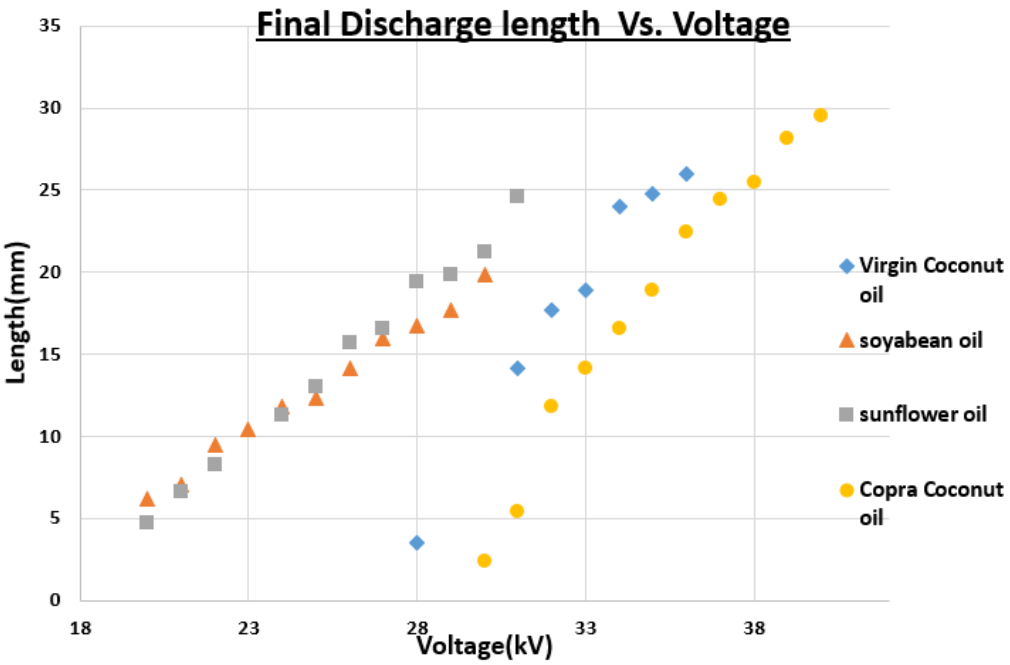

Figure 6.6: Variation of the final discharge length of the creeping discharges propagating over the solid samples versus the applied AC voltage for different oil samples.

The tangential electric field is considered as the driving forces of creeping discharges over dielectric materials [137]. The variation of the tangential electric field at the tip of the point electrode is obtained for the modelled apparatus. The plane electrode is

Table 6.2: Dielectric properties of oil samples

	Sample 1	Sample 2	Sample 3	Sample 4
Breakdown Voltage(kV)	15.8	15	15.4	15
Dielectric Constant	2.9	2.9	2.65	2.68
Breakdown Voltage of Solid Samples(kV)	36	40	30	32

grounded and voltage of 1 kV is applied to the point electrode. Table 6.3 shows the variation of the tangential and normal electric field at the tip of the point electrode upon the oil type.

Table 6.3: Electric field components at the tip of the point electrode obtained using COMSOL package for different oil samples, for a voltage U = 1 kV and a solid thickness e = 5 mm

	Sample 1	Sample 2	Sample 3	Sample 4
Dielectric constant	2.9	2.9	2.65	2.68
Tangent electric field at the tip(kV/cm)	41.3	41.3	44.6	44.2
Normal electric filed at the tip(kV/cm)	187.8	187.8	228.0	222.6

Figures 6.7a and 6.7b show the distribution of the electric fields vectors at the tip of the point electrode when the dielectric liquids are sample 1 and sample 3. The visual observation does not show any variation between the magnitude and the direction of vectors. Therefore, a dielectric liquid is defined of which dielectric constant is 4.5 to see the variation of electric field vectors clearly. Figure 6.8 shows the corresponding simulated electric field distribution. The result shows the significance of the dielectric constant of the liquid over the intensity of the electric field at the tip of the point electrode.

6.7 Conclusions

In this chapter, experiments are carried out with a high-speed camera to investigate the effect the dielectric liquid on the creeping discharge propagation on the surface of

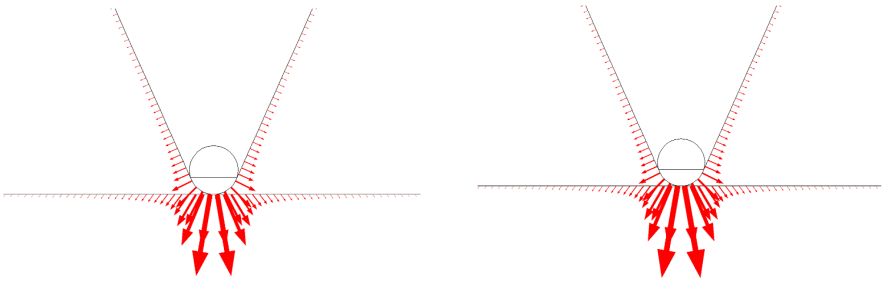

(a) $\varepsilon_{oil} = 2.9$ (b) $\varepsilon_{oil} = 2.65$

Figure 6.7: Electric field distribution at the tip of the point electrode

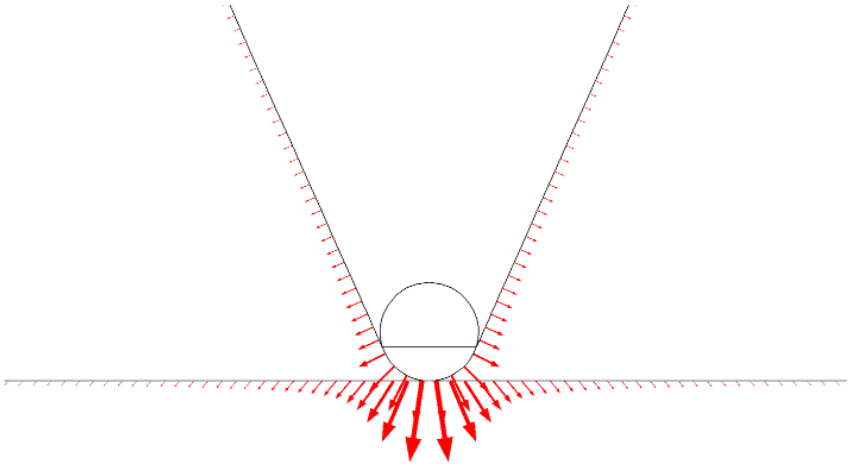

Figure 6.8: Electric Field distribution at the tip of the point electrode $\varepsilon_{oil} = 4.5$

glass under AC divergent electric field considering four different vegetable oils; Virgin coconut oil, copra type coconut oil, sunflower oil and soybean oil.

It is identified that the effect of permittivity mismatch can be used to explain the characteristics of creeping propagation such a size and discharge length. Discharge lengths increase as the voltage increases as observed in previous chapters. As the permittivity difference increases, the electric field at the triple junction is enhanced increasing both tangential and direct components. It facilitates more discharges decreasing the voltage at which the glass material is punched due to direct field component. Therefore, there

is an inverse relationship between the dielectric constant of the liquid dielectric and corresponding discharge lengths and fractal dimension values.

CHAPTER 7

CONCLUSIONS AND FUTURE WORKS

Solid/liquid interfaces can be seen in oil filled high voltage apparatus such as transformer, switchgear, circuit breakers and capacitors. The composite insulation system is supposed to enhance the condition of the insulation system of a high voltage asset. However, the solid/liquid interface facilitates creeping discharge development when the electric field strength exceeds a threshold value. Nowadays the world is looking forward to use alternative liquid as a substitute of mineral oil due to some of the disadvantages of petroleum-based mineral oil. Researches are being conducted to add nano-fillers to improve the dielectric properties of insulating polymers. However, there are less studies regarding the creeping discharge propagation associated with alternative liquid and solid materials. Therefore, manufacturers are not willing to take a risk the consequence of designing HV apparatus with nano-dielectric materials and natural ester oils without a proper understanding about the discharge behaviour under a divergent electric field. This thesis focused on studying the fractal characteristics of creeping discharge patterns propagating on solid materials immersed in insulating oil to minimize the effect of damages occurred due to creeping discharge activity.

In this thesis, Experimental studies were carried out in order to carry out fractal analysis of creeping discharges propagating over various solid/liquid interfaces. A test cell with a point-plane electrode configuration was developed in order to study the characteristics of creeping discharge propagation over solid insulators immersed in insulation oil. A three dimensional model of the test cell was developed using COMSOL Multiphysics which allows finite element analysis, to simulate the electric field distribution inside the test cell,which governs the creeping discharge inception and propagation

characteristics.

An outline of the thesis is given below.

1. An investigation was performed to adopt the fractal analysis method to analyse creeping discharge patterns.

2. Experimental studies were carried out to investigate the creeping discharge propagation over glass, acrylic, pure epoxy and nano-composite surface under AC stress. Amount of tree formation on each surface was compared in terms of discharge lengths, fractal dimension and surface profile.

3. A detail investigation was carried out using a laboratory setup to analyse two factors that can affect the creeping discharge propagation on solid/liquid interface, namely material thickness and oil level. Computer simulation of electric field variation was studied to support the experimental observations.

4. Experimental studies were carried out to find out the suitability of four different type of ester oils; copra type coconut oil, virgin coconut oil, soybean oil and sunflower oil, according to the amount of tree formation on glass material samples immersed in the liquid oil.

Following sections will present the major findings in this research program, conclusions and recommendations for future work.

7.1 Conclusions

Firstly, creeping discharge tree formation on nano-composite epoxy insulating material was compared with that of other materials such as glass and acrylic. Those two materials, along with the pure epoxy and nano-composite epoxy samples have been tested to verify the nano -silica effect on the creeping discharge characteristics. The research work reveals that considered nano- silica indeed can enhance the dielectric

properties in terms of dielectric breakdown strength. However, nano-particles affect the creeping discharge propagation negatively. The main reason is the relative permittivity increment of the epoxy material with the introduction of nano-particles. It was suggested that the particles size is not sufficient to reduce the mobility of polymer chains. However, the fractal dimension corresponding to the pattern propagation over nano-composite was slightly lower than that corresponds to the pure epoxy material because nano-particles have reduced the electron emission from the surface. Therefore, it reduces the amount of ramification.

It could be seen that the permittivity value depended capacitive effect has increased the corresponding discharge length values. Smooth surfaces allow the creeping discharges to creep into the material and the surface profile has a significant effect on the discharge propagation. Therefore, the results show that just by considering the dielectric constant of the materials, it is not possible to predict their amount of tree formation.

This thesis next studied the effect of insulation geometry over creeping discharge propagation. The capacitance of the insulator could contribute the pattern propagation in two ways.

1. Amount of stored charges on the surface on the insulator depend on the capacitance.
2. The electric field at the tip of point electrode is enhanced upon increasing the capacitance.

Therefore, it could be seen that with the increase of the material thickness, inception voltage became lower facilitating more discharge on the insulator surface.

The thesis next studied the effect of oil pressure on creeping discharge propagation. The results showed that when the oil level is increased, the amount of ramification and discharge lengths decrease. The effect of the tangential electric field at the tip of the point electrode on the pattern propagation becomes a constant after a threshold oil level

and then the pattern propagation solely depends on the pressure. However, it is not a good idea to reduce the oil level significantly as mass transfer/electro-hydrodynamic motion leads to concentrate the space charge more around the point electrode increasing the amount of tree formation. Therefore, two methods could be identified on which the propagation depends with the variation of the oil level.

1. On tangential components of the electric field at the tip of the point electrode, which is considered to be the driving force of creeping discharge
2. On the pressure on the solid/liquid interface generated by the mass of the oil.

This thesis next studied the effect of using alternative dielectric liquids on creeping discharge propagation. It could be seen that the amount of tree formation changes with the type of oil that is being used. Permittivity mismatch between the liquid and the solid can be used to explain the characteristics of creeping propagation on the insulation. Permittivity mismatch affects the electric field strength on the insulator surface. The results showed that there is an inverse relationship between the dielectric constant of the liquid, and discharge lengths and fractal dimension.

7.2 Future Works

Creeping discharge activity can be observed on solid/liquid interfaces inside high voltage assets and they can lead to the failure of the composite insulation system when the electric field exceeds a threshold value. A proper understanding of creeping discharge initiation and propagation is necessary in the design stage of oil filled high voltage apparatus. However, the creeping discharge propagation involves a complicated mechanism and the discharge may initiate unexpectedly without any obvious cause. Although environmentally friendly vegetable oils and a few types of insulating material including nano composite have been taken into the investigations, a few recommendations are also given for future work in this area of research.

1. The amount of moisture absorbed by the oils may depend on few conditions. Even if moisture-free samples are taken into the investigation and the atmospheric condition is kept constant throughout the test period, the amount of moisture absorbed by the oil depends on properties of the oil. Therefore, the effect of moisture amount of dielectric liquid on the behaviour of creeping discharges should be investigated in detail.

2. When the particle size of the silicon dioxide increases, it increases the dielectric constant of the material facilitating more discharges. Therefore creeping discharge behaviour on nano-composite samples with different type of fillers, different filler loading and particle sizes should be investigated.

3. Most of the Creeping discharge test on alternative liquid and solid material have been limited to AC voltage and impulse voltages. Investigation on different types of voltages is necessary to optimize the high voltage assets.

BIBLIOGRAPHY

[1] L. Kebbabi and A. Beroual, "Optical and electrical characterization of creeping discharges over solid/liquid interfaces under lightning impulse voltage," *IEEE Transactions on Dielectrics and Electrical Insulation*, vol. 13, no. 3, pp. 565–571, June 2006.

[2] X. Yi, "Characteristics of creepage discharges along ester-pressboard interfaces under ac stress," Ph.D. dissertation, The University of Manchester (United Kingdom), 2012.

[3] E. A. Goodman, "Today's transformer insulation systems," *IEEE Transactions on Industry Applications*, vol. IA-8, no. 4, pp. 404–411, July 1972.

[4] M. Wang, A. J. Vandermaar, and K. D. Srivastava, "Review of condition assessment of power transformers in service," *IEEE Electrical Insulation Magazine*, vol. 18, no. 6, pp. 12–25, Nov 2002.

[5] A. Zouaghi and A. Beroual, "Barrier effect on the dielectric strength of oil gaps under dc voltage," in *Conference Record of the 1998 IEEE International Symposium on Electrical Insulation (Cat. No.98CH36239)*, vol. 2, June 1998, pp. 640–643 vol.2.

[6] A. Beroual and A. Boubakeur, "Influence of barriers on the lightning and switching impulse strength of mean air gaps in point/plane arrangements," *IEEE Transactions on Electrical Insulation*, vol. 26, no. 6, pp. 1130–1139, Dec 1991.

[7] I. Fofana, A. Beroual, and A. Boubakeur, "Influence of insulating barriers on positive long air gaps in divergent field," in *1999 Eleventh International Symposium on High Voltage Engineering*, vol. 3, Aug 1999, pp. 321–324 vol.3.

[8] K. Siodla, W. Ziomek, and E. Kuffel, "The volume and area effect in transformer oil," in *Conference Record of the the 2002 IEEE International Symposium on Electrical Insulation (Cat. No.02CH37316)*, April 2002, pp. 359–362.

[9] Y. Kawaguchi, H. Murata, and M. Ikeda, "Breakdown of transformer oil," *IEEE Transactions on Power Apparatus and Systems*, vol. PAS-91, no. 1, pp. 9–23, Jan 1972.

[10] Y. Bertrand and L. C. Hoang, "Vegetal oils as substitute for mineral oils," in *Proceedings of the 7th International Conference on Properties and Applications of Dielectric Materials (Cat. No.03CH37417)*, vol. 2, June 2003, pp. 491–494 vol.2.

[11] M. Eklund, "Mineral insulating oils; functional requirements, specifications and production," in *Conference Record of the 2006 IEEE International Symposium on Electrical Insulation*, June 2006, pp. 68–72.

[12] F. Murdiya, "Research on creeping discharge phenomena in insulating oils: vegetable-based oils as substitute of mineral oil," Ph.D. dissertation, Ph. D Thesis, Department of Electrical and Electronic Engineering, Kanazawa Institute of Technology (KIT), Japan, 2015.

[13] Q. Liu and Z. D. Wang, "Streamer characteristic and breakdown in synthetic and natural ester transformer liquids with pressboard interface under lightning impulse voltage," *IEEE Transactions on Dielectrics and Electrical Insulation*, vol. 18, no. 6, pp. 1908–1917, December 2011.

[14] I. Fofana, J. S. N'cho, J. C. Olivares-Galvan, R. Escarela-Perez, and P. S. Georgilakis, "Comparative studies of the stabilities to oxidation and electrical discharge between ester fluids and transformer oils," in *2011 North American Power Symposium*, Aug 2011, pp. 1–4.

[15] B. Ellis, *Chemistry and Technology of Epoxy Resins*. Springer Netherlands, 01 1993.

[16] S. Singha and M. J. Thomas, "Dielectric properties of epoxy nanocomposites," *IEEE Transactions on Dielectrics and Electrical Insulation*, vol. 15, no. 1, pp. 12–23, February 2008.

[17] C. Zhang, R. Mason, and G. C. Stevens, "Dielectric properties of alumina-polymer nanocomposites," in *CEIDP '05. 2005 Annual Report Conference on Electrical Insulation and Dielectric Phenomena, 2005.*, Oct 2005, pp. 721–724.

[18] C. Zou, J. C. Fothergill, and S. W. Rowe, "The effect of water absorption on the dielectric properties of epoxy nanocomposites," *IEEE Transactions on Dielectrics and Electrical Insulation*, vol. 15, no. 1, pp. 106–117, February 2008.

[19] S.-H. Xie, B.-K. Zhu, J.-B. Li, X.-Z. Wei, and Z.-K. Xu, "Preparation and properties of polyimide/aluminum nitride composites," *Polymer testing*, vol. 23, no. 7, pp. 797–801, 2004.

[20] J. Wang and X.-S. Yi, "Preparation and the properties of pmr-type polyimide composites with aluminum nitride," *Journal of applied polymer science*, vol. 89, no. 14, pp. 3913–3917, 2003.

[21] C. P. Wong and R. S. Bollampally, "Comparative study of thermally conductive fillers for use in liquid encapsulants for electronic packaging," *IEEE Transactions on Advanced Packaging*, vol. 22, no. 1, pp. 54–59, Feb 1999.

[22] T. Tanaka, Y. Ohki, M. Ochi, M. Harada, and T. Imai, "Enhanced partial discharge resistance of epoxy/clay nanocomposite prepared by newly developed organic modification and solubilization methods," *IEEE Transactions on Dielectrics and Electrical Insulation*, vol. 15, no. 1, pp. 81–89, February 2008.

[23] L. Schadler, L. Brinson, and W. Sawyer, "Polymer nanocomposites: a small part of the story," *Jom*, vol. 59, no. 3, pp. 53–60, 2007.

[24] H. Zainuddin, "Study of surface discharge behaviour at the oil-pressboard interface," Ph.D. dissertation, University of Southampton, 2013.

[25] K. Jang, “Creepage discharge behaviour and numerical model analysis at the oil/pressboard interface with the effect of nano composite coating,” Ph.D. dissertation, , 2017.

[26] J. A. Lapworth and A. Wilson, “Transformer internal over-voltages caused by remote energisation,” in *2007 IEEE Power Engineering Society Conference and Exposition in Africa - PowerAfrica*, July 2007, pp. 1–6.

[27] P. Jarman, Z. Wang, Q. Zhong, and M. Ishak, “End-of-life modelling for power transformers in aged power system networks,” 08 2009.

[28] A. Beroual and L. Kebbabi, “Influence of hydrostatic pressure on morphology and final length of creeping discharges over solid/liquid interfaces under impulse voltages,” in *2008 IEEE International Conference on Dielectric Liquids*, June 2008, pp. 1–4.

[29] Partial discharge. [Online]. Available: http://rbswitchgeargroup.com/partial-discharge

[30] J. Lucas, D. Abeysundara, C. Weerakoon, K. Perera, K. Obadage, and K. Gunatunga, “Coconut oil insulated distribution transformer,” in *IEE Sri Lanka Annual Conference*, 2001, pp. 1–5.

[31] B. S. H. M. S. Y. Matharage, M. A. R. M. Fernando, M. A. A. P. Bandara, G. A. Jayantha, and C. S. Kalpage, “Performance of coconut oil as an alternative transformer liquid insulation,” *IEEE Transactions on Dielectrics and Electrical Insulation*, vol. 20, no. 3, pp. 887–898, June 2013.

[32] J. G. C. Samuel, G. Lucas, M. Fu, P. J. Howard, and S. Lafon-Placette, “Nanodielectrics research for application to high voltage insulation systems,” in *2012 47th International Universities Power Engineering Conference (UPEC)*, Sept 2012, pp. 1–6.

[33] K. Y. Lau and M. Piah, "Polymer nanocomposites in high voltage electrical insulation perspective: a review," *Malaysian Polymer Journal*, vol. 6, no. 1, pp. 58–69, 2011.

[34] M. Liang and K. Wong, "Improving the long-term performance of composite insulators use nanocomposite: A review," *Energy Procedia*, vol. 110, pp. 168–173, 2017.

[35] L. Niemeyer, L. Pietronero, and H. J. Wiesmann, "Fractal dimension of dielectric breakdown," *Physical Review Letters - PHYS REV LETT*, vol. 52, pp. 1033–1036, 03 1984.

[36] T. Cavallo *et al.*, "Ii. an account of some new experiments in electricity, with the description and use of two new electrical instruments," *Philosophical Transactions of the Royal Society of London*, vol. 70, pp. 15–29, 1780.

[37] B. Silliman Jr and W. H. Goode, "A daguerreotype experiment by galvanic light," *Journal of the Franklin Institute*, vol. 35, no. 1, pp. 68–70, 1843.

[38] J. A. De Luc, *Idées sur la météorologie*. Spilsbury, 1786, vol. 1.

[39] J. M. Eder, *Ausführliches handbuch der photographie*. W. Knapp, 1884, vol. 1.

[40] Y. Takahashi, "Two hundred years of lichtenberg figures," *Journal of Electrostatics*, vol. 6, no. 1, pp. 1 – 13, 1979. [Online]. Available: http://www.sciencedirect.com/science/article/pii/0304388679900202

[41] G. C. Lichtenberg and H. Pupke, *Über eine neue Methode, die Natur und die Bewegung der Elektrischen Materie zu erforschen:" Lichtenbergsche Figuren"*. Akademische Verlagsgesellschaft Geest & Portig, 1956, no. 246.

[42] R. Hewa Lunuwilage, "Study of pole-top fire development in power distribution networks," Ph.D. dissertation, URMIT University, 2013.

[43] O. N. Rood, "Art. xxii.–on the study of the electric spark by the aid of photography," *American Journal of Science and Arts (1820-1879)*, vol. 33, no. 98, p. 219, 1862.

[44] M. Toepler, “Über den inneren aufbau von gleitbüscheln und die gesetze ihrer leuchtfäden,” *Annalen der Physik*, vol. 358, no. 11, pp. 217–234, 1917.

[45] C. E. Magnusson, “Lichtenberg figures,” *Journal of the A.I.E.E.*, vol. 47, no. 11, pp. 828–835, Nov 1928.

[46] P. O. Pedersen, *On the Lichtenberg figures*. Høst, 1919.

[47] F. H. Merrill and A. Von Hippel, “The atomphysical interpretation of lichtenberg figures and their application to the study of gas discharge phenomena,” *Journal of Applied Physics*, vol. 10, no. 12, pp. 873–887, 1939. [Online]. Available: https://doi.org/10.1063/1.1707274

[48] J. G. Anderson and T. W. Liao, “Propagation mechanism of discharge on oil surfaces,” *Electrical Engineering*, vol. 74, no. 10, pp. 909–909, Oct 1955.

[49] A. M. Thomas, “”heat developed” and ”powder” lichtenberg figures and the ionization of dielectric surfaces produced by electrical impulses,” *British Journal of Applied Physics*, vol. 2, no. 4, p. 98, 1951. [Online]. Available: http://stacks.iop.org/0508-3443/2/i=4/a=303

[50] E. Nasser, “Some physical properties of electrical discharges on contaminated-surfaces,” *IEEE Transactions on Power Apparatus and Systems*, vol. PAS-87, no. 4, pp. 957–963, April 1968.

[51] E. Nasser and D. C. Schroder, “Secondary leader channels in the impulse breakdown of air and nitrogen,” *Journal of Applied Physics*, vol. 40, no. 7, pp. 2793–2799, 1969. [Online]. Available: https://doi.org/10.1063/1.1658077

[52] E. Nasser, “Development of spark in air from a negative point,” *Journal of Applied Physics*, vol. 42, no. 7, pp. 2839–2847, 1971. [Online]. Available: https://doi.org/10.1063/1.1660636

[53] B. Gross, “Irradiation effects in plexiglas,” *Journal of Polymer Science*, vol. 27, no. 115, pp. 135–143, 1958. [Online]. Available: https://onlinelibrary.wiley.com/doi/abs/10.1002/pol.1958.1202711511

[54] J. D. Cross, K. D. Srivastava, and J. A. Chavez, "Optical observations of discharges across dielectric surfaces in vacuum and in sf lt;inf gt;6 lt;/inf gt;," in *Conference on Electrical Insulation Dielectric Phenomena - Annual Report 1972*, Oct 1972, pp. 91–97.

[55] A. Kawashima and S. Hoh, "Lichtenberg figures on various electrical insulating materials," *IEEE Transactions on Electrical Insulation*, vol. EI-13, no. 1, pp. 51–56, Feb 1978.

[56] P. M. Mitchinson, "Surface tracking in the inter-phase region of large transformers," Ph.D. dissertation, University of Southampton, 2008.

[57] A. H. Sharbaugh, J. C. Devins, and S. J. Rzad, "Progress in the field of electric breakdown in dielectric liquids," *IEEE Transactions on Electrical Insulation*, vol. EI-13, no. 4, pp. 249–276, Aug 1978.

[58] J. C. Devins and S. J. Rzad, "Streamer propagation in liquids and over liquid-solid interfaces," in *Conference on Electrical Insulation Dielectric Phenomena - Annual Report 1982*, Oct 1982, pp. 383–394.

[59] S. Ohgaki and Y. Tsunoda, "A study of the positive streamer growth under surface discharge configuration in liquid paraffin," *IEEE Transactions on Electrical Insulation*, vol. EI-19, no. 6, pp. 594–601, Dec 1984.

[60] P. Atten and A. Sakker, "Streamer propagation over a liquid-solid interface," in *10th International Conference on Conduction and Breakdown in Dielectric Liquids*, Sept 1990, pp. 441–445.

[61] R. Hanaoka, T. Kohrin, T. Miyagawa, and T. Nishi, "Creepage discharge characteristics over solid-liquid interfaces with grounded side electrode," *IEEE Transactions on Dielectrics and Electrical Insulation*, vol. 9, no. 2, pp. 308–315, April 2002.

[62] A. Beroual and N. K. Bedoui, "Influence of hydrostatic pressure on the characteristics of discharges propagating on solid/liquid insulating interfaces under

ac and dc voltages," in *Proceedings of 2002 IEEE 14th International Conference on Dielectric Liquids. ICDL 2002 (Cat. No.02CH37319)*, July 2002, pp. 207–210.

[63] L. Kebbabi and A. Beroual, "Influence of the properties of materials and the hydrostatic pressure on creepage discharge characteristics over solid/liquid interfaces," in *2003 Annual Report Conference on Electrical Insulation and Dielectric Phenomena*, Oct 2003, pp. 293–296.

[64] ——, "Fractal analysis of creeping discharge patterns propagating at solid/liquid interfaces-influence of the nature and geometry of solid insulators," in *CEIDP '05. 2005 Annual Report Conference on Electrical Insulation and Dielectric Phenomena, 2005.*, Oct 2005, pp. 132–135.

[65] A. Beroual and L. Kebbabi, "Influence of hydrostatic pressure on morphology and final length of creeping discharges over solid/liquid interfaces under impulse voltages," in *2008 IEEE International Conference on Dielectric Liquids*, June 2008, pp. 1–4.

[66] ——, "Influence of capacitive effects on the characteristics of creeping discharges propagating over solid/liquid interfaces under impulse voltages," in *2008 Annual Report Conference on Electrical Insulation and Dielectric Phenomena*, Oct 2008, pp. 357–360.

[67] ——, "Analysis of cumulative number and polarity of creeping discharges initiated at solid/liquid interfaces subjected to ac voltage," in *2009 IEEE Conference on Electrical Insulation and Dielectric Phenomena*, Oct 2009, pp. 380–383.

[68] A. Beroual, M. L. Coulibaly, O. Aitken, and A. Girodet, "Study of creeping discharges propagating over epoxy resin insulators in presence of different gases and mixtures," in *2010 International Conference on High Voltage Engineering and Application*, Oct 2010, pp. 89–92.

[69] A. Beroual and V. Dang, "Fractal analysis of creeping discharge propagating over pressboard immersed in mineral and vegetable oils," in *2011 Annual Report*

Conference on Electrical Insulation and Dielectric Phenomena, Oct 2011, pp. 501–504.

[70] V. Dang and A. Beroual, "Investigations on creeping discharges propagating over pressboard immersed in mineral and vegetable oils submitted to impulse voltage," in *2011 Annual Report Conference on Electrical Insulation and Dielectric Phenomena*, Oct 2011, pp. 411–414.

[71] S. Zohdi, K. L. Wong, H. L. Rasara, and C. Henschke, "Study of creeping discharge on hardwood timber under ac and dc voltages," in *2013 Australasian Universities Power Engineering Conference (AUPEC)*, Sept 2013, pp. 1–5.

[72] Y. Z. Lv, Y. Zhou, C. R. Li, K. B. Ma, Q. Wang, W. Wang, S. N. Zhang, and Z. Y. Jin, "Nanoparticle effects on creeping flashover characteristics of oil/pressboard interface," *IEEE Transactions on Dielectrics and Electrical Insulation*, vol. 21, no. 2, pp. 556–562, April 2014.

[73] F. Sadaoui and A. Beroual, "Ac creeping discharges propagating over solid amp;8211;gas interfaces," *IET Science, Measurement Technology*, vol. 8, no. 6, pp. 595–600, 2014.

[74] M. A. Douar, A. Beroual, and X. Souche, "Propagation of creeping discharges in air depending on the electric field direction and insulator materials under lightning impulse voltage," in *2015 IEEE Conference on Electrical Insulation and Dielectric Phenomena (CEIDP)*, Oct 2015, pp. 880–883.

[75] Y. Lv, Y. Zhou, C. Li, Y. Ge, and B. Qi, "Creeping discharge characteristics of nanofluid-impregnated pressboards under ac stress," *IEEE Transactions on Plasma Science*, vol. 44, no. 11, pp. 2589–2593, Nov 2016.

[76] X. Zhou, H. B. Shi, M. Kuhnke, P. Werle, E. Gockenbach, and H. Borsi, "Evolution and discharge pattern of creeping discharge at aged oil/pressboard interface," in *2016 IEEE Conference on Electrical Insulation and Dielectric Phenomena (CEIDP)*, Oct 2016, pp. 1053–1056.

[77] A. Beroual and F. Sadaoui, “Analysis of partial discharges and their development into creeping discharges at solid/gas interface under ac voltage,” in *2017 IEEE Electrical Insulation Conference (EIC)*, June 2017, pp. 38–41.

[78] T. Nishikawa, R. Hanaoka, K. Miyagi, K. Takamoto, and S. Nishikawa, “Creeping discharge at vegetable-based oil/pressboard interface under rectangular impulse voltage,” in *2017 IEEE 19th International Conference on Dielectric Liquids (ICDL)*, June 2017, pp. 1–4.

[79] Y. Sawada, S. Ohta, M. Yamazaki, and H. Honjo, “Self-similarity and a phase-transition-like behavior of a random growing structure governed by a nonequilibrium parameter,” *Phys. Rev. A*, vol. 26, pp. 3557–3563, Dec 1982. [Online]. Available: https://link.aps.org/doi/10.1103/PhysRevA.26.3557

[80] R. McLeod, D. Liu, W. Pries, K. Kao, and H. Card, “Polarity dependence of fractal geometry in partial discharge in dielectrics,” *Solid state communications*, vol. 56, no. 2, pp. 197–199, 1985.

[81] S. Satpathy, “Dielectric breakdown in three dimensions,” in *Fractals in Physics*. Elsevier, 1986, pp. 173–176.

[82] H. J. Wiesmann and H. R. Zeller, “A fractal model of dielectric breakdown and prebreakdown in solid dielectrics,” in *Conference on Electrical Insulation Dielectric Phenomena - Annual Report 1986*, Nov 1986, pp. 385–390.

[83] S. Fujimori, “Analysis of electric discharge with fractal dimension,” in *Conference on Electrical Insulation Dielectric Phenomena - Annual Report 1984*, Oct 1984, pp. 374–380.

[84] K. Kudo and S. Maruyama, “Fractals of computer simulated tree,” in *Annual Conference on Electrical Insulation and Dielectric Phenomena*, Oct 1990, pp. 502–507.

[85] T. Czaszejko, "3-d electrical network model of water tree," in *Proceedings of Conference on Electrical Insulation and Dielectric Phenomena - CEIDP '96*, vol. 2, Oct 1996, pp. 799–802 vol.2.

[86] L. A. Dissado, J. C. Fothergill, N. Wise, and J. Cooper, "A deterministic model for branched structures in the electrical breakdown of solid polymeric dielectrics," *Journal of Physics D: Applied Physics*, vol. 33, no. 19, p. L109, 2000. [Online]. Available: http://stacks.iop.org/0022-3727/33/i=19/a=103

[87] H. Uehara and K. Kudo, "Temporal propagation characteristics of simulation tree considering growth probability," in *Proceedings of 2005 International Symposium on Electrical Insulating Materials, 2005. (ISEIM 2005).*, vol. 1, June 2005, pp. 17–20 Vol. 1.

[88] D. Amarasinghe and U. Sonnadara, "Fractal characteristics of simulated electrical discharges," *Journal of the National Science Foundation of Sri Lanka*, vol. 36, no. 2, pp. 137–143, 2008.

[89] A. Garg, A. Agrawal, and A. Negi, "A review on natural phenomenon of fractal geometry," *International Journal of Computer Application*, vol. 86, no. 4, 2014.

[90] J. Theiler, "Estimating fractal dimension," *JOSA A*, vol. 7, no. 6, pp. 1055–1073, 1990.

[91] K. Kudo, "Fractal analysis of electrical trees," *IEEE Transactions on Dielectrics and Electrical Insulation*, vol. 5, no. 5, pp. 713–727, Oct 1998.

[92] ——, "On the regularity of the branching structure of electrical trees," in *Proceedings of the Twenty-First Symposium on Electrical Insulating Materials*, Sept 1988, pp. 203–206.

[93] S. M. Prigarin, K. Sandau, M. Kazmierczak, and K. Hahn, "Estimation of fractal dimension: A survey with numerical experiments and software description," *International Journal of Biomathematics and Biostatistics*, vol. 2, no. 1, pp. 167–180, 2013.

[94] L. Kebbabi and A. Beroual, "Fractal analysis of creeping discharge patterns propagating at solid/liquid interfaces: influence of the nature and geometry of solid insulators," *Journal of Physics D: Applied Physics*, vol. 39, no. 1, p. 177, 2005.

[95] P. Grassberger and I. Procaccia, "Measuring the strangeness of strange attractors," *Physica D: Nonlinear Phenomena*, vol. 9, no. 1-2, pp. 189–208, 1983.

[96] Z. Kalantan and J. Einbeck, "On the computation of the correlation integral for fractal dimension estimation," in *2012 International Conference on Statistics in Science, Business and Engineering (ICSSBE)*, Sept 2012, pp. 1–6.

[97] A. Beroual, L. Kebbabi, E. A. Al-Ammar, and M. I. Qureshi, "Analysis of creeping discharges activity at solid/liquid interfaces subjected to ac voltage," *IET Generation, Transmission Distribution*, vol. 5, no. 9, pp. 973–978, September 2011.

[98] A. Beroual, M. L. Coulibaly, O. Aitken, and A. Girodet, "Effect of micro-fillers in polytetrafluoroethylene insulators on the characteristics of surface discharges in presence of SF6 CO2 and SF6-CO mixture," *IET Generation, Transmission and Distribution*, vol. 6, no. 10, pp. 951 – 957, Oct. 2012. [Online]. Available: https://hal.archives-ouvertes.fr/hal-00742439

[99] A. Beroual and M. Coulibaly, "Fractal analysis of creeping discharge propagating over solid insulators immersed in gases at different pressures," in *2012 Annual Report Conference on Electrical Insulation and Dielectric Phenomena*, Oct 2012, pp. 335–338.

[100] A. Beroual, "Relationship between the physicochemical properties of materials and the fractal dimension of creeping discharges propagating at solid/fluid interfaces," in *2016 IEEE International Power Modulator and High Voltage Conference (IPMHVC)*, July 2016, pp. 296–299.

[101] W. E. P. S. Ediriweera, K. L. I. M. P. B. Jayarathna, J. R. Lucas, and R. Samarasinghe, "Effect of the shape of the insulator on fractal characteristics of creeping

discharges," in *2018 Moratuwa Engineering Research Conference (MERCon)*, May 2018, pp. 506–510.

[102] F. Murdiya, "Research on creeping discharge phenomena in insulating oils: vegetable-based oils as substitute of mineral oil," Ph.D. dissertation, Ph. D Thesis, Department of Electrical and Electronic Engineering, Kanazawa Institute of Technology (KIT), Japan, 2015.

[103] H. Lee and S. Lee, "Finite element analysis of positive streamer propagation with lightning impulse voltage," in *2010 International Conference on Electrical Machines and Systems*, Oct 2010, pp. 1836–1839.

[104] M. Akyuz, L. Gao, V. Cooray, T. G. Gustavsson, S. M. Gubanski, and A. Larsson, "Positive streamer discharges along insulating surfaces," *IEEE Transactions on Dielectrics and Electrical Insulation*, vol. 8, no. 6, pp. 902–910, Dec 2001.

[105] C. W. Reed, "Functionalization of nanocomposite dielectrics," in *2010 IEEE International Symposium on Electrical Insulation*, June 2010, pp. 1–4.

[106] R. Kochetov, *Thermal and electrical properties of nanocomposites, including material processing*, 2012.

[107] B. Raju, B. Suresha, R. Swamy, and K. Bharath, "The effect of silicon dioxide filler on the wear resistance of glass fabric reinforced epoxy composites," *polymer composites*, vol. 18, p. 20, 2012.

[108] M. Reading and A. S. Vaughan, "Comparison of rheological, thermal and electrical properties of poly(ethylene oxide) composites with micro and nano sized silicon dioxide filler," in *2010 10th IEEE International Conference on Solid Dielectrics*, July 2010, pp. 1–4.

[109] N. Loganathan and S. Chandrasekar, "Physicochemical properties investigation in nano sized sio lt;inf gt;2 lt;/inf gt; filled silicone rubber for high voltage insu-

lation applications," in *2012 IEEE 10th International Conference on the Properties and Applications of Dielectric Materials*, July 2012, pp. 1–4.

[110] M. M. S. Shirazi, H. Borsi, and E. Gockenbach, "Evaluation of the influence of nano fillers on the electrical and dielectric properties of epoxy resin," in *2011 Electrical Insulation Conference (EIC).*, June 2011, pp. 498–501.

[111] J. Dai, Z. D. Wang, and P. Jarman, "Creepage discharge on insulation barriers in aged power transformers," *IEEE Transactions on Dielectrics and Electrical Insulation*, vol. 17, no. 4, pp. 1327–1335, August 2010.

[112] Y. Nakao, A. Mouri, T. Itooka, H. Tagashira, Y. Nakagami, M. Miyamoto, and Y. Sakai, "Propagation of creepage discharge on solid insulator in insulating oil," in *Proceedings of 1999 IEEE 13th International Conference on Dielectric Liquids (ICDL'99) (Cat. No.99CH36213)*, July 1999, pp. 257–260.

[113] L. Lundgaard, D. Linhjell, G. Berg, and S. Sigmond, "Propagation of positive and negative streamers in oil with and without pressboard interfaces," *IEEE Transactions on Dielectrics and Electrical Insulation*, vol. 5, no. 3, pp. 388–395, June 1998.

[114] M. Koch and S. Tenbohlen, "Evolution of bubbles in oil-paper insulation influenced by material quality and ageing," *IET Electric Power Applications*, vol. 5, no. 1, pp. 168–174, January 2011.

[115] O. Lesaint, A. Saker, P. Gournay, R. Tobazeon, J. Aubin, and M. Mailhot, "Streamer propagation and breakdown under ac voltage in very large oil gaps," *IEEE Transactions on Dielectrics and Electrical Insulation*, vol. 5, no. 3, pp. 351–359, June 1998.

[116] L. E. Lundgaard and O. Lesaint, "Discharges in liquids in point-plane gap under ac and impulse stress," in *Proceedings of 1995 Conference on Electrical Insulation and Dielectric Phenomena*, Oct 1995, pp. 596–599.

[117] B. F. Hampton, "Engineering problems of surface flashover," in *IEE Colloquium on Charging and Tracking of Insulators in Gaseous and Vacuum Environments*, May 1990, pp. 1/1–1/4.

[118] E. F. Kelley and R. E. Hebner, "Electro-optic field measurement at a needle tip and streamer initiation in nitrobenezene," in *Conference on Electrical Insulation Dielectric Phenomena - Annual Report 1986*, Nov 1986, pp. 272–277.

[119] P. Girdino, P. Molfino, G. Molinari, A. Viviani, G. J. Fitzpatrick, and E. O. Forster, "Effect of streamer shape and dimensions on local electric field conditions," *IEEE Transactions on Electrical Insulation*, vol. 23, no. 4, pp. 669–676, Aug 1988.

[120] W. Chadband, "On variations in the propagation of positive discharges between transformer oil and silicone fluids," *Journal of Physics D: Applied Physics*, vol. 13, no. 7, p. 1299, 1980.

[121] O. Lesaint, R. Kattan, and A. Denat, "Generation and growth of gaseous bubbles in hydrocarbon liquids under high divergent field," in *1988. Annual Report., Conference on Electrical Insulation and Dielectric Phenomena*, Oct 1988, pp. 269–274.

[122] Y. Nakao, A. Mouri, T. Itooka, H. Tagashira, Y. Nakagami, M. Miyamoto, and Y. Sakai, "Propagation of creepage discharge on solid insulator in insulating oil," in *Proceedings of 1999 IEEE 13th International Conference on Dielectric Liquids (ICDL'99) (Cat. No.99CH36213)*, July 1999, pp. 257–260.

[123] M. Krins, H. Borsi, and E. Gockenbach, "Impact of carbon particles on the electrical strength of different solid/liquid interfaces in a non-uniform field," in *Conference Record of the 1998 IEEE International Symposium on Electrical Insulation (Cat. No.98CH36239)*, vol. 2, June 1998, pp. 623–626 vol.2.

[124] K. Jang, T. Akahoshi, M. Kozako, and M. Hikita, "Nano sio2/epoxy coating effect on creepage discharge characteristics in oil/pressboard composite insulation

system," in *2016 IEEE International Conference on Dielectrics (ICD)*, vol. 1, July 2016, pp. 394–397.

[125] S. Singha and M. J. Thomas, "Dielectric properties of epoxy nanocomposites," *IEEE Transactions on Dielectrics and Electrical Insulation*, vol. 15, no. 1, pp. 12–23, February 2008.

[126] H. Zainuddin, P. Lewin, and P. Mitchinson, "Modeling the inter-phase region of high voltage transformers," in *Dielectric Liquids (ICDL), 2011 IEEE International Conference on*. IEEE, 2011, pp. 1–4.

[127] V.-H. Dang, A. Beroual, M. Coulibaly, and C. Perrier, "Investigation on creeping discharges propagating over pressboard immersed in mineral and vegetable oils submitted to ac and dc voltages," in *2012 International Conference on High Voltage Engineering and Application*, Sept 2012, pp. 215–218.

[128] T. Tanaka, "A novel concept for electronic transport in nanoscale spaces formed by islandic multi-cored nanoparticles," in *2016 IEEE International Conference on Dielectrics (ICD)*, vol. 1, July 2016, pp. 23–26.

[129] ——, "A quantum dot model for permittivity of polymer nanocomposites," in *2016 IEEE Conference on Electrical Insulation and Dielectric Phenomena (CEIDP)*, Oct 2016, pp. 40–43.

[130] A. Beroual, M.-L. Coulibaly, A. Girodet, and O. Aitken, "Relationship between the fractal dimension of creeping discharges propagating at solid/gas interfaces and the characteristics parameters of interfaces," *International Review of Electrical Engineering*, vol. 9, pp. 460–465, 01 2014.

[131] D. Faircloth, "Technological aspects: High voltage," *arXiv preprint arXiv:1404.0952*, 2014.

[132] Z. Dianchun, W. Zhengwei, Z. Dawei, and Y. Weiguo, "Effects of molecular ionization energy on liquid streamer development under dc," in *Ifost*, vol. 1, June 2013, pp. 207–211.

[133] G. J. FitzPatrick, P. J. McKenny, and E. O. Forster, "The effect of pressure on streamer inception and propagation in liquid hydrocarbons," *IEEE Transactions on Electrical Insulation*, vol. 25, no. 4, pp. 672–682, Aug 1990.

[134] O. Lesaint, R. Kattan, and A. Denat, "Generation and growth of gaseous bubbles in hydrocarbon liquids under high divergent field," in *1988. Annual Report., Conference on Electrical Insulation and Dielectric Phenomena*, Oct 1988, pp. 269–274.

[135] O. Lesaint and P. Gournay, "On the gaseous nature of positive filamentary streamers in hydrocarbon liquids. i: Influence of the hydrostatic pressure on the propagation," *Journal of Physics D: Applied Physics*, vol. 27, no. 10, p. 2111, 1994.

[136] W. H. Middendorf and G. H. Brown, "Liquid dielectrics in an electric field," *Electrical Engineering*, vol. 78, no. 12, pp. 1158–1158, Dec 1959.

[137] X. Yi and Z. Wang, "Creepage discharge on pressboards in synthetic and natural ester transformer liquids under ac stress," *IET Electric Power Applications*, vol. 7, no. 3, pp. 191–198, 2013.

[138] O. Lesaint, P. Gournay, and R. Tobazeon, "Investigations on transient currents associated with streamer propagation in dielectric liquids," *IEEE Transactions on Electrical Insulation*, vol. 26, no. 4, pp. 699–707, Aug 1991.

[139] F. Murdiya, R. Hanaoka, H. Akiyama, K. Miyagi, K. Takamoto, and T. Kano, "Creeping discharge developing on vegetable-based oil / pressboard interface under ac voltage," *IEEE Transactions on Dielectrics and Electrical Insulation*, vol. 21, no. 5, pp. 2102–2110, Oct 2014.

[140] A. Beroual and V. Dang, "Fractal analysis of creeping discharge propagating over pressboard immersed in mineral and vegetable oils," in *2011 Annual Report Conference on Electrical Insulation and Dielectric Phenomena*, Oct 2011, pp. 501–504.

[141] U. Pal, R. Patra, N. Sahoo, C. Bakhara, and M. Panda, "Effect of refining on quality and composition of sunflower oil," *Journal of food science and technology*, vol. 52, no. 7, pp. 4613–4618, 2015.

[142] "Sunflower processing." [Online]. Available: https://www.crowniron.com/oilseed-processing/sunflower-processing/

[143] A. Regitano Neto, A. Rauen, A. Mourad, E. Aparecida Henriques, and R. Alves, "Environmental effect on sunflower oil quality," *Crop Breeding and Applied Biotechnology*, vol. 16, pp. 197–204, 09 2016.

[144] *Production Method of Soyabean*. [Online]. Available: http://shodhganga.inflibnet.ac.in/bitstream/10603/88938/3/04-chapter203.pdf

[145] "Soybean oil production." [Online]. Available: http://www.oilmillmachinery.net/Soybean-Oil-Production.html

[146] B. S. H. M. S. Y. Matharage, M. A. A. P. Bandara, M. A. R. M. Fernando, G. A. Jayantha, and C. S. Kalpage, "Aging effect of coconut oil as transformer liquid insulation comparison with mineral oil," in *2012 IEEE 7th International Conference on Industrial and Information Systems (ICIIS)*, Aug 2012, pp. 1–6.

APPENDIX A

SIMULATED MODEL OF THE EXPERIMENTAL SETUP

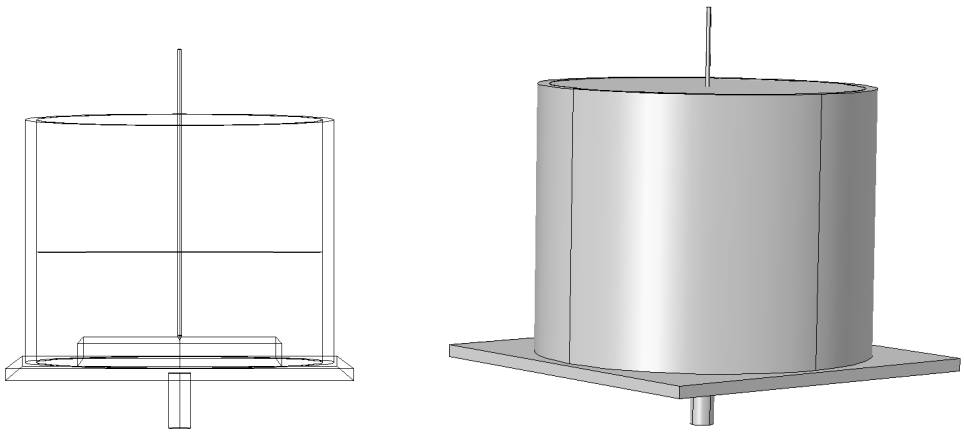

(a) Wire-frame model (b) 3D model

Figure A.1: Modelled test cell using COMSOL Multi-physics package

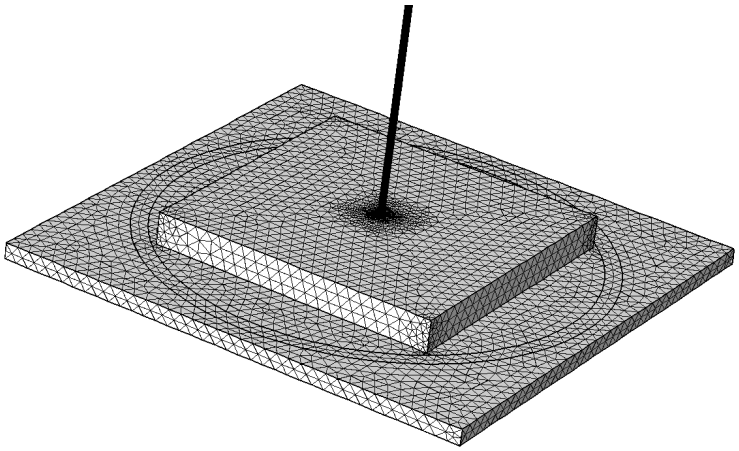

(a) on needle-bar electrode

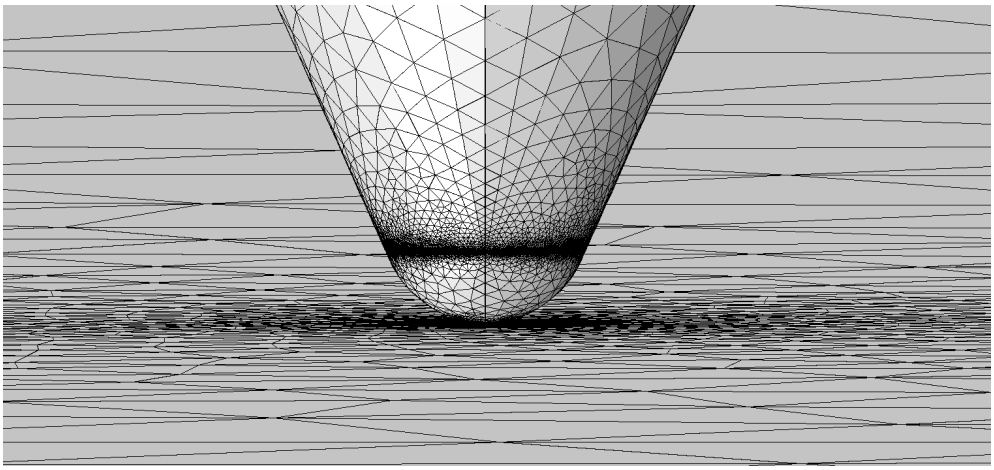

(b) on needle tip

Figure A.2: Distribution of FEM mesh

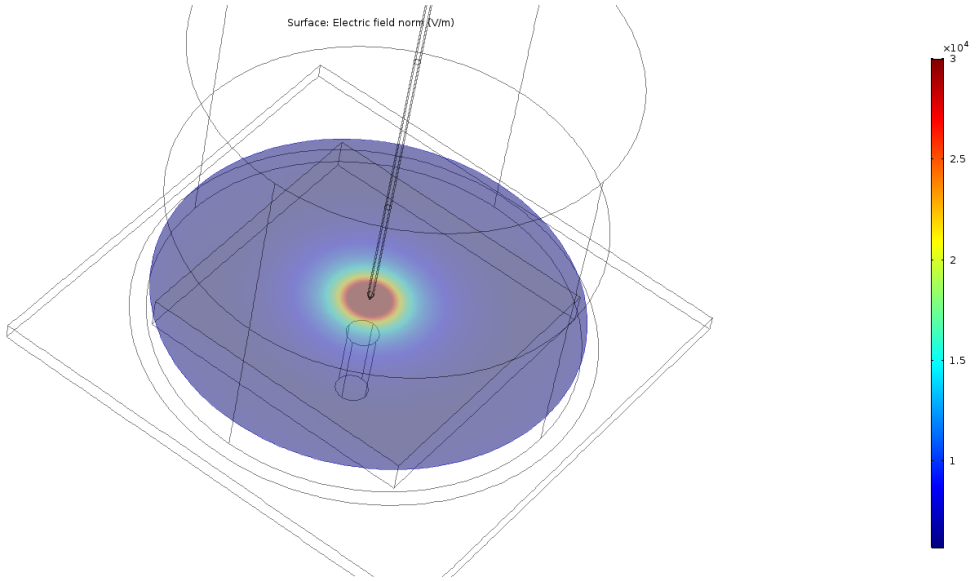

(a) surface distribution

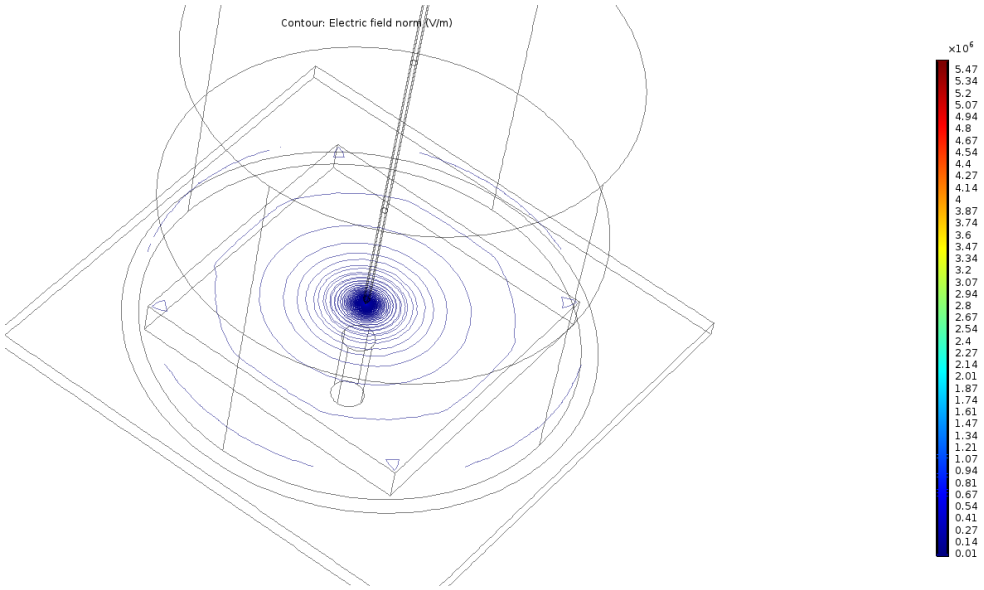

(b) contour distribution

Figure A.3: Electric field distribution on the sample surface when the point electrode is at 1kV

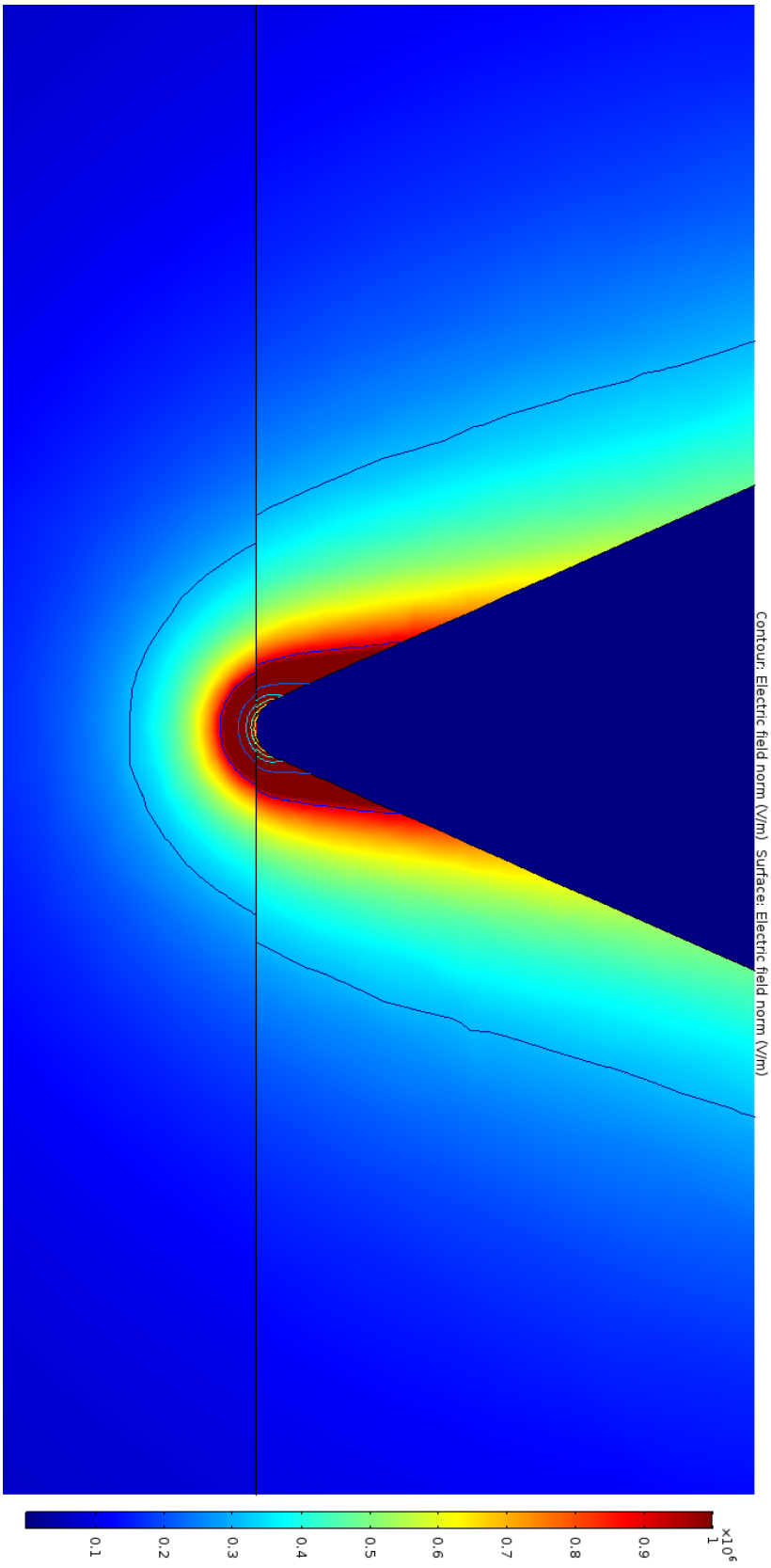

Figure A.4: Electric Field distribution at the tip of the point electrode

APPENDIX B

MATLAB PROGRAM TO CALCULATE FRACTAL DIMENSION

```
% values of width1, width2 and max1 variables should be defined by
    the user prior to the program. width1 and width2 are the side
    length of the figures. max1 is the maximum value that side length
     of the box can take

I= imread('imagename.png');    % load the image
Igray = rgb2gray(I);           % convert it into gray scale
c= ~Igray;
k=zeros(width1,width2);
N=zeros(1,width1);             % variable to store box size
R=zeros(1,width1);               % variable to store  number of boxes
gap=1;                         % define the rate at which the side
    length of the box  increases
a=0;
b=0;
q=1;

for size1 =1:gap:max1            %size of the box
k=zeros(width1, width2);
siz=size1-1;
for i=1:size1:(width1-0)
for j=1:size1:(width2-0)                                          %
    starting to cover the figure  starting from  (1,1) point.
if(j>(width2-siz) && i<=(width1-siz))          % After the pattern
    is covered with boxes ,if there is a square shaped remaining part
     of which one side length is smaller than box size.

for m=i:i+siz
for l=j:width2
if(c(m,l) ==1)                   %Check whether there  is any part of
     the  fractal pattern inside the considered box.
```

```
k(i,j)=1;
end
end
end
end

if(j<=(width2-siz) && i<=(width1-siz))                    %covering
    the pattern with boxes.
for m=i:i+siz
for l=j:j+siz
if(c(m,l) ==1)
k(i,j)=1;
end
end
end
end

if(i>(width1-siz) && j<(width2-siz))              % After the pattern
    is covered with boxes, if there is a square shaped remaining part
     of which one side length is smaller than box size.

for m=i:width1
for l=j:j+siz
if(c(m,l) ==1)
k(i,j)=1;
end
end
end
end

if(i>(width1-siz) &&  j>(width2-siz))             % After the pattern
    is covered with boxes ,if there is a square shaped remaining part
     of which both side lengths are smaller than box size.


for m=i:width1
for l=j:width2
if(c(m,l) ==1)
k(i,j)=1;
end
end

end
end
end
end
```

```
a=0;
for si=1:width1
for di=1:width2
a=a+k(si,di);            % Count the number of required boxes to
    cover the pattern.
end
end

if(a<b  && q~=1)
b=a;
N(1,q) = a;
R(1,q)=size1;
q=q+1;
end

if( q==1)                % if this is  first iteration of the for
    loop.
b=a;
N(1,q) = a;
R(1,q)=size1;
q=q+1;
end

end
n=zeros(1,q-1);
r=zeros(1,q-1);
for i=1:q-1
n(1,i)=N(1,i);
r(1,i)=R(1,i);
end

g=log(r);                % log of box size.
h=log(n);                % log of number of boxes.
g=g.';
h=h.';
r=r.';
n=n.';
q=q-1;
filename = 'testdata.xlsx';     % define a excel sheet to save data.

xlswrite(filename,r,1,'A1:Aq');    % save  calculated data in the
    defined excel sheet.
xlswrite(filename,n,1,'B1:Bq');
xlswrite(filename,g,1,'C1:Cq');
xlswrite(filename,h,1,'D1:Dq');
```